UNIVERSITY OF CALIFORNIA

Los Angeles

Protein-Polymer Nanomaterials for Therapeutic Applications

A dissertation submitted in partial satisfaction of the

requirements for the degree Doctor of Philosophy

in Chemistry

by

Nicholas Masao Matsumoto

2014

ABSTRACT OF THE DISSERTATION

Protein-Polymer Nanomaterials for Therapeutic Applications

by

Nicholas Masao Matsumoto

Doctor of Philosophy in Chemistry

University of California, Los Angeles, 2014

Professor Heather D. Maynard, Chair

Protein-polymer hybrid nanomaterials, designed for the targeted delivery of therapeutic anti-cancer agents, are at the forefront of research in biotechnology, nanotechnology, and cancer therapy. Conventional chemotherapeutics exhibit non-specific toxicity due to broad biodistribution; therefore developing nano-sized drug delivery vehicles for the targeted delivery of chemotherapeutics to tumors and cancer cells is important. Nanoparticles (ranging from 10-100 nanometers in size) accumulate in solid tumors and can be functionalized in order to encapsulate therapeutics and target cancer cells. Herein, the development of two classes of protein-polymer nanomaterials is described.

Vaults are naturally occurring protein-cages measuring 42 x 42 x 75 nm in dimension with a hollow internal cavity. Vaults are non-immunogenic, readily expressed, and can be engineered. We have developed stimuli responsive vault-polymer conjugates. A protein reactive thermo-responsive poly(*N*-isopropylacrylamide) was prepared *via* reversible addition-fragmentation chain transfer (RAFT) polymerization and conjugated to the vault, resulting in a thermo-responsive vault nanoparticle (**Chapter 2**). Dual responsive vault nanoparticles have also been developed *via* conjugation of a pH- and thermo-responsive polymer, poly(*N*-isopropylacrylamide-*co*-acrylic acid), prepared by RAFT polymerization (**Chapter 3**).

The design of nanoparticles was further explored by conjugating proteins to disulfide cross-linked poly(poly(ethylene glycol) methyl ether methacrylate) (pPEGMA) nanogels. Thiol-reactive nanogels were conjugated to thiol-enriched proteins *via* a simple disulfide exchange reaction (**Chapter 4**).

Additionally, the development of new methods for protein-polymer conjugation is described. Ring opening metathesis polymerization (ROMP) was used for the preparation of protein-reactive unsaturated poly(ethylene glycol) (PEG) analogs (**Chapter 5**). These unsaturated PEG analogs were conjugated to proteins. Due to olefins present in the polymer backbone, the polymer can be degraded from the conjugated protein by exposure to Grubbs type metathesis catalysts. Furthermore, a ROMP *grafting from* approach has also been developed, whereby the protein streptavidin (SAv) was functionalized with a biotinylated ruthenium metathesis catalyst. The SAv macrocatalyst was then used in the ROMP of a tetraethylene glycol modified norbornene monomer to yield a well defined protein-polymer conjugate (**Chapter 6**).

Lastly, the preparation of a telechelic, protein-reactive polymer by RAFT polymerization is described (**Chapter 7**). A *Boc*-protected aminooxy RAFT chain transfer agent (CTA) was

synthesized and utilized in the polymerization of poly(ethylene glycol) methyl ether acrylate (PEGA). The resulting aminooxy functionalized pPEGA was then functionalized post-polymerization to install cysteine-reactive vinyl sulfone functionality on the polymer.

The dissertation of Nicholas Masao Matsumoto is approved.

Leonard H. Rome

Miguel A. García-Garibay

Heather D. Maynard, Committee Chair

University of California, Los Angeles

2014

This is dedicated to my Mom and Dad.

Table of Contents

List of Figures

List of Tables

List of Schemes

List of Abbreviations

AA	Acrylic Acid
ADMET	Acyclic diene metathesis
AIBN	2,2'-Azobis(2-methylpropionitrile)
ATRP	Atom Transfer Radical Polymerization
AF488	Alexa Fluor® 488
BSA	Bovine Serum Albumin
CD_3CN	Deuterated Acetonitrile
$CDCl_3$	Deuterated Chloroform
$CHCl_3$	Chloroform
CM	Cross Metathesis
CRP	Controlled Radical Polymerization
CTA	Chain Transfer Agent
Cys	Cysteine
CD_2Cl_2	Deuterated Methylene Chloride
d	doublet (NMR)
Da	Dalton
DBU	1,8-diazabicycloundec-7-ene
DCC	*N,N*'-Dicyclohexylcarbodiimide
DCM	Methylene Chloride
DiI	1,1'-dioctadecyl-3,3,3',3'-tetramethylindocarbocyanine perchlorate
DLS	Dynamic light scattering

DMAP	4-Dimethylaminopyridine
DMF	*N,N*'-Dimethylformamide
DTT	dithiothreitol
EDC	1-Ethyl-3-(3-dimethylaminopropyl)carbodiimide
EDTA	ethylenediaminetetraacetic acid
EM	Electron microscopy
EPR	Enhanced permeation and retention effect
eq	Equivalents
EtOAc	Ethyl Acetate
FPLC	Fast Protein Liquid Chromatography
GPC	Gel Permeation (Size Exclusion) Chromatography
Grubbs I	Grubbs Catalyst, 1st Generation
Grubbs II	Grubbs Catalyst, 2nd Generation
Grubbs III	Grubbs Catalyst, 3rd Generation
h	Hour
HDF	Human dermal fibroblasts
Hoveyda-Grubbs II	Hoveyda-Grubbs catalyst, 2nd Generation
HRMS	High resolution mass spectrometry
IR	infrared
J	Coupling Constant (NMR)
kDa	Kilodalton
LCST	Lower critical solution temperature
Lyz	Lysozyme

m	multiplet (NMR)
MeOD	Deuterated Methanol
MeOH	Methanol
MHz	Megahertz (NMR)
mmol	Millimole
M_n	Number Average Molecular Weight
MRI	Magnetic resonance imaging
M_w	Weight Average Molecular Weight
MW	Molecular Weight
MWCO	Molecular Weight Cut Off
MVP	Major vault protein
NG	Nanogel
nm	Nanometer
NMR	Nuclear Magnetic Resonance
Norbornenyl TEG ester	(1S,2R,4S)-2-(2-(2-(2-hydroxyethoxy)ethoxy)ethoxy)ethyl bicyclo[2.2.1]hept-5-ene-2-carboxylate
NIPAAm	*N*-isopropylacrylamide
PB	Phosphate Buffer
PDI	Polydispersity Index
PDSMA	pyridyl disulfide methacrylate
PEG	Poly(ethylene glycol)
PEGA	Poly(ethylene glycol) methyl ether acrylate
PEGMA	Poly(ethylene glycol)methyl ether methacrylate

PMMA	Poly(methyl methacrylate)
ppm	Parts per million (NMR)
q	quartet (NMR)
RAFT	Reversible Addition-Fragmentation Chain Transfer
RCM	Ring Closing Metathesis
ROM	Ring Opening Metathesis
ROMP	Ring Opening Metathesis Polymerization
s	singlet (NMR)
SAv	Streptavidin
SATP	*N*-succinimidyl-*S*-acetylthiopropionate
SDS-PAGE	Sodium Dodecyl Sulfate Poly(acrylamide) Gel Electrophoresis
SEC	Size Exclusion Chromatography
t	triplet (NMR)
*t*BuOH	*tert*-Butanol
TCEP	Triscarboxyethylphosphine
TEA	Triethylamine
TEG	Tetra(ethylene glycol)
THF	Tetrahydrofuran
TLC	Thin Layer Chromatography
Tris	Tris(hydroxymethyl)aminomethane
UV-Vis	Ultraviolet-visible spectroscopy

Acknowledgements

Chapter 2 is a version of Matsumoto, N. M.; Prabhakaran, P.; Rome, L. H.; Maynard, H. D. Smart Vaults: Thermally-Responsive Protein Nanocapsules. *ACS Nano* **2013**, *7*, 867-874. Chapter 4 is a version of Matsumoto, N. M.; Gonzalez-Toro, D. C.; Chacko, R. T.; Maynard, H. D.; Thayumanavan, S. Synthesis of Nanogel-Protein Conjugates. *Polymer Chem.* **2013**, *4*, 2464-2469.

First and foremost, I would like to express my gratitude to my advisor Prof. Heather Maynard for her continued support of my education over the past six years. In the Maynard lab, I have had the opportunity to conduct a number of independent research projects of great interest to me. Due to Heather's leadership, the Maynard lab is one of the most supportive labs at UCLA and has been an amazing environment to pursue a PhD. Thank you Heather for all of the support and guidance you have given me throughout the course my graduate studies.

I would also like to thank my doctoral committee, Prof. Lenny Rome and Prof. Miguel García-Garibay. Prof. García-Garibay was instrumental in my involvement in the Organization for Cultural Diversity in Chemistry (OCDC) at UCLA. His commitment to diversity is an inspiration to me. Prof. Lenny Rome has been the best collaborator I have ever worked with. Working on vaults with Lenny and his group has been one of the highlights of my time in graduate school.

I have been fortunate to receive financial support from the NSF Competitive Edge Program, the NSF Graduate Research Fellowship Program (DGE-0707424), and the UCLA Dissertation Year Fellowship. These fellowships have allowed me to focus on research throughout graduate school. Furthermore, I would like to thank the NIH (R21 CA 137506) for research funding.

Throughout my PhD, I have worked with great collaborators. From the Rome group at the UCLA School of Medicine, I would like to thank Dr. Valerie Kickhoefer, Dr. Jan Mrazek, Dr. Daniel Buehler, and Hedi Roseboro for helping me with my vault projects. I would also like to thank Prof. S. Thayumanavan and Dr. Daniella Gonzalez-Toro, from UMass Amherst, for the opportunity to work with them on their nanogel system.

In the Maynard group, I have had the opportunity to work with a lot of really awesome people. Firstly, I would like to thank my friend and mentor Dr. Greg Grover for helping me get started in the Maynard lab and for helping me to become an independent researcher. I would like to acknowledge my next-door neighbor, coworker, and good-friend Dr. Steevens Alconcel who made the lab and our apartment building in the Palms so much fun. For the past four years, Caitlin Decker has been a close friend and excellent colleague. I am going to miss our impromptu harmonica and recorder jam sessions in the office. Dr. Chris Kolodziej and Dr. Zach Tolstyka, were senior members of the lab when I joined, and I thank them for their friendship, advice and support. I would like to thank Dr. Panchami Prabhakaran for working with me on the vault project (Chapter 2) and Eric Raftery for working with me on the ROMP PEG project (Chapter 5). I frequently enjoyed discussions with Prof. Erhan Bat, who was a post-doc in the Maynard lab, and I thank him for all of his advice and support. I would like to congratulate Juneyoung Lee, Thi Kathy Nguyen, and En-Wei Lin who also started in the Maynard Lab in 2009 and are graduating with PhD's this year. Lastly, I would like to acknowledge the current members of the Maynard group: Dr. Muhammet Kahveci, Dr. Yang Liu, Uland Lau, Natalie Boehnke, Sam Paluck, Jeonghoon Ko, and Emma Pelegri-O'Day. Thank you all for making lab so much fun.

I am very grateful for receiving an excellent undergraduate education at UC Santa Cruz and I am very proud to be a Banana Slug. I would like to thank my undergraduate research advisor Prof. Rebecca Braslau, who welcomed me into her laboratory and allowed me to pursue my own research projects. From the Braslau lab, I would like to thank my grad student mentor Wilson Chau and Dr. Frank Rivera. Prof. Joe Konopelski taught the first organic chemistry course I ever took; I am very thankful for his advice and support throughout my undergraduate education. At UCSC, I was very fortunate to be involved in the ACE community. I would like to express my extreme gratitude to the director of the ACE program, Nancy Cox-Konopelski, whose commitment to under-represented STEM students at UC Santa Cruz is unequaled. Nancy's encouragement very early in my undergraduate studies led me to pursuing chemistry research and graduate studies. At UC Santa Cruz, I had a lot of fun studying chemistry with Nick and Lexi Ball-Jones, who are wrapping up their own PhD's in organic chemistry at UC Davis.

I am blessed with a large, loud, and loving family. My Mom and Dad are a perfect team, whose love and support is responsible for at least seven college degrees (and counting) divided between my sisters Laura, Victoria, Maya, and I. Mom, thank you for instilling in me the importance of education. All of the commitment that I have for my own education comes from watching your educational journey, from mother of four in community college all the way to completing your own doctoral degree. Thank you Dr. Catherine Armas-Matsumoto, AKA Mom. Dad, through your hard work you made all of this possible for mom, my sisters, and me. Thank you Dad. I would also like to thank my Ji-Chan (grandfather), Noboru Matsumoto, who helped raise me and has given me constant encouragement and support throughout my life. I mentioned earlier, that my family is loud… this is due to my Nana (Grandmother) Carmen Armas, Tata (Grandfather) Tony Armas, Aunt Jeanette, Uncle Ross, Uncle Phil, Aunt Yani, Uncle John, and

my cousins Brandon, Sam, Briana, Andrew, Olivia, and Hannah. One of the greatest benefits of going to school in LA was being so close to all of you.

As I am writing this, my family is in the middle of a three-month celebration and I would like to acknowledge these important events. My youngest sister Maya recently graduated from Saint Mary's College (May 24th, 2014). Congrats Maya! I would like to congratulate my sister Laura and her husband Dr. Jaime Vega on the birth of their first child, Cruz Hajime Vega (born May 15th 2014). Welcome to the family Cruz! I would also like to wish my sister Victoria and future-brother-in-law Tim Lenderman all the best in their upcoming wedding (July 5th, 2014)!

Vita

Education

2009	University of California, Santa Cruz B.S., Chemistry with Highest Honors
2005	San Marcos High School San Marcos, CA

Research Experience

2009-2014	Graduate Research Assistant University of California, Los Angeles Prof. Heather D. Maynard
2006-2009	Undergraduate Research Assistant University of California, Santa Cruz Prof. Rebecca Braslau

Selected Honors & Awards

2013	UCLA Dissertation Year Fellowship
2010	NSF Graduate Research Fellowship
2009	NSF Competitive Edge Fellowship
2008	ACS Scholars Fellowship
2007	UC LEADS Scholar

Publications

6. Upton, B. M.; Gipson, R. M.; Duhović, S.; Lydon, B. R.; Matsumoto, N. M.; Maynard, H.D.; Diaconescu, P. L., "Synthesis of Ferrocene-Functionalized Monomers for Biodegradable Polymer Formation," *Inorganic Chemistry Frontiers* **2014**, *1,* 271-277.

5. Matsumoto, N.M.; González-Toro, D.C.; Chacko, R. T.; Maynard, H. D.; Thayumanavan, S. "Synthesis of Nanogel-Protein Conjugates," *Polymer Chemistry* **2013***, 4*, 2464-2469.

4. Matsumoto, N. M.; Prabhakaran, P.; Rome, L. H.; Maynard, H. D. "Smart Vaults: Thermally-Responsive Protein Nanocapsules," *ACS Nano*. **2013**, *7*, 867-874.

3. Grover, G. N.; Lee, J.; Matsumoto, N. M.; Maynard, H. D. "Aminooxy and Pyridyl Disulfide Telechelic Poly(poly(ethylene glycol) acrylate) by RAFT Polymerization," *Macromolecules* **2012**, *45*, 4958-4965.

2. Alconcel, S. N. S.; Grover, G. N.; Matsumoto, N. M.; Maynard, H. D. "Synthesis of Michael Acceptor Ionomers of Poly(4-Sulfonated Styrene-*co*-Poly(ethylene Glycol) Methyl Ether Acrylate)," *Australian Journal of Chemistry* **2009**, *62*, 1496-1500.

1. Grover, G. N.; Alconcel, S. N. S.; Matsumoto, N. M.; Maynard, H. D. "Trapping of Thiol-Terminated Acrylate Polymers with Divinyl Sulfone To Generate Well-Defined Semitelechelic Michael Acceptor Polymers," *Macromolecules* **2009**, *42*, 7657-7663.

Chapter 1

General Introduction: Protein-Polymer Nanomaterials for Therapeutic Applications

1.1. General Introduction to the Dissertation

Conjugation of proteins to synthetic polymers provides materials with enhanced physical characteristics that still retain the function of the native protein.[1-4] Thus, protein-polymer conjugates offer a diverse class of biomaterials of considerable interest for applications in biotechnology, nanotechnology, and drug delivery. Compared to native proteins, protein-polymer conjugates exhibit improved solubility, stability, and pharmacokinetic properties. Currently, protein-polymer conjugates are employed as therapeutics for the treatment of various diseases, including hepatitis C and cancer.[5]

The study of protein-polymer conjugation began with the first reports of the covalent conjugation of poly(ethylene glycol) (PEG) to proteins by Abuchowski and co-workers in 1977.[6,7] In their seminal publication, Abuchowski and co-workers showed that PEG-bovine serum albumin (BSA) conjugates exhibit longer *in vivo* circulation lifetimes as well as reduced immunogenicity than native BSA when injected into rabbits.[6] PEGylation has since been applied to the development of protein therapeutics, including 10 protein-PEG conjugates, which that are approved for use by the US FDA.[5] Longer circulation lifetimes and improved *in vivo* stability directly translate to a better quality for patients who require frequent administration of such protein drugs.

Polymer conjugation to proteins can result in materials with drastically altered physical properties compared to the native protein. An example of this is protein-"smart" polymer conjugates.[8-10] "Smart" polymers are polymers that respond to external stimuli such as temperature,[11-30] pH,[31-34] and magnetic field.[8-10] Conjugation of stimuli responsive "smart" polymers to proteins, results in active protein materials that respond to stimuli in the same manner as the conjugated polymer. Pioneering work by Hoffman and coworkers has utilized

thermo-responsive poly(*N*-isopropylacrylamide) (pNIPAAm) for the development of thermo-responsive protein-polymer conjugates, which undergoes a reversible phase-change at elevated temperatures and becomes insoluble in aqueous environments.[35,36]

In general, there are three approaches to preparing protein-polymer conjugates: *grafting to, grafting from,* and *grafting through*.[1-4] The most commonly utilized conjugation strategy is *grafting to*. This entails the covalent conjugation of a pre-formed polymer to a protein. Although *grafting to* is the predominant method used for the formation of protein-polymer conjugates, this strategy has several major drawbacks. When *grafting to,* it is often necessary to use excess molar equivalents of polymer compared to protein, which is not only inefficient but makes the purification of the resulting protein-polymer conjugate challenging. Modern biomacromolecule purification techniques are optimized for the purification of large biomacromolecules from small molecules. Such techniques include: size exclusion chromatography, gel filtration chromatography, dialysis, and ultra-centrifugation. To take advantage of these techniques, *grafting from* methods have been developed. *Grafting from* polymers is a strategy whereby a polymerization-initiating moiety is installed onto a protein, which is then used to initiate a polymerization, effectively growing a polymer chain from the protein. Purification of the large protein-polymer conjugates can then be achieved through the use of the previously mentioned techniques. The least frequently pursued conjugation strategy is *grafting through*. This strategy entails the installation of a polymerizable unit onto the protein, which can then be incorporated into a polymer. Overall, this strategy results in a polymer containing pendent protein units.

1.2. Controlled Radical Polymerization for Protein-Polymer Conjugation

To produce homogeneous protein-polymer conjugates, polymers with narrow molecular weight distributions and controlled molecular weights are essential. Controlled radical polymerization (CRP) techniques such as atom transfer radical polymerization (ATRP)[37-40] and reversible addition-fragmentation chain transfer (RAFT) polymerization[41-44] provide access to well-defined macromolecular architectures. ATRP and RAFT accommodate a diverse range of vinyl monomers, including functionalized styrenes, acrylates, methacrylates and acrylamides.[37,39,41,42]

CRP techniques, such as ATRP and RAFT, are well suited to the preparation of protein-reactive telechelic and semi-telechelic polymers. Protein-reactive end-groups have been incorporated at the chain ends of polymers by using modified ATRP organohalide initiators[45-47] and RAFT chain transfer agents (CTA).[48,49] Post-polymerization modification of end groups is also an effective way to prepare reactive polymers. ATRP polymer organohalide end-groups can be displaced with strong nucleophiles, such as azides.[50,51] The RAFT thiocarbonylthio end-group can be reduced to reveal a free-thiol, which can be utilized for a variety of efficient thiol-ene reactions or disulfide forming reactions.[52-59] Typical protein-reactive end-groups include activated esters, Michael acceptors, and protein-ligands, such as biotin.[54,55] Chemoselective end-groups reactive towards cysteine residue thiols, such as vinyl sulfone (at pH 7),[53,59] maleimide (at pH 7),[12,19,54,55,58] and pyridyl disulfide provide site-specific polymer conjugation.[46,48] Site-selective conjugation of polymers to proteins is important in order to retain bioactivity, as polymer conjugation in close proximity to the protein active site can diminish protein activity.[60] ATRP and RAFT techniques have been used extensively for *grafting from* proteins. Our group and others have developed grafting from methods *via* ATRP, whereby ATRP-initiating

organohalides have been installed onto proteins and utilized for the polymerization of vinyl monomers.[61-65] Similarly, RAFT polymerization has been utilized in the polymerization from proteins by covalent modification with RAFT CTAs, followed by subsequent polymerization of vinyl monomers.[12,66,67]

1.3. Therapeutic Nanoparticles

The development of therapeutic nanoparticles is of particular importance to the fields of drug delivery and cancer research. Due to their size, nanoparticles ranging from 70-200 nm in diameter can circulate *in vivo* with minimal renal clearance (>5.5 nm), liver uptake (<700 nm), and spleen uptake (>300 nm).[68] Furthermore, nanoparticles can passively accumulate in tumors due to the porous nature of tumor vasculature.[69] Accumulation in tumors due to poorly formed tumor vasculature is known as the enhanced permeation and retention (EPR) effect.[69] Furthermore, nanoparticles can be engineered to accommodate therapeutic payloads as well as target specific cell types. Many powerful chemotherapeutic agents exhibit poor aqueous solubility as well as non-specific biodistributions,[70,71] which can cause negative side effects. Incorporating such therapeutic molecules into nanoparticles can overcome these solubility and distribution limitations, drastically improving the quality of life for patients requiring such therapeutics. Small molecule targeting ligands such as folate, and targeting proteins, such as antibodies, have been applied towards the development of therapeutic nanoparticles.[72]

Synthetic polymers have been used as building blocks for the development of functional nanoparticles. The use of synthetic polymers allows for the development of nanoparticles with reactive functionalities, desirable physical properties, and predictable architectures. Such nanoparticles include micelles,[73-75] polymersomes,[76] cross-linked micelles,[74,77-79] and nanogels.[80-

[91] Furthermore, synthetic polymer based nanoparticles can be designed to respond to their environment. For example, nanoparticles have been engineered to release therapeutic payloads in the oxidative and acidic environments, which are inherent to diseased cells.

Nano-sized protein cages can be modified with the addition polymers, to yield complex nanostructure architectures, which are inaccessible, by synthetic methods alone. There are many examples of polymer modification of virus capsids and ferritin, which are both large protein cages found in nature.[92-108] Such polymer modified protein-cage based nanoparticles could offer more precise therapeutic than purely synthetic nanoparticles.

1.4. Aim and Structure of the Dissertation

The work described in this dissertation details the preparation and application of synthetic polymers, protein-polymer conjugates, and protein-polymer nanomaterials for therapeutic applications. The central theme of this dissertation is the development of reactive polymers for conjugation to proteins. RAFT polymerization techniques were utilized extensively in **Chapters 2-5**. New methods involving ring-opening metathesis polymerization (ROMP) were also explored, and this is described in **Chapters 6 & 7**.

In **Chapter 2**, the use of RAFT polymerization for the development of protein-reactive telechelic polymers containing aminooxy functionality is discussed. A *Boc*-protected aminooxy dithiobenzoate CTA was prepared and employed in the RAFT polymerization of poly(poly(ethylene glycol) methyl ether acrylate) (pPEGA). Post-polymerization reduction of the dithiobenzoate polymer end-group to reveal a free thiol, followed by an *in situ* Michael addition to vinyl sulfone yielded a α-*Boc*-aminooxy, ω-vinyl sulfone pPEGA.

Chapters 3 & 4 detail the modification of vault nanoparticles with stimuli-responsive polymers prepared *via* RAFT polymerization. Ubiquitous amongst eukaryotes, vaults are the largest known ribonucleoprotein particles, which measure approximately 45 x 45 x 75 nm in dimension.[109-113] These particles are composed of 78-80 copies of the major vault protein (MVP), which are assembled into a hollow barrel-like structure with protruding caps. The internal cavity of the vault measures 5 x 10^7 $Å^3$, and can accommodate hundreds of proteins in the interior.[114] Vaults are stable[115] (to pH and temperature changes, surfactants, organic solvents), non-immunogenic particles that are readily expressed[116] and modified.[117-119] For these reasons, we have pursued the vault as a platform for the development stimuli-responsive protein-polymer nanoparticles. In **Chapter 3**, the development of thermally-responsive vault-pNIPAAm conjugates is discussed. The vault-pNIPAAm conjugate was shown to undergo a thermally triggered reversible aggregation. **Chapter 4** details the modification of vaults with multiple stimuli-responsive poly(*N*-isopropylacrylamide-*co*-acrylic acid) p(NIPAAm-*co*-AA). These vault-p(NIPAAm-*co*-AA) conjugates undergo a reversible thermally-triggered aggregation in slightly acidic conditions (pH 5-6) while remaining stable at neutral pH.

In **Chapter 5**, the preparation of protein-decorated polymeric nanogels is discussed. Polymeric nanogels, composed of poly(poly(ethylene glycol) methyl ether methacrylate-*co*--pyridyl disulfide methacrylate) p(PEGMA-*co*-PDSMA), were prepared and modified at the nanogel surface with the model protein BSA. Conjugation occurred *via* disulfide exchange of thiol-enriched BSA with existing pyridyl disulfide moieties on the p(PEGMA-*co*-PDSMA) nanogel.

CRP techniques, such as ATRP and RAFT, have been used extensively for the development of protein-polymer materials. To date, however, there have only been several

reports of the use of ROMP or ROMP derived polymers for the preparation of protein-polymer conjugates.[120,121] **Chapters 6 & 7**, describe the development of ROMP based methods for protein-polymer conjugation.

In **Chapter 6**, the preparation and application of protein-reactive unsaturated PEG analogs is discussed. The unsaturated PEG analogs were prepared *via* ROMP of a previously reported unsaturated crown-ether analog.[122,123] Amine-reactive aldehyde functionality was introduced onto the polymer end-group, by terminating the polymerization with vinylene carbonate.[124] These unsaturated PEG analogs were readily conjugated to T4 lysozyme (Lyz). The resulting conjugates could be chemoselectively degraded by incubation with a Grubbs' type catalyst.

Chapter 7 discusses the development of ROMP based *grafting from* protein-polymer conjugation methods. A streptavidin (SAv) macro-catalyst was prepared *via* the introduction of a biotinylated Grubbs' catalyst. The SAv macro-catalyst was subsequently utilized to initiate ROMP of a tetra(ethylene glycol) modified norbornene monomer resulting in a well-defined SAv-polymer conjugate.

The work described in **Chapters 3 & 5** has been published.[24,125]

1.5 References

1. Broyer, R. M.; Grover, G. N.; Maynard, H. D. Emerging Synthetic Approaches for Protein-Polymer Conjugations. *Chem. Commun.* **2011**, *47*, 2212-2226.
2. Grover, G. N.; Maynard, H. D. Protein-Polymer Conjugates: Synthetic Approaches by Controlled Radical Polymerizations and Interesting Applications. *Curr. Opin. Chem. Biol.* **2010**, *14*, 818-827.
3. Jung, B.; Theato, P. In *Bio-Synthetic Polymer Conjugates*; Schlaad, H., Ed.; Springer-Verlag Berlin: Berlin, 2013; Vol. 253, p 37-70.
4. Le Droumaguet, B.; Nicolas, J. Recent Advances in the Design of Bioconjugates from Controlled/Living Radical Polymerization. *Polym. Chem.* **2010**, *1*, 563-598.
5. Alconcel, S. N. S.; Baas, A. S.; Maynard, H. D. Fda-Approved Poly(Ethylene Glycol)-Protein Conjugate Drugs. *Polym. Chem.* **2011**, *2*, 1442-1448.
6. Abuchowski, A.; Vanes, T.; Palczuk, N. C.; Davis, F. F. Alteration of Immunological Properties of Bovine Serum-Albumin by Covalent Attachment of Polyethylene-Glycol. *J. Biol. Chem.* **1977**, *252*, 3578-3581.
7. Abuchowski, A.; McCoy, J. R.; Palczuk, N. C.; Vanes, T.; Davis, F. F. Effect of Covalent Attachment of Polyethylene-Glycol on Immunogenicity and Circulating Life of Bovine Liver Catalase. *J. Biol. Chem.* **1977**, *252*, 3582-3586.
8. Borner, H. G.; Kuhnle, H.; Hentschel, J. Making "Smart Polymers" Smarter: Modern Concepts to Regulate Functions in Polymer Science. *Journal of Polymer Science Part a-Polymer Chemistry* **2010**, *48*, 1-14.
9. Hoffman, A. S. Stimuli-Responsive Polymers: Biomedical Applications and Challenges for Clinical Translation. *Advanced Drug Delivery Reviews* **2013**, *65*, 10-16.

10. Roy, D.; Brooks, W. L. A.; Sumerlin, B. S. New Directions in Thermoresponsive Polymers. *Chem. Soc. Rev.* **2013**, *42*, 7214-7243.

11. Cummings, C.; Murata, H.; Koepsel, R.; Russell, A. J. Tailoring Enzyme Activity and Stability Using Polymer-Based Protein Engineering. *Biomaterials* **2013**, *34*, 7437-7443.

12. De, P.; Li, M.; Gondi, S. R.; Sumerlin, B. S. Temperature-Regulated Activity of Responsive Polymer-Protein Conjugates Prepared by Grafting-from Via Raft Polymerization. *J. Am. Chem. Soc.* **2008**, *130*, 11288-+.

13. Dong, H. C.; Matyjaszewski, K. Thermally Responsive P(M(Eo)(2)Ma-Co-Oeoma) Copolymers Via Aget Atrp in Miniemulsion. *Macromolecules* **2010**, *43*, 4623-4628.

14. Hoffman, A. S.; Stayton, P. S. Conjugates of Stimuli-Responsive Polymers and Proteins. *Progress in Polymer Science* **2007**, *32*, 922-932.

15. Hu, Z. B.; Cai, T.; Chi, C. L. Thermoresponsive Oligo(Ethylene Glycol)-Methacrylate-Based Polymers and Microgels. *Soft Matter* **2010**, *6*, 2115-2123.

16. Huang, X.; Yin, Y. Z.; Jiang, X.; Tang, Y.; Xu, J. Y.; Liu, J. Q.; Shen, J. C. Construction of Smart Glutathione Peroxidase Mimic Based on Hydrophilic Block Copolymer with Temperature Responsive Activity. *Macromolecular Bioscience* **2009**, *9*, 1202-1210.

17. Ku, T. H.; Chien, M. P.; Thompson, M. P.; Sinkovits, R. S.; Olson, N. H.; Baker, T. S.; Gianneschi, N. C. Controlling and Switching the Morphology of Micellar Nanoparticles with Enzymes. *J. Am. Chem. Soc.,* **2011**, *133*, 8392-8395.

18. Li, M.; De, P.; Gondi, S. R.; Sumerlin, B. S. Responsive Polymer-Protein Bioconjugates Prepared by Raft Polymerization and Copper-Catalyzed Azide-Alkyne Click Chemistry. *Macromol. Rapid Commun.* **2008**, *29*, 1172-1176.

19. Li, M.; De, P.; Li, H. M.; Sumerlin, B. S. Conjugation of Raft-Generated Polymers to Proteins by Two Consecutive Thiol-Ene Reactions. *Polym. Chem.* **2010**, *1*, 854-859.

20. Li, W.; Zhang, A.; Feldman, K.; Walde, P.; Schluter, A. D. Thermoresponsive Dendronized Polymers. *Macromolecules* **2008**, *41*, 3659-3667.

21. Lin, Y.; Gao, J. W.; Liu, H. W.; Li, Y. S. Synthesis and Characterization of Hyperbranched Poly(Ether Amide)S with Thermoresponsive Property and Unexpected Strong Blue Photoluminescence. *Macromolecules* **2009**, *42*, 3237-3246.

22. Lutz, J. F.; Andrieu, J.; Uzgun, S.; Rudolph, C.; Agarwal, S. Biocompatible, Thermoresponsive, and Biodegradable: Simple Preparation of "All-in-One" Biorelevant Polymers. *Macromolecules* **2007**, *40*, 8540-8543.

23. Ma, Z. W.; Hong, Y.; Nelson, D. M.; Pichamuthu, J. E.; Leeson, C. E.; Wagner, W. R. Biodegradable Polyurethane Ureas with Variable Polyester or Polycarbonate Soft Segments: Effects of Crystallinity, Molecular Weight, and Composition on Mechanical Properties. *Biomacromolecules* **2011**, *12*, 3265-3274.

24. Matsumoto, N. M.; Prabhakaran, P.; Rome, L. H.; Maynard, H. D. Smart Vaults: Thermally-Responsive Protein Nanocapsules. *Acs Nano* **2013**, *7*, 867-874.

25. Rauwald, U.; del Barrio, J.; Loh, X. J.; Scherman, O. A. "On-Demand" Control of Thermoresponsive Properties of Poly(N-Isopropylacrylamide) with Cucurbit 8 Uril Host-Guest Complexes. *Chem. Commun.* **2011**, *47*, 6000-6002.

26. Shimoboji, T.; Larenas, E.; Fowler, T.; Hoffman, A. S.; Stayton, P. S. Temperature-Induced Switching of Enzyme Activity with Smart Polymer-Enzyme Conjugates. *Bioconjugate Chem.* **2003**, *14*, 517-525.

27. Walther, A.; Barner-Kowollik, C.; Muller, A. H. E. Mixed, Multicompartment, or Janus Micelles? A Systematic Study of Thermoresponsive Bis-Hydrophilic Block Terpolymers. *Langmuir* **2010**, *26*, 12237-12246.

28. Weber, C.; Hoogenboom, R.; Schubert, U. S. Temperature Responsive Bio-Compatible Polymers Based on Poly(Ethylene Oxide) and Poly(2-Oxazoline)S. *Prog. Polym. Sci.* **2012**, *37*, 686-714.

29. Zarafshani, Z.; Obata, T.; Lutz, J. F. Smart Pegylation of Trypsin. *Biomacromolecules* **2010**, *11*, 2130-2135.

30. Zhu, J. Y.; Zhang, Y. F.; Lu, D. N.; Zare, R. N.; Ge, J.; Liu, Z. Temperature-Responsive Enzyme-Polymer Nanoconjugates with Enhanced Catalytic Activities in Organic Media. *Chem. Commun.* **2013**, *49*, 6090-6092.

31. Lee, H. I.; Boyce, J. R.; Nese, A.; Sheiko, S. S.; Matyjaszewski, K. Ph-Induced Conformational Changes of Loosely Grafted Molecular Brushes Containing Poly(Acrylic Acid) Side Chains. *Polymer* **2008**, *49*, 5490-5496.

32. Manganiello, M. J.; Cheng, C.; Convertine, A. J.; Bryers, J. D.; Stayton, P. S. Diblock Copolymers with Tunable Ph Transitions for Gene Delivery. *Biomaterials* **2012**, *33*, 2301-2309.

33. Truong, M. Y.; Dutta, N. K.; Choudhury, N. R.; Kim, M.; Elvin, C. M.; Hill, A. J.; Thierry, B.; Vasilev, K. A Ph-Responsive Interface Derived from Resilin-Mimetic Protein Rec1-Resilin. *Biomaterials* **2010**, *31*, 4434-4446.

34. Zhu, L. P.; Smith, P. P.; Boyes, S. G. Ph-Responsive Polymers for Imaging Acidic Biological Environments in Tumors. *J. Polym. Sci., Part B: Polym. Phys.* **2013**, *51*, 1062-1067.

35. Chen, G. H.; Hoffman, A. S. Preparation and Properties of Thermoreversible, Phase-Separating Enzyme-Oligo(N-Isopropylacrylamide) Conjugates. *Bioconjugate Chem.* **1993**, *4*, 509-514.

36. Stayton, P. S.; Shimoboji, T.; Long, C.; Chilkoti, A.; Chen, G. H.; Harris, J. M.; Hoffman, A. S. Control of Protein-Ligand Recognition Using a Stimuli-Responsive Polymer. *Nature* **1995**, *378*, 472-474.

37. Kamigaito, M.; Ando, T.; Sawamoto, M. Metal-Catalyzed Living Radical Polymerization. *Chem. Rev.* **2001**, *101*, 3689-3745.

38. Kato, M.; Kamigaito, M.; Sawamoto, M.; Higashimura, T. Polymerization of Methyl-Methacrylate with the Carbon-Tetrachloride Dichlorotris(Triphenylphosphine)Ruthenium(Ii) Methylaluminum Bis(2,6-Di-Tert-Butylphenoxide) Initiating System - Possibility of Living Radical Polymerization. *Macromolecules* **1995**, *28*, 1721-1723.

39. Matyjaszewski, K.; Xia, J. H. Atom Transfer Radical Polymerization. *Chem. Rev.* **2001**, *101*, 2921-2990.

40. Wang, J. S.; Matyjaszewski, K. Controlled Living Radical Polymerization - Atom-Transfer Radical Polymerization in the Presence of Transition-Metal Complexes. *J. Am. Chem. Soc.* **1995**, *117*, 5614-5615.

41. Moad, G.; Rizzardo, E.; Thang, S. H. Living Radical Polymerization by the Raft Process. *Aust. J. Chem.* **2005**, *58*, 379-410.

42. Moad, G.; Rizzardo, E.; Thang, S. H. Living Radical Polymerization by the Raft Process - a Third Update. *Aust. J. Chem.* **2012**, *65*, 985-1076.

43. Boyer, C.; Bulmus, V.; Davis, T. P.; Ladmiral, V.; Liu, J.; Perrier, S. Bioapplications of Raft Polymerization. *Chem. Rev.* **2009**, *109*, 5402-5436.

44. Chiefari, J.; Chong, Y. K.; Ercole, F.; Krstina, J.; Jeffery, J.; Le, T. P. T.; Mayadunne, R. T. A.; Meijs, G. F.; Moad, C. L.; Moad, G.; Rizzardo, E.; Thang, S. H. Living Free-Radical Polymerization by Reversible Addition-Fragmentation Chain Transfer: The Raft Process. *Macromolecules* **1998**, *31*, 5559-5562.

45. Sayers, C. T.; Mantovani, G.; Ryan, S. M.; Randev, R. K.; Keiper, O.; Leszczyszyn, O. I.; Blindauer, C.; Brayden, D. J.; Haddleton, D. M. Site-Specific N-Terminus Conjugation of Poly(Mpeg(1100)) Methacrylates to Salmon Calcitonin: Synthesis and Preliminary Biological Evaluation. *Soft Matter* **2009**, *5*, 3038-3046.

46. Vazquez-Dorbatt, V.; Tolstyka, Z. P.; Chang, C. W.; Maynard, H. D. Synthesis of a Pyridyl Disulfide End-Functionalized Glycopolymer for Conjugation to Biomolecules and Patterning on Gold Surfaces. *Biomacromolecules* **2009**, *10*, 2207-2212.

47. Vazquez-Dorbatt, V.; Tolstyka, Z. P.; Maynard, H. D. Synthesis of Aminooxy End-Functionalized Pnipaam by Raft Polymerization for Protein and Polysaccharide Conjugation. *Macromolecules* **2009**, *42*, 7650-7656.

48. Heredia, K. L.; Nguyen, T. H.; Chang, C. W.; Bulmus, V.; Davis, T. P.; Maynard, H. D. Reversible Sirna-Polymer Conjugates by Raft Polymerization. *Chem. Commun.* **2008**, 3245-3247.

49. Heredia, K. L.; Tolstyka, Z. P.; Maynard, H. D. Aminooxy End-Functionalized Polymers Synthesized by Atrp for Chemoselective Conjugation to Proteins. *Macromolecules* **2007**, *40*, 4772-4779.

50. van Dongen, S. F. M.; Nallani, M.; Cornelissen, J.; Nolte, R. J. M.; van Hest, J. C. M. A Three-Enzyme Cascade Reaction through Positional Assembly of Enzymes in a Polymersome Nanoreactor. *Chem.-Eur. J.* **2009**, *15*, 1107-1114.

51. Xu, F. J.; Neoh, K. G.; Kang, E. T. Bioactive Surfaces and Biomaterials Via Atom Transfer Radical Polymerization. *Prog. Polym. Sci.* **2009**, *34*, 719-761.

52. Boyer, C.; Liu, J. Q.; Bulmus, V.; Davis, T. P. Raft Polymer End-Group Modification and Chain Coupling/Conjugation Via Disulfide Bonds. *Aust. J. Chem.* **2009**, *62*, 830-847.

53. Grover, G. N.; Alconcel, S. N. S.; Matsumoto, N. M.; Maynard, H. D. Trapping of Thiol-Terminated Acrylate Polymers with Divinyl Sulfone to Generate Well-Defined Semitelechelic Michael Acceptor Polymers. *Macromolecules* **2009**, *42*, 7657-7663.

54. Heredia, K. L.; Grover, G. N.; Tao, L.; Maynard, H. D. Synthesis of Heterotelechelic Polymers for Conjugation of Two Different Proteins. *Macromolecules* **2009**, *42*, 2360-2367.

55. Heredia, K. L.; Tao, L.; Grover, G. N.; Maynard, H. D. Heterotelechelic Polymers for Capture and Release of Protein-Polymer Conjugates. *Polym. Chem.* **2010**, *1*, 168-170.

56. Spruell, J. M.; Levy, B. A.; Sutherland, A.; Dichtel, W. R.; Cheng, J. Y.; Stoddart, J. F.; Nelson, A. Facile Postpolymerization End-Modification of Raft Polymers. *J. Polym. Sci., Part A: Polym. Chem.* **2009**, *47*, 346-356.

57. Tao, L.; Kaddis, C. S.; Loo, R. R. O.; Grover, G. N.; Loo, J. A.; Maynard, H. D. Synthetic Approach to Homodimeric Protein-Polymer Conjugates. *Chem. Commun.* **2009**, 2148-2150.

58. Tao, L.; Kaddis, C. S.; Loo, R. R. O.; Grover, G. N.; Loo, J. A.; Maynard, H. D. Synthesis of Maleimide-End-Functionalized Star Polymers and Multimeric Protein-Polymer Conjugates. *Macromolecules* **2009**, *42*, 8028-8033.

59. Alconcel, S. N. S.; Grover, G. N.; Matsumoto, N. M.; Maynard, H. D. Synthesis of Michael Acceptor Ionomers of Poly(4-Sulfonated Styrene-Co-Poly(Ethylene Glycol) Methyl Ether Acrylate). *Australian Journal of Chemistry* **2009**, *62*, 1496-1500.

60. Kochendoerfer, G. G. Site-Specific Polymer Modification of Therapeutic Proteins. *Curr. Opin. Chem. Biol.* **2005**, *9*, 555-560.

61. Bontempo, D.; Maynard, H. D. Streptavidin as a Macroinitiator for Polymerization: In Situ Protein-Polymer Conjugate Formation. *J. Am. Chem. Soc.* **2005**, *127*, 6508-6509.

62. Gao, W. P.; Liu, W. G.; Christensen, T.; Zalutsky, M. R.; Chilkoti, A. In Situ Growth of a Peg-Like Polymer from the C Terminus of an Intein Fusion Protein Improves Pharmacokinetics and Tumor Accumulation. *Proc. Natl. Acad. Sci. U. S. A.* **2010**, *107*, 16432-16437.

63. Gao, W. P.; Liu, W. G.; Mackay, J. A.; Zalutsky, M. R.; Toone, E. J.; Chilkoti, A. In Situ Growth of a Stoichiometric Peg-Like Conjugate at a Protein's N-Terminus with Significantly Improved Pharmacokinetics. *Proc. Natl. Acad. Sci. U. S. A.* **2009**, *106*, 15231-15236.

64. Heredia, K. L.; Bontempo, D.; Ly, T.; Byers, J. T.; Halstenberg, S.; Maynard, H. D. In Situ Preparation of Protein - "Smart" Polymer Conjugates with Retention of Bioactivity. *J. Am. Chem. Soc.* **2005**, *127*, 16955-16960.

65. Magnusson, J. P.; Bersani, S.; Salmaso, S.; Alexander, C.; Caliceti, P. In Situ Growth of Side-Chain Peg Polymers from Functionalized Human Growth Hormone-a New

Technique for Preparation of Enhanced Protein-Polymer Conjugates. *Bioconjugate Chem.* **2010**, *21*, 671-678.

66. Boyer, C.; Bulmus, V.; Liu, J. Q.; Davis, T. P.; Stenzel, M. H.; Barner-Kowollik, C. Well-Defined Protein-Polymer Conjugates Via in Situ Raft Polymerization. *J. Am. Chem. Soc.* **2007**, *129*, 7145-7154.

67. Liu, J. Q.; Bulmus, V.; Herlambang, D. L.; Barner-Kowollik, C.; Stenzel, M. H.; Davis, T. P. In Situ Formation of Protein-Polymer Conjugates through Reversible Addition Fragmentation Chain Transfer Polymerization. *Angew. Chem.-Int. Edit.* **2007**, *46*, 3099-3103.

68. Liu, D. X.; Mori, A.; Huang, L. Role of Liposome Size and Res Blockade in Controlling Biodistribution and Tumor Uptake of Gm1-Containing Liposomes. *Biochim Biophys Acta* **1992**, *1104*, 95-101.

69. Maeda, H.; Nakamura, H.; Fang, J. The Epr Effect for Macromolecular Drug Delivery to Solid Tumors: Improvement of Tumor Uptake, Lowering of Systemic Toxicity, and Distinct Tumor Imaging in Vivo. *Adv. Drug Delivery Rev.* **2013**, *65*, 71-79.

70. Torchilin, V. P. Targeted Polymeric Micelles for Delivery of Poorly Soluble Drugs. *CMLS, Cell. Mol. Life Sci.* **2004**, *61*, 2549-2559.

71. Allen, T. M.; Cullis, P. R. Drug Delivery Systems: Entering the Mainstream. *Science* **2004**, *303*, 1818-1822.

72. Byrne, J. D.; Betancourt, T.; Brannon-Peppas, L. Active Targeting Schemes for Nanoparticle Systems in Cancer Therapeutics. *Adv. Drug Delivery Rev.* **2008**, *60*, 1615-1626.

73. Rieger, J.; Grazon, C.; Charleux, B.; Alaimo, D.; Jerome, C. Pegylated Thermally Responsive Block Copolymer Micelles and Nanogels Via in Situ Raft Aqueous Dispersion Polymerization. *J. Polym. Sci., Part A: Polym. Chem.* **2009**, *47*, 2373-2390.

74. Rijcken, C. J.; Snel, C. J.; Schiffelers, R. M.; van Nostrum, C. F.; Hennink, W. E. Hydrolysable Core-Crosslinked Thermosensitive Polymeric Micelles: Synthesis, Characterisation and in Vivo Studies. *Biomaterials* **2007**, *28*, 5581-5593.

75. Savic, R.; Eisenberg, A.; Maysinger, D. Block Copolymer Micelles as Delivery Vehicles of Hydrophobic Drugs: Micelle-Cell Interactions. *J. Drug Targeting* **2006**, *14*, 343-355.

76. van Dongen, S. F. M.; Nallani, M.; Cornelissen, J. J. L. M.; Nolte, R. J. M.; van Hest, J. C. M. A Three-Enzyme Cascade Reaction through Positional Assembly of Enzymes in a Polymersome Nanoreactor. *Chem.--Eur. J.* **2009**, *15*, 1107-1114.

77. Cheng, C.; Qi, K.; Germack, D. S.; Khoshdel, E.; Wooley, K. L. Synthesis of Core-Crosslinked Nanoparticles with Controlled Cylindrical Shape and Narrowly-Dispersed Size Via Core-Shell Brush Block Copolymer Templates. *Adv. Mater.* **2007**, *19*, 2830-2835.

78. Thurmond, K. B.; Kowalewski, T.; Wooley, K. L. Water-Soluble Knedel-Like Structures: The Preparation of Shell-Cross-Linked Small Particles. *J. Am. Chem. Soc.* **1996**, *118*, 7239-7240.

79. Liu, S. Y.; Weaver, J. V. M.; Tang, Y. Q.; Billingham, N. C.; Armes, S. P. Synthesis of Shell Cross-Linked Micelles with Ph-Responsive Cores Using Abc Triblock Copolymers. *Macromolecules* **2002**, *35*, 6121-6131.

80. Asadian-Birjand, M.; Sousa-Herves, A.; Steinhilber, D.; Cuggino, J. C.; Calderon, M. Functional Nanogels for Biomedical Applications. *Curr. Med. Chem.* **2012**, *19*, 5029-5043.

81. Bickerton, S.; Jiwpanich, S.; Thayumanavan, S. Interconnected Roles of Scaffold Hydrophobicity, Drug Loading, and Encapsulation Stability in Polymeric Nanocarriers. *Mol. Pharm.* **2012**, *9*, 3569-3578.

82. Gonzalez-Toro, D. C.; Ryu, J.-H.; Chacko, R. T.; Zhuang, J.; Thayumanavan, S. Concurrent Binding and Delivery of Proteins and Lipophilic Small Molecules Using Polymeric Nanogels. *J. Am. Chem. Soc.* **2012**, *134*, 6964-6967.

83. Lee, H.; Mok, H.; Lee, S.; Oh, Y. K.; Park, T. G. Target-Specific Intracellular Delivery of Sirna Using Degradable Hyaluronic Acid Nanogels. *J. Control. Release* **2007**, *119*, 245-252.

84. Oh, J. K.; Drumright, R.; Siegwart, D. J.; Matyjaszewski, K. The Development of Microgels/Nanogels for Drug Delivery Applications. *Progress in Polymer Science* **2008**, *33*, 448-477.

85. Raemdonck, K.; Demeester, J.; De Smedt, S. Advanced Nanogel Engineering for Drug Delivery. *Soft Matter* **2009**, *5*, 707-715.

86. Ryu, J.-H.; Bickerton, S.; Zhuang, J.; Thayumanavan, S. Ligand-Decorated Nanogels: Fast One-Pot Synthesis and Cellular Targeting. *Biomacromolecules* **2012**, *13*, 1515-1522.

87. Ryu, J.-H.; Chacko, R. T.; Jiwpanich, S.; Bickerton, S.; Babu, R. P.; Thayumanavan, S. Self-Cross-Linked Polymer Nanogels: A Versatile Nanoscopic Drug Delivery Platform. *J. Am. Chem. Soc.* **2010**, *132*, 17227-17235.

88. Ryu, J. H.; Jiwpanich, S.; Chacko, R.; Bickerton, S.; Thayumanavan, S. Surface-Functionalizable Polymer Nanogels with Facile Hydrophobic Guest Encapsulation Capabilities. *J. Am. Chem. Soc.* **2010**, *132*, 8246-8247.

89. Shen, W. Q.; Chang, Y. L.; Liu, G. Y.; Wang, H. F.; Cao, A. N.; An, Z. S. Biocompatible, Antifouling, and Thermosensitive Core-Shell Nanogels Synthesized by Raft Aqueous Dispersion Polymerization. *Macromolecules* **2011**, *44*, 2524-2530.

90. Yallapu, M. M.; Jaggi, M.; Chauhan, S. C. Design and Engineering of Nanogels for Cancer Treatment. *Drug Discov. Today* **2011**, *16*, 457-463.

91. Zha, L.; Banik, B.; Alexis, F. Stimulus Responsive Nanogels for Drug Delivery. *Soft Matter* **2011**, *7*, 5908-5916.

92. Patterson, D. P.; Prevelige, P. E.; Douglas, T. Nanoreactors by Programmed Enzyme Encapsulation inside the Capsid of the Bacteriophage P22. *ACS Nano* **2012**, *6*, 5000-5009.

93. Ma, Y. J.; Nolte, R. J. M.; Cornelissen, J. Virus-Based Nanocarriers for Drug Delivery. *Adv. Drug Delivery Rev.* **2012**, *64*, 811-825.

94. Manchester, M.; Singh, P. Virus-Based Nanoparticles (Vnps): Platform Technologies for Diagnostic Imaging. *Adv. Drug Delivery Rev.* **2006**, *58*, 1505-1522.

95. Douglas, T.; Young, M. Virus Particles as Templates for Materials Synthesis. *Adv. Mater.* **1999**, *11*, 679-681.

96. Uchida, M.; Klem, M. T.; Allen, M.; Suci, P.; Flenniken, M.; Gillitzer, E.; Varpness, Z.; Liepold, L. O.; Young, M.; Douglas, T. Biological Containers: Protein Cages as Multifunctional Nanoplatforms. *Adv. Mater.* **2007**, *19*, 1025-1042.

97. Manzenrieder, F.; Luxenhofer, R.; Retzlaff, M.; Jordan, R.; Finn, M. G. Stabilization of Virus-Like Particles with Poly(2-Oxazoline)S. *Angew. Chem.-Int. Edit.* **2011**, *50*, 2601-2605.

98. Comellas-Aragones, M.; de la Escosura, A.; Dirks, A. J.; van der Ham, A.; Fuste-Cune, A.; Cornelissen, J.; Nolte, R. J. M. Controlled Integration of Polymers into Viral Capsids. *Biomacromolecules* **2009**, *10*, 3141-3147.

99. Raja, K. S.; Wang, Q.; Gonzalez, M. J.; Manchester, M.; Johnson, J. E.; Finn, M. G. Hybrid Virus-Polymer Materials. 1. Synthesis and Properties of Peg-Decorated Cowpea Mosaic Virus. *Biomacromolecules* **2003**, *4*, 472-476.

100. Endo, M.; Fujitsuka, M.; Majima, T. Porphyrin Light-Harvesting Arrays Constructed in the Recombinant Tobacco Mosaic Virus Scaffold. *Chem.-Eur. J.* **2007**, *13*, 8660-8666.

101. Garcea, R. L.; Gissmann, L. Virus-Like Particles as Vaccines and Vessels for the Delivery of Small Molecules. *Curr. Opin. Biotechnol.* **2004**, *15*, 513-517.

102. Soto, C. M.; Ratna, B. R. Virus Hybrids as Nanomaterials for Biotechnology. *Curr. Opin. Biotechnol.* **2010**, *21*, 426-438.

103. O'Riordan, C. R.; Lachapelle, A.; Delgado, C.; Parkes, V.; Wadsworth, S. C.; Smith, A. E.; Francis, G. E. Pegylation of Adenovirus with Retention of Infectivity and Protection from Neutralizing Antibody in Vitro and in Vivo. *Hum. Gene Ther.* **1999**, *10*, 1349-1358.

104. Pokorski, J. K.; Breitenkamp, K.; Liepold, L. O.; Qazi, S.; Finn, M. G. Functional Virus-Based Polymer-Protein Nanoparticles by Atom Transfer Radical Polymerization. *J. Am. Chem. Soc.* **2011**, *133*, 9242-9245.

105. Schlick, T. L.; Ding, Z.; Kovacs, E. W.; Francis, M. B. Dual-Surface Modification of the Tobacco Mosaic Virus. *Journal of the American Chemical Society* **2005**, *127*, 3718-3723.

106. Lucon, J.; Qazi, S.; Uchida, M.; Bedwell, G. J.; LaFrance, B.; Prevelige, P. E.; Douglas, T. Use of the Interior Cavity of the P22 Capsid for Site-Specific Initiation of Atom-Transfer Radical Polymerization with High-Density Cargo Loading. *Nat. Chem.* **2012**, *4*, 781-788.

107. Comellas-Aragones, M.; Engelkamp, H.; Claessen, V. I.; Sommerdijk, N.; Rowan, A. E.; Christianen, P. C. M.; Maan, J. C.; Verduin, B. J. M.; Cornelissen, J.; Nolte, R. J. M. A Virus-Based Single-Enzyme Nanoreactor. *Nat. Nanotechnol.* **2007**, *2*, 635-639.

108. Sikkema, F. D.; Comellas-Aragones, M.; Fokkink, R. G.; Verduin, B. J. M.; Cornelissen, J. J. L. M.; Nolte, R. J. M. Monodisperse Polymer-Virus Hybrid Nanoparticles. *Organic & Biomolecular Chemistry* **2007**, *5*, 54-57.

109. Kedersha, N. L.; Heuser, J. E.; Chugani, D. C.; Rome, L. H. Vaults .3. Vault Ribonucleoprotein-Particles Open into Flower-Like Structures with Octagonal Symmetry. *J. Cell Biol.* **1991**, *112*, 225-235.

110. Kedersha, N. L.; Rome, L. H. Isolation and Characterization of a Novel Ribonucleoprotein Particle - Large Structures Contain a Single Species of Small Rna. *J. Cell Biol.* **1986**, *103*, 699-709.

111. Tanaka, H.; Kato, K.; Yamashita, E.; Sumizawa, T.; Zhou, Y.; Yao, M.; Iwasaki, K.; Yoshimura, M.; Tsukihara, T. The Structure of Rat Liver Vault at 3.5 Angstrom Resolution. *Science* **2009**, *323*, 384-388.

112. Kong, L. B.; Siva, A. C.; Rome, L. H.; Stewart, P. L. Structure of the Vault, a Ubiquitous Cellular Component. *Structure with Folding & Design* **1999**, *7*, 371-379.

113. Kedersha, N. L.; Miquel, M. C.; Bittner, D.; Rome, L. H. Vaults .2. Ribonucleoprotein Structures Are Highly Conserved among Higher and Lower Eukaryotes. *J. Cell Biol.* **1990**, *110*, 895-901.

114. Poderycki, M. J.; Kickhoefer, V. A.; Kaddis, C. S.; Raval-Fernandes, S.; Johansson, E.; Zink, J. I.; Loo, J. A.; Rome, L. H. The Vault Exterior Shell Is a Dynamic Structure That Allows Incorporation of Vault-Associated Proteins into Its Interior. *Biochemistry* **2006**, *45*, 12184-12193.

115. Esfandiary, R.; Kickhoefer, V. A.; Rome, L. H.; Joshi, S. B.; Middaugh, C. R. Structural Stability of Vault Particles. *J. Pharm. Sci.* **2009**, *98*, 1376-1386.

116. Stephen, A. G.; Raval-Fernandes, S.; Huynh, T.; Torres, M.; Kickhoefer, V. A.; Rome, L. H. Assembly of Vault-Like Particles in Insect Cells Expressing Only the Major Vault Protein. *J. Biol. Chem.* **2001**, *276*, 23217-23220.

117. Kickhoefer, V. A.; Garcia, Y.; Mikyas, Y.; Johansson, E.; Zhou, J. C.; Raval-Fernandes, S.; Minoofar, P.; Zink, J. I.; Dunn, B.; Stewart, P. L.; Rome, L. H. Engineering of Vault Nanocapsules with Enzymatic and Fluorescent Properties. *Proc. Natl. Acad. Sci. U. S. A.* **2005**, *102*, 4348-4352.

118. Kickhoefer, V. A.; Han, M.; Raval-Fernandes, S.; Poderycki, M. J.; Moniz, R. J.; Vaccari, D.; Silvestry, M.; Stewart, P. L.; Kelly, K. A.; Rome, L. H. Targeting Vault Nanoparticles to Specific Cell Surface Receptors. *Acs Nano* **2009**, *3*, 27-36.

119. Goldsmith, L. E.; Pupols, M.; Kickhoefer, V. A.; Rome, L. H.; Monbouquette, H. G. Utilization of a Protein "Shuttle" to Load Vault Nanocapsules with Gold Probes and Proteins. *ACS Nano* **2009**, *3*, 3175-3183.

120. Carrillo, A.; Gujraty, K. V.; Rai, P. R.; Kane, R. S. Design of Water-Soluble, Thiol-Reactive Polymers of Controlled Molecular Weight: A Novel Multivalent Scaffold. *Nanotechnology* **2005**, *16*, S416-S421.

121. Chen, B. Z.; Metera, K.; Sleiman, H. F. Biotin-Terminated Ruthenium Bipyridine Ring-Opening Metathesis Polymerization Copolymers: Synthesis and Self-Assembly with Streptavidin. *Macromolecules* **2005**, *38*, 1084-1090.

122. Marsella, M. J.; Maynard, H. D.; Grubbs, R. H. Template-Directed Ring-Closing Metathesis: Synthesis and Polymerization of Unsaturated Crown Ether Analogs. *Angew. Chem.-Int. Edit. Engl.* **1997**, *36*, 1101-1103.

123. Maynard, H. D.; Grubbs, R. H. Synthesis of Functionalized Polyethers by Ring-Opening Metathesis Polymerization of Unsaturated Crown Ethers. *Macromolecules* **1999**, *32*, 6917-6924.

124. Hilf, S.; Grubbs, R. H.; Kilbinger, A. F. M. End Capping Ring-Opening Olefin Metathesis Polymerization Polymers with Vinyl Lactones. *J. Am. Chem. Soc.* **2008**, *130*, 11040-11048.

125. Matsumoto, N. M.; Gonzalez-Toro, D. C.; Chacko, R. T.; Maynard, H. D.; Thayumanavan, S. Synthesis of Nanogel-Protein Conjugates. *Polym. Chem.* **2013**, *4*, 2464-2469.

Chapter 2

Smart Vaults: Thermally-Responsive Protein Nanocapsules[†]

2.1. Introduction

Naturally derived protein cages, such as virus capsids and ferritin, serve as excellent templates for functional biohybrid materials with precise architectures that are unattainable by purely synthetic processes.[1-5] Such materials have been developed for applications in the fields of nanotechnology,[4,6] biotechnology,[5,7] electronic materials,[8] catalysis,[9] and drug delivery.[10-13] The regular arrangement of protein sub-units within protein cage structures allows for synthetic modification of specific regions and surfaces of the protein cage, such as the exterior shell or interior cavity. The conjugation of synthetic polymers to viruses, such as adenovirus, cowpea mosaic virus, tobacco mosaic virus, and others has been investigated.[14-17] For example, poly(ethylene glycol) has been attached to adenovirus and cowpea mosaic virus, and its conjugation has been shown to decrease immunogenicity of the particles.[14,16] Recently, Douglas and coworkers have polymerized 2-aminoethyl methacrylate from the interior of P22 capsids creating a particle capable of encapsulating magnetic resonance imaging (MRI) contrast agents.[18] Although there are several examples of polymer conjugation to protein cages, to our knowledge there are no examples of stimuli-responsive smart polymers conjugated to protein cages. Yet such materials can reversibly alter the physical characteristics of the nanobiomaterial by an externally controlled trigger.

Smart polymers are responsive to external stimuli such as heat, pH, magnetic field, *etc.,*[19] and the analysis of the micro- and nano-assembly transitions have been undertaken.[20] Poly(*N*-isopropylacrylamide) (pNIPAAm) is a well-known temperature responsive polymer that undergoes a reversible phase transition and becomes insoluble in water above the lower critical solution temperature (LCST).[19] We and others have previously reported the preparation of protein-pNIPAAm conjugates, which exhibit the pNIPAAm phase behavior while retaining the

bioactivity of the protein.[21-28] Conjugation of pNIPAAm results in altered properties upon exposure to heat. For example, ligand binding sites can be closed, proteins can be reversibly aggregated, and the polymer can be used to purify biomolecules by mild precipitation.[21-28] In this paper, we report that the thermally-responsive polymer can be added to vault nanocapsules without disrupting the structure of the capsule.

First reported in 1986 by Rome and Kedersha, vaults are highly conserved ribonucleoprotein complexes found in high concentrations in almost all eukaryotic cells.[30-32] These massive particles weigh approximately 13 MDa and have a unique structure composed of a barrel waist and protruding caps at both ends (Scheme 2.1).[33] In recent years, high-resolution crystal structures have confirmed low resolution cryo-EM structures.[34] Naturally occurring vaults are comprised of several highly conserved proteins, with one protein, the 104 kDa major vault protein (MVP), accounting for over 70% of the vault mass. The MVP provides the basis for the vault structure, with 78 MVPs aligned from C- to N-terminus from the cap of the vault to the waist, with all of the N-termini facing towards the interior. Vaults are dynamic; although the MVPs are non-covalently associated, they have a kinetic off rate such that they can dynamically open and close to accommodate small molecules which slip into the inner cavity or large proteins or other macromolecules which bind to their interior.[29] Vaults are also highly stable *in vivo* and *in vitro* to a variety of biological and physical stresses.[35]

Expression of MVP in insect cells results in the spontaneous assembly of non-native vault structures that measure 45 x 45 x 75 nm and are composed of ~78 copies of MVP.[36] Although the natural biological function of vaults is unknown, recombinant vaults can be engineered for a variety of applications.[37] For example, the N-terminus of MVP can be modified

to contain a cysteine-rich (4 cysteine residues) 12 amino acid peptide sequence to form CP-MVP. Vaults assembled from this fusion protein have increased particle stability.[37] Cell-specific targeting vaults have also been engineered by incorporating IgG binding peptides into recombinant MVPs for attachment of targeting antibodies.[38] While in nature vaults contain multiple copies of two large proteins (VPARP and TEP1) and one or more small RNAs (vRNAs), recombinant vaults have a hollow interior with an approximate volume of 5 x 10^7 $Å^3$, which is large enough to accommodate hundreds of proteins and many more small molecules.[29,33,39-41] For example, gold nanoparticles were packaged and conducting polymers were non-covalently incorporated into the vault interior.[40,41] A number of proteins have been packaged into the vault, taking advantage of a binding site on MVP which faces the internal vault lumen. This site recognizes the vault protein VPARP through a protein domain at the VPARP C-terminus, which is referred to as INT for MVP interaction domain.[37] INT fusion proteins bind with high affinity to the vault lumen, but they are slowly released. This strategy has been used to package antigens into vaults so that the vault can be used as an adjuvant and to package a chemokine to activate the immune system.[42-44] Herein we report the feasibility of preparing smart vault nanoparticle conjugates by the synthesis of a vault-poly(*N*-isopropylacrylamide) conjugate (Scheme 2.1). The synthesis and characterization of responsive properties are described.

Scheme 2.1. Preparation of thermo-responsive vault-pNIPAAm conjugates. The vault image was adapted from cryoEM reconstructions of recombinant vaults. Cryo-EM reconstruction of the vault by P. Stewart, Case Western Reserve University, Department of Pharmacology.[29]

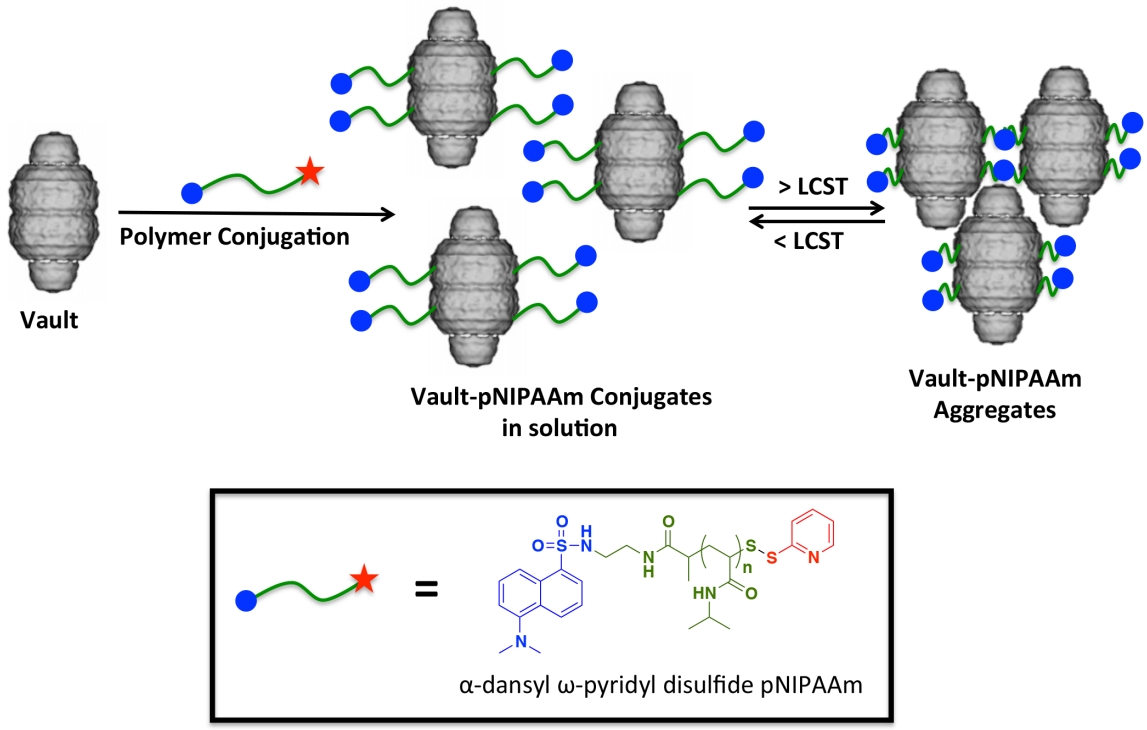

2.2. Results and Discussion

2.2.1. Polymer Synthesis

Our approach to developing thermo-responsive vault nanoparticles is based upon the conjugation of thiol-reactive pNIPAAm to cysteine-rich CP-MVP vaults. We and others have prepared cysteine-reactive polymers by reversible addition-fragmentation chain transfer (RAFT) polymerization.[45,46] RAFT is suitable for this application because it results in polymers with narrow molecular weight distributions.[47,48] Well-defined polymers are particularly important for this study because they exhibit sharp LCSTs. We chose to use a pyridyl-disulfide pNIPAAm in order to achieve reversible conjugation to the vault. We also introduced a dansyl group as a fluorophore at the other end group for ease of visualization.

The polymer was prepared as follows (Scheme 2.2). First, a dansyl-modified CTA was prepared by coupling *N*-(2-aminoethyl)-5-(dimethylamino) naphthalene-1-sulfonamide with 2-(((ethylthio)carbonothioyl)thio)propanoic acid. The product was obtained in 64% yield. This CTA was then utilized in the RAFT polymerization of NIPAAm with AIBN in DMF at 80 ºC. The polymerization was stopped after 1 h at 81% monomer conversion by ^{1}H NMR spectroscopy. **Polymer 1** was obtained after extensive dialysis against MeOH. The number-average molecular weight (M_n) was determined by ^{1}H NMR to be 12.4 kDa and the polydispersity index (PDI) by GPC was 1.02. The trithiocarbonate end-group of **polymer 1** was transformed into a cysteine reactive pyridyl-disulfide *via* aminolysis of the trithiocarbonate to the free thiol with ethanolamine, followed by an *in situ* disulfide exchange with Aldrithiol®. After dialysis of the reaction mixture against MeOH, the α-dansyl ω-pyridyl disulfide pNIPAAm, **polymer 2**, was obtained. Molecular weight analysis indicated that the polymer had not coupled during the end group transformation because the M_n and PDI (12.4 kDa and 1.03, respectively)

were the same as before the reaction. By comparing the integration of the peaks corresponding to the pyridyl disulfide to the dansyl group in the ^{1}H NMR spectrum, the conversion of the disulfide exchange was determined to be 81%.

Scheme 2.2. Synthesis of thiol-reactive pNIPAAm polymer for conjugation to the CP-MVP vault**.**

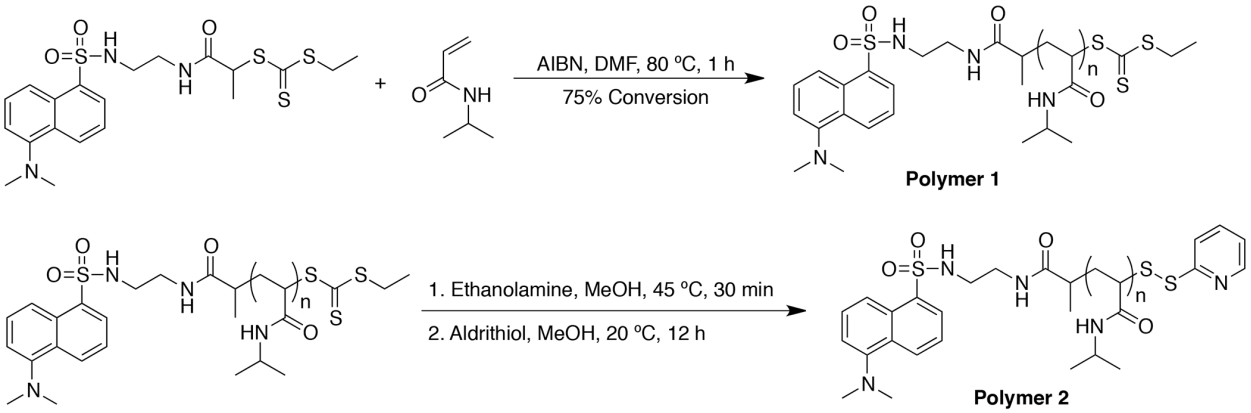

2.2.2. Vault Conjugation

Polymer 2 was conjugated to CP-MVP vault by incubating the CP-MVP vault at a ratio of 100:1 polymer:CP-MVP vault (Scheme 2.3). The resulting conjugate was analyzed by SDS-PAGE and compared to unmodified CP-MVP vault. Under non-reducing conditions there is a clear shift to higher molecular weight compared to the ~100 kDa CP-MVP vault (Figure 2.1.a., lanes 5 *versus* 4), and under reducing conditions, SDS-PAGE stained with Coomassie blue showed no difference in molecular weight as expected because of the reversibility of the disulfide bond of the polymer connection (Figure 2.1.a., lanes 2 and 3). Visualization of the gel with ultra-violet light confirmed conjugation; the dansyl fluorophore of the polymer appeared at

the same position (Figure 2.1b, lane 3) as the protein in the Coomassie stained gel (Figure 2.1a, lane 3). The results demonstrate that the conjugate with the CP-MVP vault was prepared and that the conjugation was reversible.

Scheme 2.3. Synthesis of CP-MVP vault-pNIPAAm conjugates.

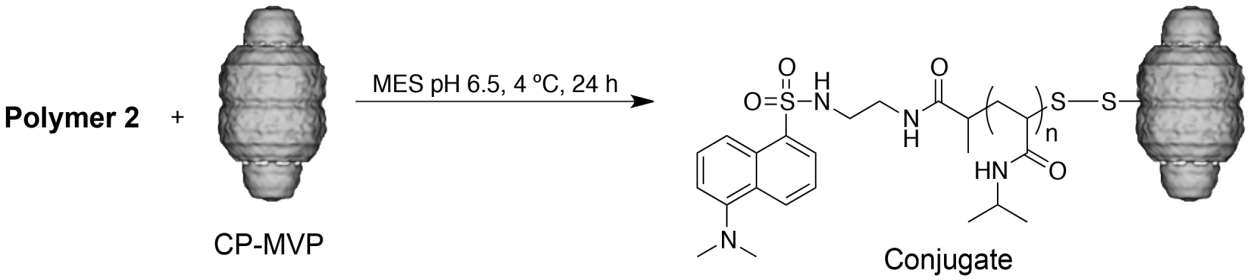

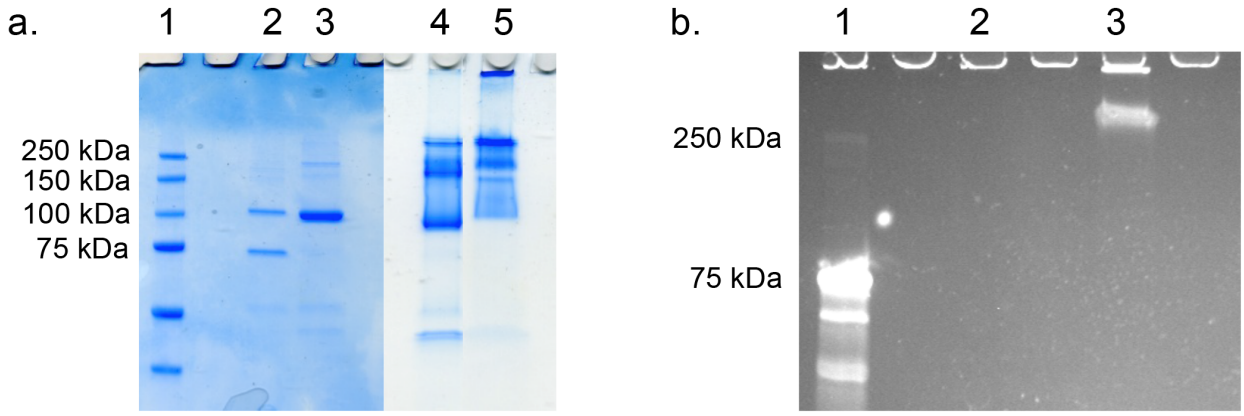

Figure 2.1. SDS-PAGE of CP-MVP vault and conjugate visualized by a) Coomassie blue staining (Lane 1: protein marker; Lane 2: CP-MVP vault reducing conditions; Lane 3: Conjugate reducing conditions; Lane 4: CP-MVP vault non-reducing conditions; Lane 5: Conjugate non-reducing conditions) and b) UV-Vis excitation (Lane 1: protein marker; Lane 2: CP-MVP vault under non-reducing conditions; Lane 3: Conjugate under non-reducing conditions).

2.2.3. Thermo-Responsive Properties of Vault-pNIPAAm Conjugates

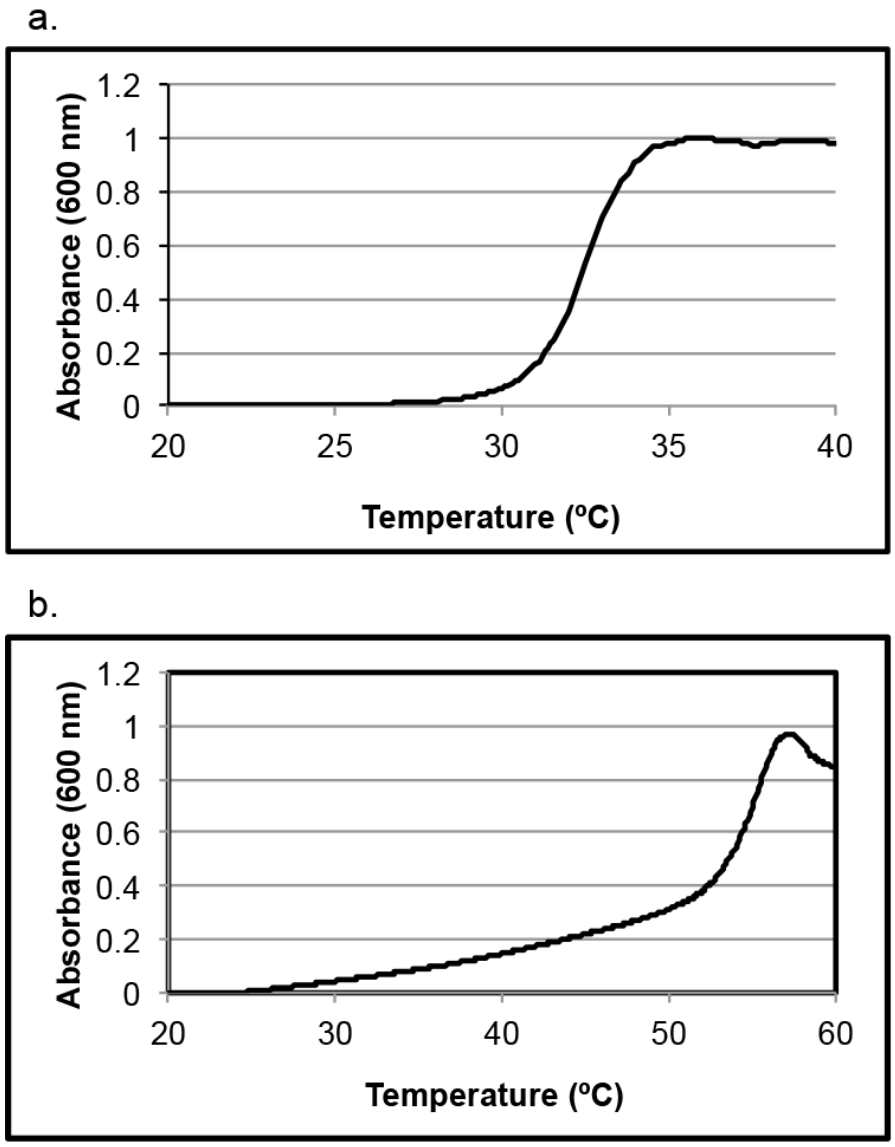

Figure 2.2. UV-Vis turbidity study of a) **polymer 2** and b) CP-MVP-vault-**polymer 2** conjugate. LCST is 10% of the maximum absorbance.

The thermo-responsive properties of the conjugate were studied by UV-Vis turbidity measurements. From UV-Vis turbidity studies (Figure 2.2), the LCST of **polymer 2** was

determined to be 30.5 ºC. The phase transition was sharp, as expected for a narrow molecular weight distribution polymer. The hydrophobic dansyl group lowered the LCST from the typical value of 32 ºC. Once the polymer was conjugated to the hydrophilic CP-MVP vault, the LCST was increased by the proximity of the hydrophilic protein to 35.9 ºC. The phase transition was broad, potentially due to a distribution of number of polymers and attachment sites. The vault itself had no LCST as expected (see experimental section, Figure 2.11); no visible aggregation of the vault structure was observed up to at least 50 ºC, indicating that the phase transition for the conjugate was due to the polymer. The results together confirmed that the polymer is covalently attached to the protein and that the polymer confers thermal responsiveness to the vault.

Dynamic light scattering (DLS) studies at different temperatures were performed to investigate the size of the conjugate (Figure 2.3). At 25 ºC, the conjugate closely resembled the unmodified CP-MVP vault (49.7 nm ± 2.2 nm, *versus* 48.69 nm ± 0.44 nm, respectively). However, upon heating above the LCST of the polymer to 40 ºC the conjugate aggregated into micron-sized particles, while the size of the unmodified CP-MVP vault at that temperature did not change (53.98 nm ± 5.0). Upon cooling, the observed aggregates disappeared and the conjugate returned to approximately its original size (58.76 nm ± 1.5 nm), thereby demonstrating that the aggregation was reversible.

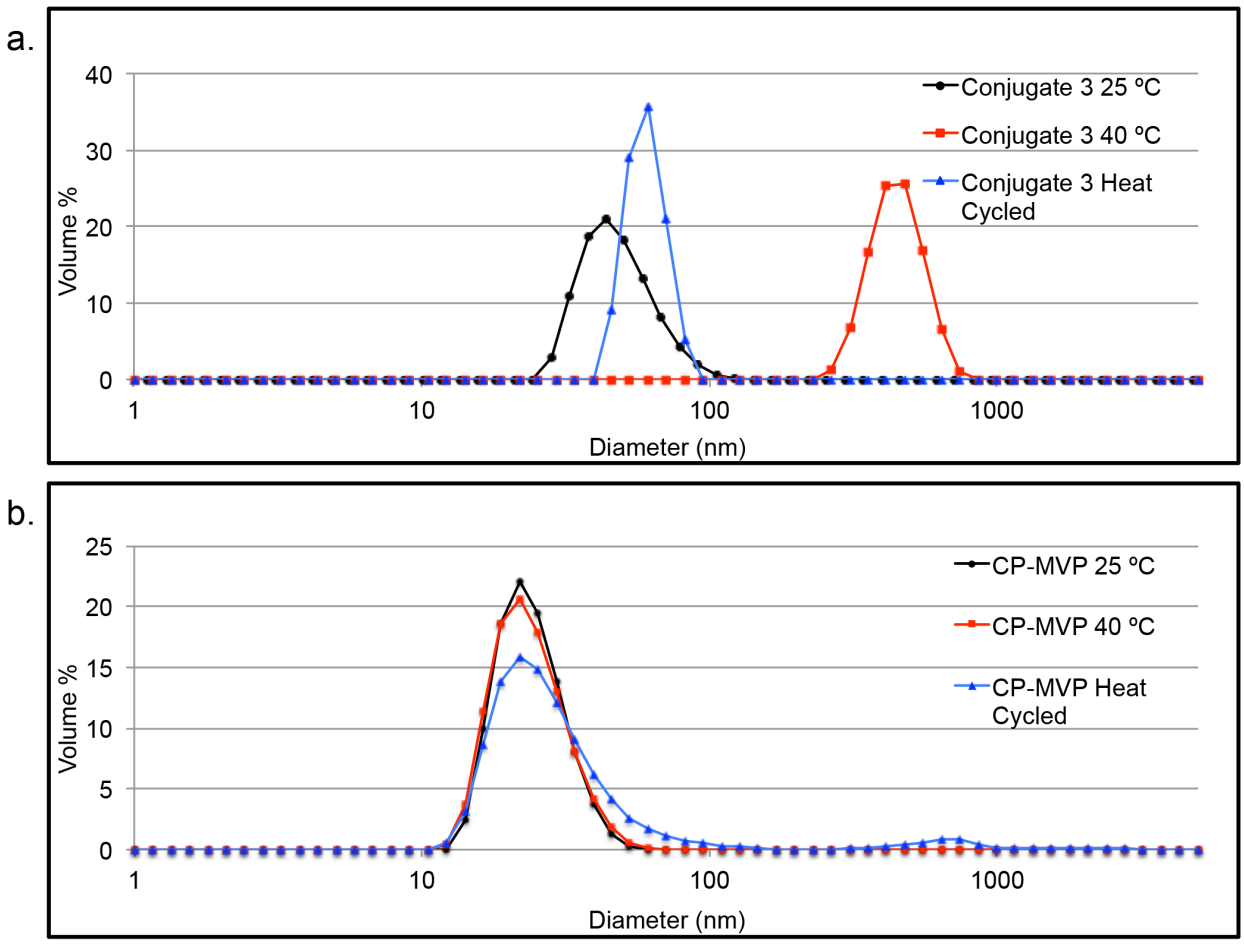

Figure 2.3. a) DLS analysis of conjugate at 25 ºC, 40 ºC, and heat cycled (25 ºC to 40 ºC to 25 ºC) conjugate cooled to 25 ºC. b) DLS analysis of unmodified CP-MVP vaults at 25 ºC, 40 ºC, and heat cycled (25 ºC to 40 ºC to 25 ºC).

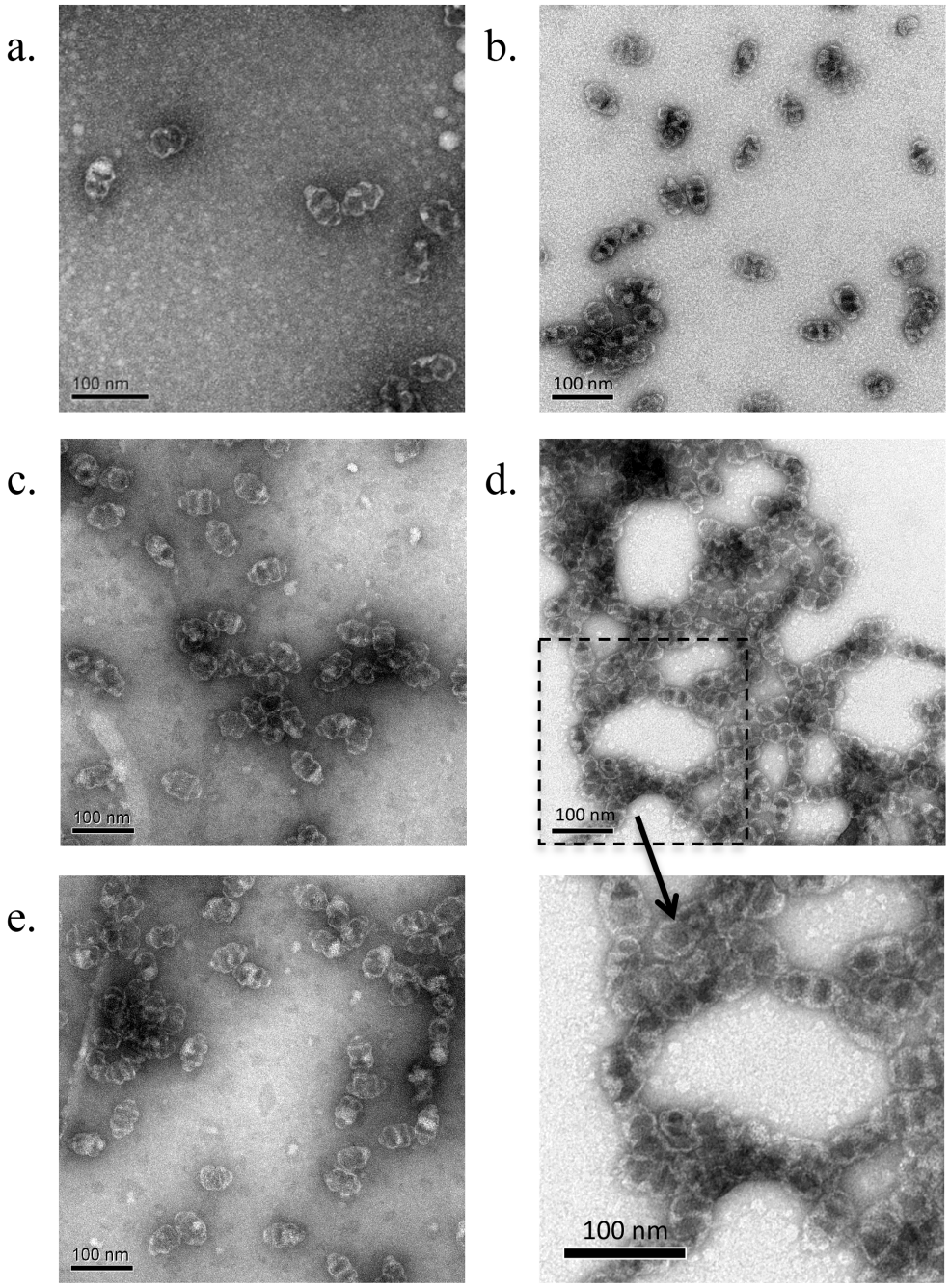

Figure 2.4. Negative stain TEM of unmodified CP-MVP vaults at a) 35 ºC and b) 45 ºC; **Polymer 2**-CP-MVP vault conjugates at c) 35 ºC, d) 45 ºC (lower right is blow up of 4d), e) after cooling back down to 4 ºC.

This result was further investigated by electron microscopy. EM images of the conjugate and unmodified CP-MVP vault at 35 ºC showed intact vault structures (Figure 2.4. a, c, respectively). This indicated that modification of CP-MVP vaults with **polymer 2** did not alter the vault structure. However, when the samples were heated above the LCST to 45 ºC, the conjugate appeared aggregated, yet with intact vault structures still recognizable within the aggregates (Figure 2.4.d), while the unmodified CP-MVP vault structures were unchanged (Figure 2.4.b). Again, when the conjugate was cooled back down to 4 ºC, the vault structures were no longer aggregated and looked the same as before heating (Figure 2.4.e).

The data together demonstrate that conjugation of the pNIPAAm does not interfere with or disrupt vault structure. Yet, the polymer once attached allows for reversible aggregation of vaults without destroying their structure. This result is interesting because it implies that cargo could be potentially loaded within the vault, while the polymer could be used to precipitate the vaults at a site of interest. It is well known that pNIPAAm can form aggregates at tumors while remaining soluble in other tissue due to the differential in temperatures between the cancerous and normal tissues.[49,50] An aggregating vault conjugate would potentially undergo similar selectivity, yet at the same time allow for protein or drug delivery from the vault nanocapsules. Drug loading and delivery within the vault is possible and has been demonstrated with vaults engineered to contain lipids.[39]

It is not known if the pNIPAAm is attached to the cysteine-rich region at the N-terminus in the interior or to free cysteines at the exterior. Upon examination of the crystal structure of the rat MVP,[33] there are six cysteines on the exterior of the vault, however but only all but one appear to be inaccessible on the surface accessible. Cysteine 356 may be exposed or at least partially exposed. CP-MVP is engineered to contain an additional four cysteines near the N-

terminus of the protein, which is in the interior of the vault. Due to the dynamic nature of the CP-MVP vaults, polymer should be able to enter the structure to react. Thus, the polymer is likely attached to both the exterior and interior. It also may be possible that polymer in the interior could thread out and participate in aggregation of the vaults. Our initial attempts to investigate the location(s) of the chains were to associate gold nanoparticles with polymers that had biotin groups instead of a dansyl (see the experimental section for polymer synthesis and conjugation). However, the location of the polymer was unclear. Cysteine mutagenesis experiments may provide the desired information. Nevertheless, it is clear from the results that attachment of the polymer to the vault does not disrupt the structure, as full vault structures were observed. We have also demonstrated the synthesis of conjugates with pNIPAAm that contain a fluorophore. This implies that other end groups could be prepared, and multifunctional vaults could be made with this strategy. Vaults are stable, non-immunogenic, readily engineered and expressed, making them a versatile platform for the development of sophisticated hybrid nanomaterials. Thus, we envision that the thermally-responsive vaults described herein are an interesting and versatile nanoplatform for drug delivery and other applications.

2.3. Experimental

2.3.1. Materials

Chemicals were purchased from Sigma-Aldrich, Fisher Scientific, and Acros. AIBN was recrystallized twice from acetone. NIPAAm was recrystallized twice from hexanes. 2-(((Ethylthio)carbonothioyl)thio)propanoic acid was synthesized according to a literature procedure.[51] *N*-(2-aminoethyl)-5-(dimethylamino) naphthalene-1-sulfonamide was synthesized according to a literature procedure.[52] Biotinylated CTA 2 was prepared following literature procedure.[22] Rat CP-MVP was expressed from a baculovirus system in *Sf9* insect cells, which do not contain endogenous vaults according to our literature procedure.[37]

2.3.2. Analytical Techniques

NMR spectra were obtained on Bruker 500 MHz ARX, 500 MHz DRX, and 600 MHZ DRX spectrometers. Proton NMR spectra were acquired with a relaxation delay of 2 sec for small molecules. Proton NMR spectra were acquired with a relaxation delay of 30 sec for all polymers. Mass spectra were obtained on a Waters LCT Premier with ACQUITY LC and autosampler. Infrared absorption spectra were recorded using a PerkinElmer FT-IR equipped with an ATR accessory. UV-Vis spectra were obtained on a Biomate 5 Thermo Spectronic UV-Vis spectrometer and a Hewlett-Packard HP8453 diode-array UV-Vis spectrophotometer with Peltier temperature control spectrometer with quartz cells. GPC was conducted on a Shimadzu HPLC system equipped with a refractive index detector RID-10A, one Polymer Laboratories PLgel guard column, and two Polymer Laboratories PLgel 5 μm mixed D columns. LiBr (0.1 M) in DMF at 40 °C was used as an eluent (flow rate: 0.80 mL/min). Calibration was performed using near-monodisperse PMMA standards from Polymer Laboratories. DLS was performed on a

Malvern Zetasizer Nano-S. SDS-PAGE was performed using Bio-Rad Any kD Mini-PROTEAN-TGX gels.

2.3.3. Methods

Scheme 2.4. Synthesis of the dansyl-trithiocarbonate CTA

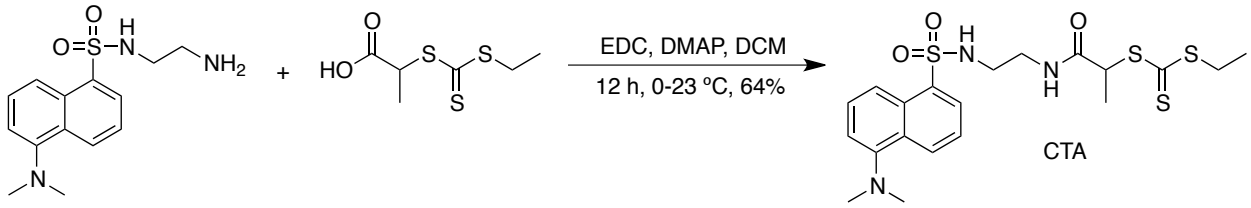

Synthesis of dansyl-trithiocarbonate CTA: *N*-(2-aminoethyl)-5-(dimethylamino) naphthalene-1-sulfonamide (dansyl amine) (0.62 g, 2.95 mmol) was dissolved in dry methylene chloride (80 mL) in a flame dried flask with a stirring bar and cooled to 0 ºC. *N*-(3-dimethylaminopropyl)-*N*'-ethylcarbodiimide (EDC) hydrochloride (0.46 g, 2.96 mmol) and 4-(dimethylamino)pyridine (DMAP) (0.04 g, 0.33 mmol) were added to the solution containing the dansyl amine and stirred for 1 h at 0 ºC. 2-(((Ethylthio)carbonothioyl)thio)propanoic acid (0.43, 1.47 mmol) was dissolved in 20 mL dry methylene chloride and added drop wise to the solution containing the dansyl amine, EDC, and DMAP. This solution was allowed to warm to room temperature and stirred for 12 h. Then the solution was washed 2 x 100 mL H_2O and 2 x 100 mL saturated $NaHCO_3$ solution. The organic layer was dried with $MgSO_4$, filtered, and solvent was removed *in vacuo*. The crude product was purified via silica gel chromatography using a 2:1 hexanes:ethyl acetate eluent. The resulting CTA was obtained in 64% yield. ^{1}H NMR (600 MHz, $CDCl_3$) δ: 8.54 (d, 8.53 Hz, 1H), 8.26 (d, 8.81 Hz, 1H), 8.21 (d, 5.87 Hz, 1H), 7.57 (t, 8.32 Hz, 1H), 7.51 (t,

7.83 Hz, 1H), 7.18 (d, 7.39 Hz, 1H), 6.65 (m, 1H), 5.51 (t, 6.11 Hz, 1H), 4.52 (q, 7.17 Hz, 1H), 4.11 (q, 7.17 Hz, 1H), 3.39-3.72 (m, 2H), 3.24-3.17 (m 1H), 3.06-2.96 (m, 2H), 2.88 (s, 6H), 1.45 (d, 6.99 Hz, 3H), 1.34 (t, 7.64 Hz, 3H). ^{13}C NMR (500 MHz, $CDCl_3$) δ: 223.64, 171.40, 152.08, 134.48, 130.65, 129.93, 129.63, 129.51, 128.65, 123.22, 118.66, 115.37, 48.16, 45.44, 42.90, 39.69, 31.88, 16.32, 12.90. IR: 3282, 2931, 2868, 2831, 2788, 2254, 1654, 1612, 1587, 1573, 1527, 1452, 1406, 1372, 1354, 1312, 1264, 1231, 1201, 1160, 1141, 1076, 1028, 943, 907, 876, 814, 787, 682 cm^{-1}. HRMS (ESI) calculated for $C_{20}H_{27}N_3O_3S_4$ $[M + H]^+$ 486.1013, found 486.1003.

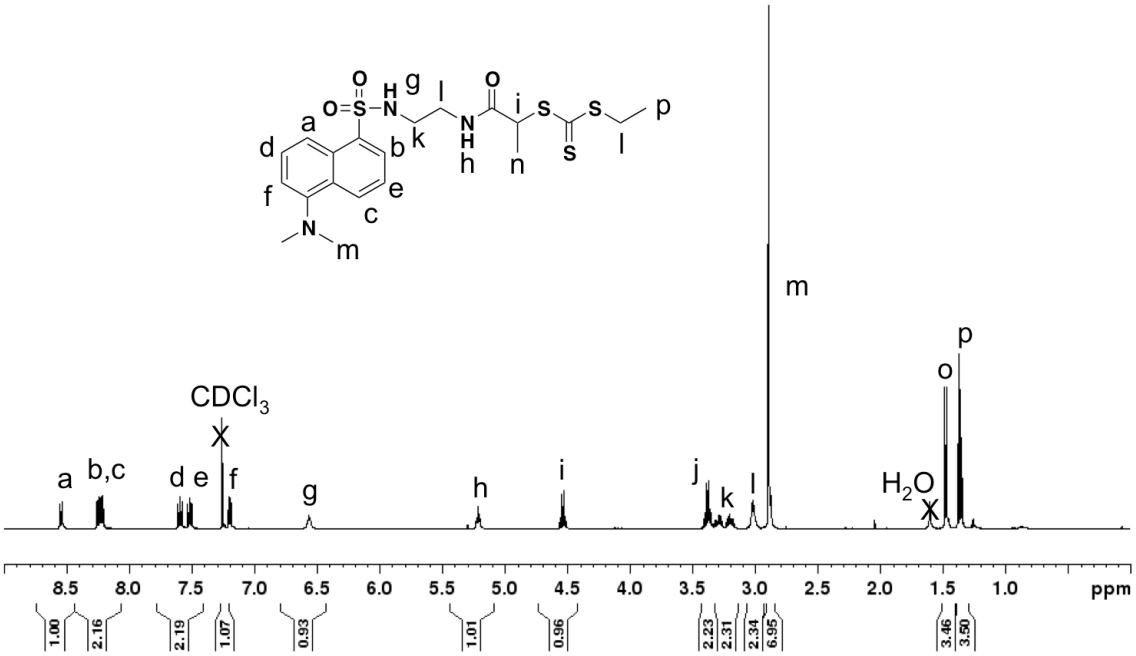

Figure 2.5. ^{1}H NMR (600 MHz, $CDCl_3$) of the dansyl-trithiocarbonate CTA.

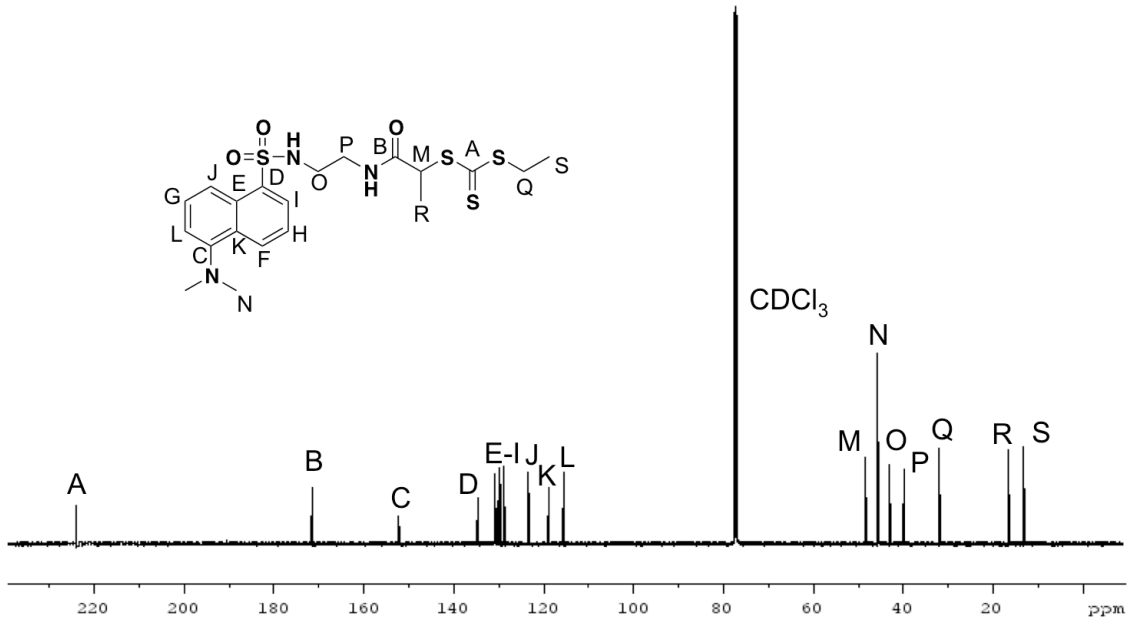

Figure 2.6. ^{13}C NMR (500 MHz, $CDCl_3$) of the dansyl-trithiocarbonate CTA.

Polymerization of NIPAAm in the presence of dansyl CTA to afford α-dansyl pNIPAAm: The dansyl CTA (46 mg, 0.095 mmol), NIPAAm (1.4 g, 12.0 mmol), and AIBN (1.6 mg, 0.0097 mmol) were added to a Schlenk tube containing a stirring bar, and DMF (1.9 mL) was added to dissolve the solids. Freeze-pump-thaw cycles were repeated five times and the reaction was performed at 70 ºC in an oil bath. The reaction was stopped after 1 h at 81% monomer conversion by cooling with liquid nitrogen and exposing the reaction to atmosphere. **Polymer 1** was purified by dialyzing against MeOH (MWCO 3,500 g/mol) giving the **α** -dansyl pNIPAAm. ^{1}H NMR (600 MHz, MeOD) δ: 8.55 (d), 8.36-8.28 (m), 8.24-8.15 (m), 8.12-7.35 (NH, pNIPAAM), 7.26 (d), 4.60 (s), 4.13-3.77 (bs), 3.43-3.23 (m), 2.86 (s), 2.25-1.80 (CH, pNIPAAm), 1.78-1.45 (CH_2, pNIPAAm), 1.26-0.93 (NCH_3, pNIPAAm). M_n by ^{1}H NMR was 12,400 g/mol (targeted 12,000 g/mol). M_n(GPC) was 14,200 g/mol and the PDI was 1.02.

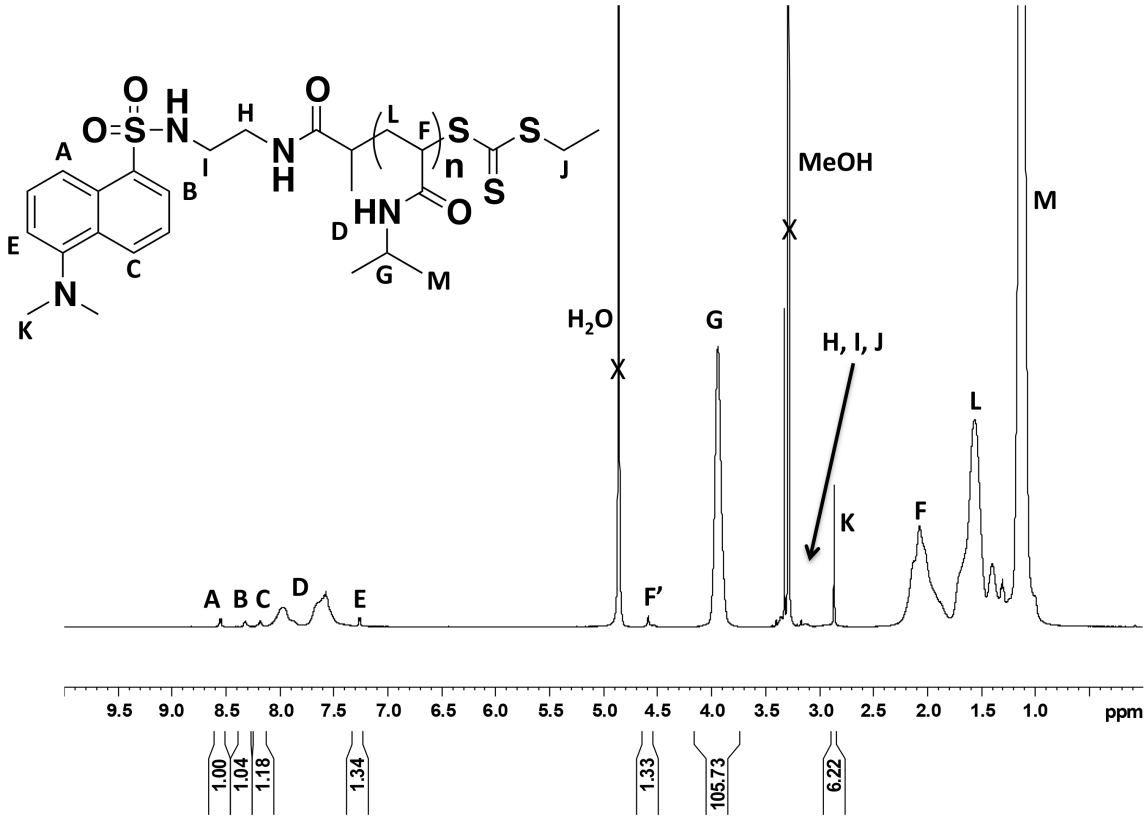

Figure 2.7. [1]H NMR (600 MHz, MeOD) of **polymer 1**.

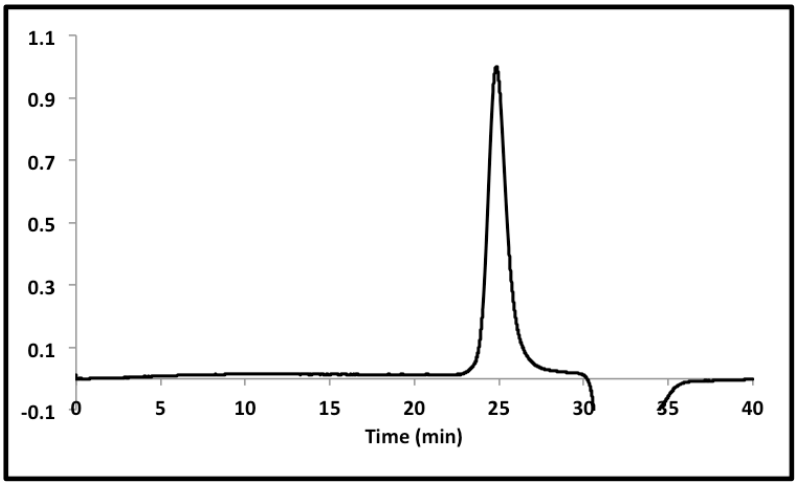

Figure 2.8. GPC chromatogram of **polymer 1,** normalized and analyzed by comparison with monodisperse PMMA standards.

In situ aminolysis and disulfide exchange of dansyl pNIPAAm with Aldrithiol® to form polymer 2: Polymer 1 (70 mg, 0.005 mmol) was added to a Schlenk tube equipped with a stirring bar and dissolved in MeOH (0.7 mL). In a second Schlenk tube equipped with a stirring bar, ethanolamine (14 μg, 0.230 μmol) was added. In a third Schlenk tube equipped with a stirring bar, Aldrithiol® (75 mg, 0.340 mmol) was dissolved in MeOH (0.7 mL). All three Schlenk tubes were subjected to five freeze-pump-thaw cycles. The contents of the first Schlenk tube, containing a-dansyl pNIPAAm and MeOH, were then transferred into the second Schlenk tube, containing ethanolamine, using a syringe. The second Schlenk tube was then immersed in an oil bath at 45 ºC and the solution was allowed to stir. After 30 min, the second Schlenk tube was removed from the oil bath and the contents, dansyl pNIPAAm, MeOH, and ethanolamine, were transferred to the third Schlenk tube, containing Aldrithiol and MeOH, via syringe. The third Schlenk tube containing dansyl pNIPAAm, ethanolamine, Aldrithiol® and MeOH was stirred at 20 ºC for 12 h. The product was purified by dialyzing against MeOH (MWCO 3,500 g/mol) giving **polymer 2**. End-group conversion of the trithiocarbonate to a pyridyl disulfide was 81% by ^{1}H-NMR. ^{1}H NMR (600 MHz, MeOD) δ: 8.55 (d, Ar CH), 8.40-8.27 (m, Ar CH), 8.24-8.14 (NH, pNIPAAm), 7.26 (Ar CH), 7.22-7.15 (Ar CH), 3.95 (CH_3, pNIPAAm), 3.45-3.20 (CH_2CH_2), 2.87 (NCH_3), 2.34-1.76 (CH, pNIPAAm), 1.76-1.46 (CH_2, pNIPAAM), 1.26-1.20 (NCH_3, pNIPAAm). M_n (^{1}H NMR) = 12,400 g/mol; M_n (GPC) = 14,200 g/mol; PDI = 1.03.

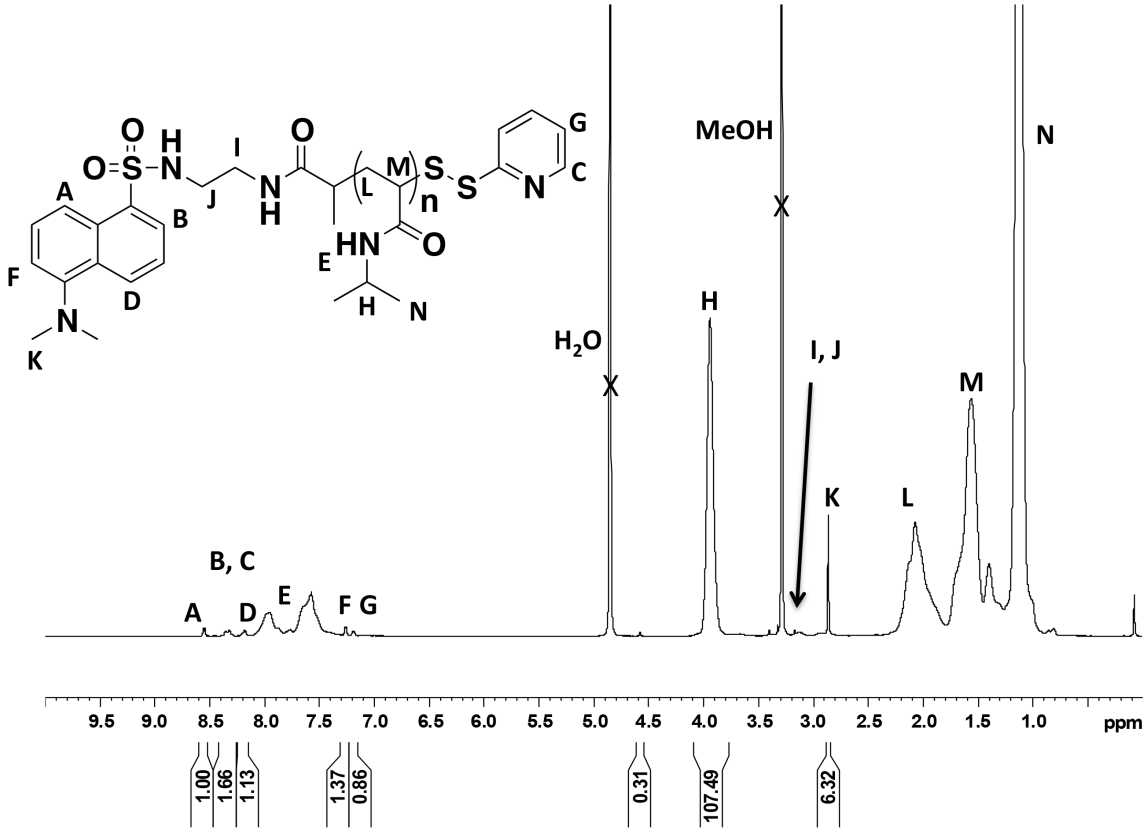

Figure 2.9. ^{1}H NMR (600 MHz, MeOD) of **polymer 2**.

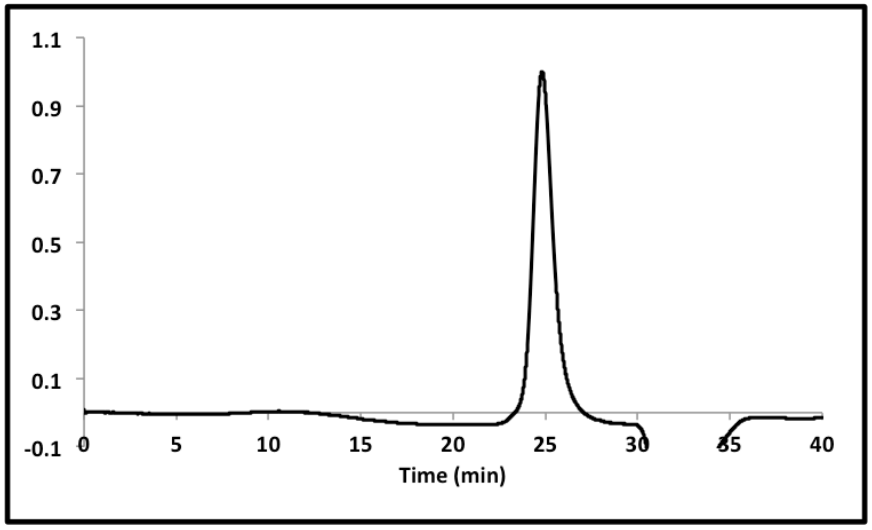

Figure 2.10. GPC chromatogram of **polymer 2**, normalized and analyzed by comparison with monodisperse PMMA standards.

pNIPAAm conjugation to CP-MVP: A pH 6.5 20 mM 2-(*N*-morpholino) ethanesulfonic acid) (MES) buffer was degassed with argon gas for 30 min. CP-MVP (0.50 mg, 0.05 μmol) in 250 μL buffer was treated with triscarboxylethylphosphine (TCEP) resin for 2 h at 4 ºC, then filtered through a 0.22 μm syringe filter. **Polymer 2** (6.20 mg, 5.00 μmol) was dissolved in 250 μL of buffer. The filtered CP-MVP solution was added to the solution containing **polymer 2**. The reaction was allowed to stand at 4 ºC for 24 h before purification by ultrafiltration (MWCO 100,000 g/mol) to give the conjugate.

LCST determination: A solution of the polymer, conjugate, or unmodified CP-Vault-pNIPAAm conjugate at a concentration of 1 mg mL^{-1} in pH 6.5 20 mM MES was placed in a 100 μL quartz cuvette. The cuvette was placed in a Hewlett-Packard HP8453 diode-array UV-Vis spectrophotometer with Peltier temperature control. The following temperature program was used: temperature was elevated at 0.5 ºC min^{-1} and held for 30 s prior to measuring the absorbance at 600 nm. The LCST was determined at 10% of the maximum absorbance. The LCST was reported as the average of three experiments.

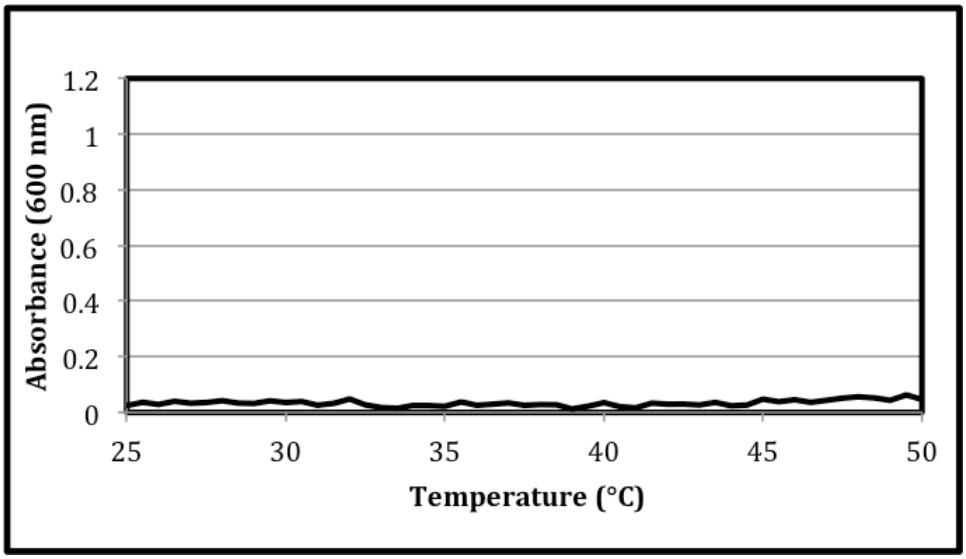

Figure 2.11. UV-Vis turbidity study of unmodified CP-MVP vaults. No LCST observed.

DLS size determination: A solution of CP-Vault-pNIPAAm conjugate at a concentration of 1 mg mL^{-1} in pH 6.5, 20 mM MES was placed in a 40 μL disposable cuvette. The cuvette was placed in a Malvern Zetasizer Nano-S. The temperature was allowed to equilibrate for three minutes before beginning the DLS measurement. This process was repeated three times, and sizes are reported as an average of three measurements.

Preparation of the TEM sample: A 40 μL aliquot of a 0.2 μg μL^{-1} solution of CP-Vault-pNIPAAm conjugate was warmed to a set temperature (35 ºC or 45 ºC or heated to 45 ºC then cooled to 4 ºC) and incubated for 7 min. 20 μL of each solution was then pipetted onto the surface of a heating block at the set temperature. A carbon-coated EM grid was floated up-side down on the sample to allow the conjugate to adsorb to the grid surface. After 7 min, the grid was removed from the sample and blotted on filter paper to remove excess liquid. The grid was then floated up-side down in 500 μL of a 1% uranyl acetate solution at the set temperatures.

After 7 min, the grid was removed from the uranyl acetate solution and blotted on filter paper. TEM was conducted on a JEOL JEM1200-EX transmission electron microscope. Images were taken using a Gatan BioScan 600W 1 x 1K digital camera and Digital Micrograph acquisition software.

Scheme 2.5. Synthesis of Biotinylated pNIPAAm **polymer 3.**

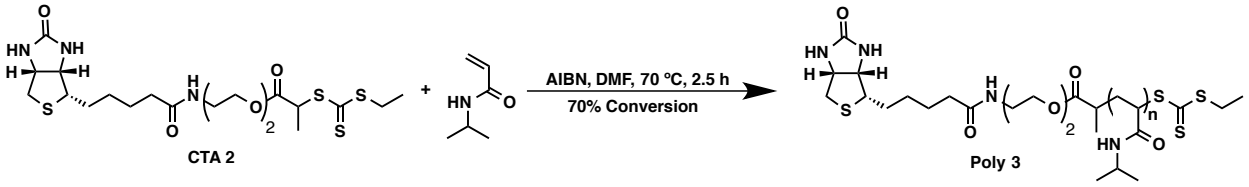

*Polymerization of NIPAAm in the presence of **CTA 2** to afford biotin-pNIPAAm (**polymer 3**):* Biotinylated CTA (46.1 mg, 0.880 mmol), AIBN (1.45 mg, 0.0883 mmol), and NIPAAm (0.996 g, 8.80 mmol) were loaded into a Schlenk tube. DMF (1.76 mL) was added to give a 50 mM solution of **CTA 2**, and then the flask was subjected to four freeze-pump-thaw cycles under argon. Immersion of the Schlenk tube into a 70 °C oil bath initiated the polymerization. After 2.5 h (70.0 % conversion) the reaction flask was removed from the oil bath and opened to the atmosphere to give crude **poly3**. The polymer was purified by dialysis against 1/1 EtOAc/MeOH (MWCO 2,000 Da). Polymer conversions were calculated from the ^{1}H NMR spectra by averaging of the integrations of the vinylic proton peaks of NIPAAm and the peak at 3.89 ppm (NC**H**$(CH_3)_2$ of pNIPAAm and NIPAAm in MeOD). ^{1}H NMR (500 MHz, D_2O) δ: 8.11-7.46 (NH), 4.61-4.59, 4.42-4.40 (CH), 4.30-4.20 (CH), 3.89 ($CHMe_2$), 3.4-3.26, 3.19 (CH), 3.00-2.88 (CH), 2.78-2.76 (CH), 2.27-2.25, 2.12-2.00 (CHC=O), 1.70-1.45 (CH_2), 1.33-1.32, 1.14 (CH_3). M_n(^{1}H NMR) = 16,000 g/mol. M_n (GPC) = 14,920 g/mol. PDI (GPC) = 1.09.

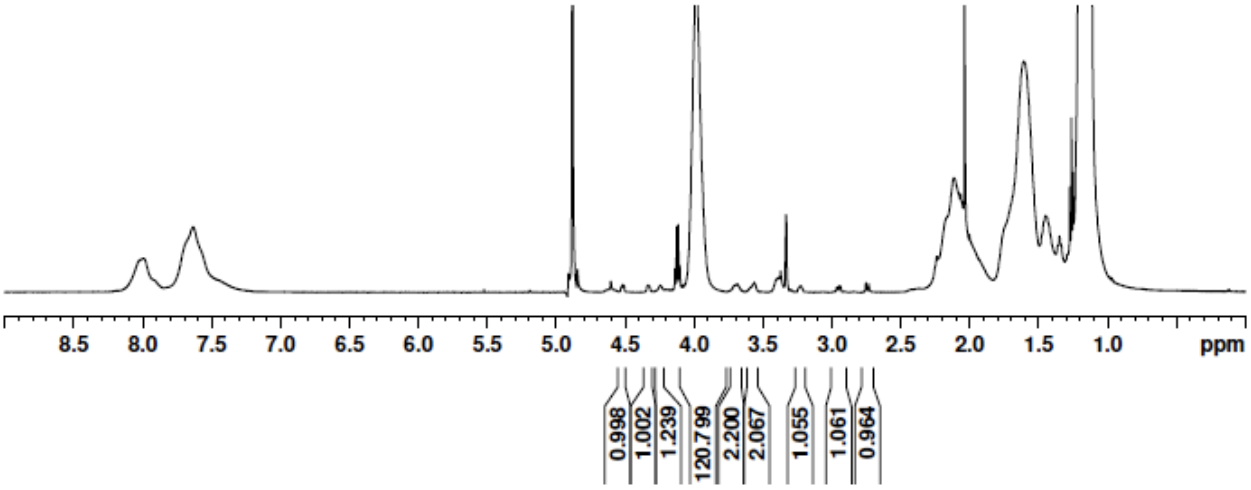

Figure 2.12. ^{1}H NMR (500 MHz, D_2O) of **poly 3**.

Scheme 2.6. Aminolysis and *in situ* disulfide exchange with Aldrithiol® of **polymer 3** to yield **polymer 4**.

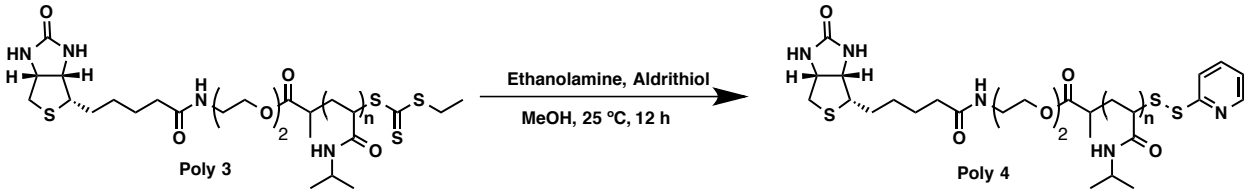

*Aminolysis and in situ conjugation of **polymer 3** with Aldrithiol® to afford Biotin-pNIPAAm-Pyridyl Disulfide (**polymer 4**)*: **poly3** (0.111 g, 0.069 mmol) and Aldrithiol® (0.761 g, 3.36 mmol) were dissolved in MeOH (3.45 mL) in Schlenk tube 1. 2-Aminoethanol (0.021 mg, 0.344 mmol) was dissolved in MeOH (3.45 mL) in Schlenk tube 2. Both tubes were subjected to three freeze-pump-thaw cycles under argon. The contents of tube 2 were added to tube 1, and stirred for 12 h at 25 ºC. The polymer was purified by dialysis against 1/1 EtOAc/MeOH (MWCO 2,000 Da). End group retention was determined *via* ^{1}H-NMR, by comparing the integration of

the peaks at 8.41 ppm, which correspond the ω-pyridine group to the peaks at 4.53 and 4.33 ppm, which correspond to the α-biotin end group. M_n (^{1}H NMR) = 16000 g/mol. M_n (0.1 M LiBr DMF GPC): 15,179. PDI = 1.10.

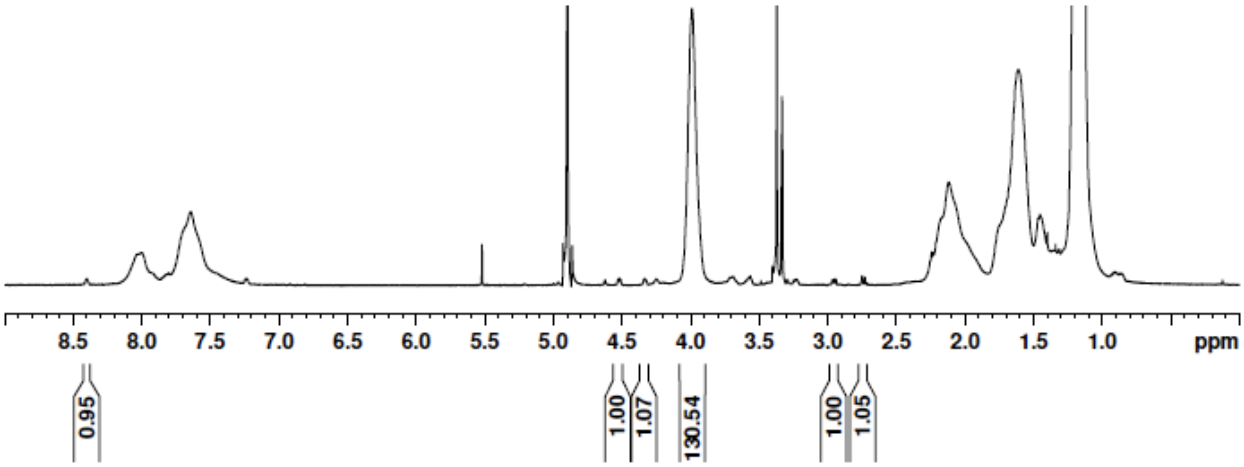

Figure 2.13. ^{1}H NMR (500 MHz, D_2O) of **polymer 4**.

*Typical Conjugation of **polymer 4** to CP-MVP*: A solution of CP-MVP (350 µg, 3.65 µmol) in 20mM MES pH 6.5 buffer (170 µL) was added to a solution of **poly3** (5.25 mg, 0.328 mmol) in 20 mM MES pH 6.5 buffer (180 µL) to bring the final concentration of protein in solution to 1 mg/ml. This solution was allowed to stand at 4 ºC for 24 h. The pNIPAAm-CP-MVP conjugate was purified by centrifuge filtration (MWCO 50000 Da). Conjugates were analyzed by SDS-PAGE under reducing and non-reducing conditions.

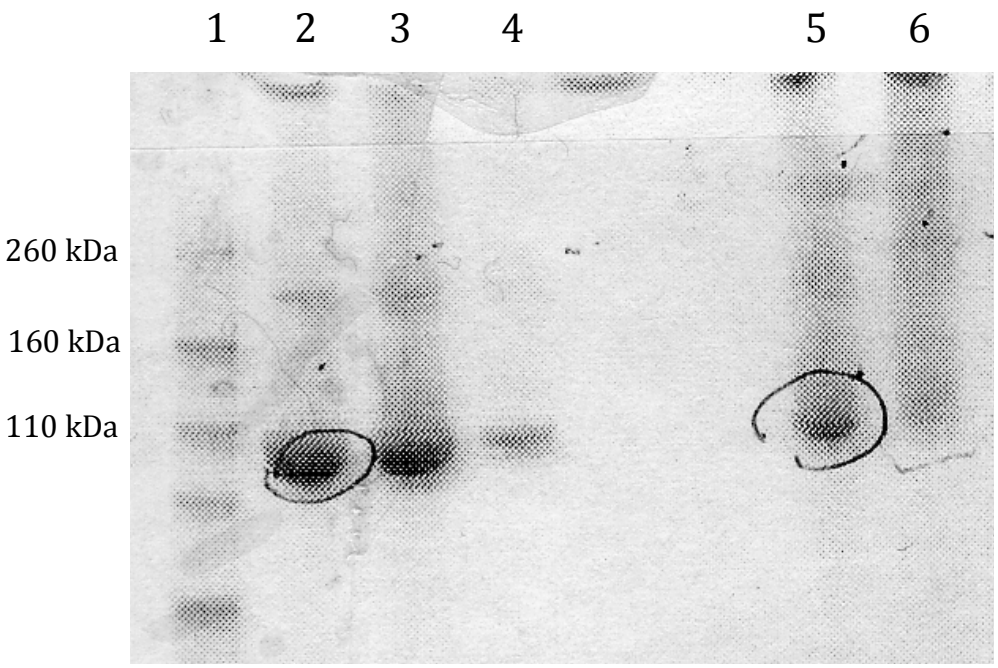

Figure 2.14. SDS PAGE Lane 1: Protein Marker; Lane 2: CP-MVP (reducing); Lane 3: CP-MVP-**poly4** conjugate (reducing 5 μg); Lane 4: CP-MVP-**poly4** conjugate (reducing, 2 μg); Lane 5: CP-MVP; Lane 6: CP-MVP-**poly4** conjugate.

2.4. Conclusions

Novel biohybrid nanoparticles have been synthesized through covalent conjugation of pNIPAAm to recombinant CP-MVP vaults. Pyridyl disulfide pNIPAAm with a dansyl group at the other end group were conjugated to CP-MVP vaults *via* reaction with free cysteines. The resulting conjugates were thermally-responsive. UV-Vis turbidity measurements showed that the conjugates had an LCST of 35.9 ºC. DLS studies demonstrated that upon heating, aggregates formed, which were reversible with upon cooling. This result was confirmed by EM studies, whereby reversible aggregation of polymer-modified vaults was observed, while the vault nanocapsules remained intact regardless of the temperature. We envision that these smart vault conjugates may be used for drug delivery applications in conjunction with previously reported vault based hydrophobic drug delivery methods and hyperthermia therapy, which is an *in vivo* localized heating technique,[39,53,54] to build up depots of therapeutic drugs in tumors for a sustained release of drugs to tumor cells and other interesting medical and biotechnology applications.

2.5 References

†Portions of Chapter 2 have been published as: Matsumoto, N. M.; Prabhakaran, P.; Rome, L. H.; Maynard, H. D. Smart Vaults: Thermally-Responsive Protein Nanocapsules. *ACS Nano* **2013**, *7*, 867-874.

1. Douglas, T.; Young, M. Virus Particles as Templates for Materials Synthesis. *Adv. Mater.* **1999**, *11*, 679-681.
2. Witus, L. S.; Francis, M. B. Using Synthetically Modified Proteins to Make New Materials. *Acc. Chem. Res.* **2011**, *44*, 774-783.
3. Lee, L. A.; Niu, Z. W.; Wang, Q. Viruses and Virus-Like Protein Assemblies-Chemically Programmable Nanoscale Building Blocks. *Nano Res.* **2009**, *2*, 349-364.
4. Uchida, M.; Klem, M. T.; Allen, M.; Suci, P.; Flenniken, M.; Gillitzer, E.; Varpness, Z.; Liepold, L. O.; Young, M.; Douglas, T. Biological Containers: Protein Cages as Multifunctional Nanoplatforms. *Adv. Mater.* **2007**, *19*, 1025-1042.
5. Soto, C. M.; Ratna, B. R. Virus Hybrids as Nanomaterials for Biotechnology. *Curr. Opin. Biotechnol.* **2010**, *21*, 426-438.
6. Jutz, G.; Boker, A. Bionanoparticles as Functional Macromolecular Building Blocks - a New Class of Nanomaterials. *Polymer* **2011**, *52*, 211-232.
7. Steinmetz, N. F.; Evans, D. J. Utilisation of Plant Viruses in Bionanotechnology. *Org. Biomol. Chem.* **2007**, *5*, 2891-2902.
8. Endo, M.; Fujitsuka, M.; Majima, T. Porphyrin Light-Harvesting Arrays Constructed in the Recombinant Tobacco Mosaic Virus Scaffold. *Chem.-Eur. J.* **2007**, *13*, 8660-8666.

9. Nam, K. T.; Kim, D.-W.; Yoo, P. J.; Chiang, C.-Y.; Meethong, N.; Hammond, P. T.; Chiang, Y.-M.; Belcher, A. M. Virus-Enabled Synthesis and Assembly of Nanowires for Lithium Ion Battery Electrodes. *Science* **2006**, *312*, 885-888.

10. MaHam, A.; Tang, Z. W.; Wu, H.; Wang, J.; Lin, Y. H. Protein-Based Nanomedicine Platforms for Drug Delivery. *Small* **2009**, *5*, 1706-1721.

11. Manchester, M.; Singh, P. Virus-Based Nanoparticles (Vnps): Platform Technologies for Diagnostic Imaging. *Adv. Drug Deliv. Rev.* **2006**, *58*, 1505-1522.

12. Ma, Y. J.; Nolte, R. J. M.; Cornelissen, J. Virus-Based Nanocarriers for Drug Delivery. *Adv. Drug Deliv. Rev.* **2012**, *64*, 811-825.

13. Garcea, R. L.; Gissmann, L. Virus-Like Particles as Vaccines and Vessels for the Delivery of Small Molecules. *Curr. Opin. Biotechnol.* **2004**, *15*, 513-517.

14. Raja, K. S.; Wang, Q.; Gonzalez, M. J.; Manchester, M.; Johnson, J. E.; Finn, M. G. Hybrid Virus-Polymer Materials. 1. Synthesis and Properties of Peg-Decorated Cowpea Mosaic Virus. *Biomacromolecules* **2003**, *4*, 472-476.

15. Schlick, T. L.; Ding, Z.; Kovacs, E. W.; Francis, M. B. Dual-Surface Modification of the Tobacco Mosaic Virus. *J. Am. Chem. Soc.* **2005**, *127*, 3718-3723.

16. O'Riordan, C. R.; Lachapelle, A.; Delgado, C.; Parkes, V.; Wadsworth, S. C.; Smith, A. E.; Francis, G. E. Pegylation of Adenovirus with Retention of Infectivity and Protection from Neutralizing Antibody in Vitro and in Vivo. *Hum. Gene Ther.* **1999**, *10*, 1349-1358.

17. Sikkema, F. D.; Comellas-Aragones, M.; Fokkink, R. G.; Verduin, B. J. M.; Cornelissen, J. J. L. M.; Nolte, R. J. M. Monodisperse Polymer-Virus Hybrid Nanoparticles. *Org. Biomol. Chem.* **2007**, *5*, 54-57.

18. Lucon, J.; Qazi, S.; Uchida, M.; Bedwell, G. J.; LaFrance, B.; Prevelige, P. E.; Douglas, T. Use of the Interior Cavity of the P22 Capsid for Site-Specific Initiation of Atom-Transfer Radical Polymerization with High-Density Cargo Loading. *Nat. Chem.* **2012**, *4*, 781-788.

19. Alarcon, C. d. l. H.; Pennadam, S.; Alexander, C. Stimuli Responsive Polymers for Biomedical Applications. *Chem. Soc. Rev.* **2005**, *34*, 276-285.

20. Antipina, M. N.; Sukhorukov, G. B. Remote Control over Guidance and Release Properties of Composite Polyelectrolyte Based Capsules. *Adv. Drug Deliv. Rev.* **2011**, *63*, 716-729.

21. Chang, C.-W.; Nguyen, T. H.; Maynard, H. D. Thermoprecipitation of Glutathione S-Transferase by Glutathione-Poly(N-Isopropylacrylamide) Prepared by Raft Polymerization. *Macromol. Rapid Commun.* **2010**, *31*, 1691-1695.

22. Heredia, K. L.; Grover, G. N.; Tao, L.; Maynard, H. D. Synthesis of Heterotelechelic Polymers for Conjugation of Two Different Proteins. *Macromolecules* **2009**, *42*, 2360-2367.

23. Tao, L.; Kaddis, C. S.; Loo, R. R. O.; Grover, G. N.; Loo, J. A.; Maynard, H. D. Synthesis of Maleimide-End-Functionalized Star Polymers and Multimeric Protein-Polymer Conjugates. *Macromolecules* **2009**, *42*, 8028-8033.

24. Vazquez-Dorbatt, V.; Tolstyka, Z. P.; Maynard, H. D. Synthesis of Aminooxy End-Functionalized Pnipaam by Raft Polymerization for Protein and Polysaccharide Conjugation. *Macromolecules* **2009**, *42*, 7650-7656.

25. Hoffman, A. S.; Stayton, P. S. Conjugates of Stimuli-Responsive Polymers and Proteins. *Prog. Polym. Sci.* **2007**, *32*, 922-932.

26. Gauthier, M. A.; Klok, H. A. Polymer-Protein Conjugates: An Enzymatic Activity Perspective. *Polym. Chem.* **2010**, *1*, 1352-1373.

27. Heredia, K. L.; Bontempo, D.; Ly, T.; Byers, J. T.; Halstenberg, S.; Maynard, H. D. In Situ Preparation of Protein - "Smart" Polymer Conjugates with Retention of Bioactivity. *J. Am. Chem. Soc.* **2005**, *127*, 16955-16960.

28. Hoffman, A. S.; Stayton, P. S.; Bulmus, V.; Chen, G. H.; Chen, J. P.; Cheung, C.; Chilkoti, A.; Ding, Z. L.; Dong, L. C.; Fong, R.; Lackey, C. A.; Long, C. J.; Miura, M.; Morris, J. E.; Murthy, N.; Nabeshima, Y.; Park, T. G.; Press, O. W.; Shimoboji, T.; Shoemaker, S.; Yang, H. J.; Monji, N.; Nowinski, R. C.; Cole, C. A.; Priest, J. H.; Harris, J. M.; Nakamae, K.; Nishino, T.; Miyata, T. Really Smart Bioconjugates of Smart Polymers and Receptor Proteins. *J. Biomed. Mater. Res.* **2000**, *52*, 577-586.

29. Poderycki, M. J.; Kickhoefer, V. A.; Kaddis, C. S.; Raval-Fernandes, S.; Johansson, E.; Zink, J. I.; Loo, J. A.; Rome, L. H. The Vault Exterior Shell Is a Dynamic Structure That Allows Incorporation of Vault-Associated Proteins into Its Interior. *Biochemistry* **2006**, *45*, 12184-12193.

30. Kedersha, N. L.; Rome, L. H. Isolation and Characterization of a Novel Ribonucleoprotein Particle - Large Structures Contain a Single Species of Small Rna. *J. Cell Biol.* **1986**, *103*, 699-709.

31. Kedersha, N. L.; Miquel, M. C.; Bittner, D.; Rome, L. H. Vaults .2. Ribonucleoprotein Structures Are Highly Conserved among Higher and Lower Eukaryotes. *J. Cell Biol.* **1990**, *110*, 895-901.

32. Suprenant, K. A. Vault Ribonucleoprotein Particles: Sarcophagi, Gondolas, or Safety Deposit Boxes? *Biochemistry* **2002**, *41*, 14447-14454.

33. Kong, L. B.; Siva, A. C.; Rome, L. H.; Stewart, P. L. Structure of the Vault, a Ubiquitous Cellular Component. *Struct. Fold. Des.* **1999**, *7*, 371-379.

34. Tanaka, H.; Kato, K.; Yamashita, E.; Sumizawa, T.; Zhou, Y.; Yao, M.; Iwasaki, K.; Yoshimura, M.; Tsukihara, T. The Structure of Rat Liver Vault at 3.5 Angstrom Resolution. *Science* **2009**, *323*, 384-388.

35. Kedersha, N. L.; Heuser, J. E.; Chugani, D. C.; Rome, L. H. Vaults .3. Vault Ribonucleoprotein-Particles Open into Flower-Like Structures with Octagonal Symmetry. *J. Cell Biol.* **1991**, *112*, 225-235.

36. Stephen, A. G.; Raval-Fernandes, S.; Huynh, T.; Torres, M.; Kickhoefer, V. A.; Rome, L. H. Assembly of Vault-Like Particles in Insect Cells Expressing Only the Major Vault Protein. *J. Biol. Chem.* **2001**, *276*, 23217-23220.

37. Kickhoefer, V. A.; Garcia, Y.; Mikyas, Y.; Johansson, E.; Zhou, J. C.; Raval-Fernandes, S.; Minoofar, P.; Zink, J. I.; Dunn, B.; Stewart, P. L.; Rome, L. H. Engineering of Vault Nanocapsules with Enzymatic and Fluorescent Properties. *P. Natl. Acad. Sci. U.S.A.* **2005**, *102*, 4348-4352.

38. Kickhoefer, V. A.; Han, M.; Raval-Fernandes, S.; Poderycki, M. J.; Moniz, R. J.; Vaccari, D.; Silvestry, M.; Stewart, P. L.; Kelly, K. A.; Rome, L. H. Targeting Vault Nanoparticles to Specific Cell Surface Receptors. *ACS Nano* **2009**, *3*, 27-36.

39. Buehler, D. C.; Toso, D. B.; Kickhoefer, V. A.; Zhou, Z. H.; Rome, L. H. Vaults Engineered for Hydrophobic Drug Delivery. *Small* **2011**, *7*, 1432-1439.

40. Goldsmith, L. E.; Pupols, M.; Kickhoefer, V. A.; Rome, L. H.; Monbouquette, H. G. Utilization of a Protein "Shuttle" to Load Vault Nanocapsules with Gold Probes and Proteins. *ACS Nano* **2009**, *3*, 3175-3183.

41. Ng, B. C.; Yu, M.; Gopal, A.; Rome, L. H.; Monbouquette, H. G.; Tolbert, S. H. Encapsulation of Semiconducting Polymers in Vault Protein Cages. *Nano Lett.* **2008**, *8*, 3503-3509.

42. Champion, C. I.; Kickhoefer, V. A.; Liu, G. C.; Moniz, R. J.; Freed, A. S.; Bergmann, L. L.; Vaccari, D.; Raval-Fernandes, S.; Chan, A. M.; Rome, L. H.; Kelly, K. A. A Vault Nanoparticle Vaccine Induces Protective Mucosal Immunity. *Plos One* **2009**, *4*, e5409.

43. Kar, U. K.; Jiang, J. N.; Champion, C. I.; Salehi, S.; Srivastava, M.; Sharma, S.; Rabizadeh, S.; Niazi, K.; Kickhoefer, V.; Rome, L. H.; Kelly, K. A. Vault Nanocapsules as Adjuvants Favor Cell-Mediated over Antibody-Mediated Immune Responses Following Immunization of Mice. *Plos One* **2012**, *7*, e38553.

44. Kar, U. K.; Srivastava, M. K.; Andersson, A.; Baratelli, F.; Huang, M.; Kickhoefer, V. A.; Dubinett, S. M.; Rome, L. H.; Sharma, S. Novel Ccl21-Vault Nanocapsule Intratumoral Delivery Inhibits Lung Cancer Growth. *Plos One* **2011**, *6*, e18758.

45. Boyer, C.; Bulmus, V.; Davis, T. P.; Ladmiral, V.; Liu, J.; Perrier, S. Bioapplications of Raft Polymerization. *Chem. Rev.* **2009**, *109*, 5402-5436.

46. Grover, G. N.; Maynard, H. D. Protein-Polymer Conjugates: Synthetic Approaches by Controlled Radical Polymerizations and Interesting Applications. *Curr. Opin. Chem. Biol.* **2010**, *14*, 818-827.

47. Chiefari, J.; Chong, Y. K.; Ercole, F.; Krstina, J.; Jeffery, J.; Le, T. P. T.; Mayadunne, R. T. A.; Meijs, G. F.; Moad, C. L.; Moad, G.; Rizzardo, E.; Thang, S. H. Living Free-Radical Polymerization by Reversible Addition-Fragmentation Chain Transfer: The Raft Process. *Macromolecules* **1998**, *31*, 5559-5562.

48. Moad, G.; Rizzardo, E.; Thang, S. H. Living Radical Polymerization by the Raft Process. *Aust. J. Chem.* **2005**, *58*, 379-410.

49. Bawa, P.; Pillay, V.; Choonara, Y. E.; Toit, L. C. d. Stimuli-Responsive Polymers and Their Applications in Drug Delivery. *Biomed. Mater.* **2009**, *4*, 022001.

50. Xu, J.; Liu, S. Y. Polymeric Nanocarriers Possessing Thermoresponsive Coronas. *Soft Matter* **2008**, *4*, 1745-1749.

51. Ferguson, C. J.; Hughes, R. J.; Nguyen, D.; Pham, B. T. T.; Gilbert, R. G.; Serelis, A. K.; Such, C. H.; Hawkett, B. S. Ab Initio Emulsion Polymerization by Raft-Controlled Self-Assembly. *Macromolecules* **2005**, *38*, 2191-2204.

52. Doyle, E. L.; Hunter, C. A.; Phillips, H. C.; Webb, S. J.; Williams, N. H. Cooperative Binding at Lipid Bilayer Membrane Surfaces. *J. Am. Chem. Soc.* **2003**, *125*, 4593-4599.

53. Skirtach, A. G.; Javier, A. M.; Kreft, O.; Kohler, K.; Alberola, A. P.; Mohwald, H.; Parak, W. J.; Sukhorukov, G. B. Laser-Induced Release of Encapsulated Materials inside Living Cells. *Angew. Chem.-Int. Edit.* **2006**, *45*, 4612-4617.

54. Javier, A. M.; del Pino, P.; Bedard, M. F.; Ho, D.; Skirtach, A. G.; Sukhorukov, G. B.; Plank, C.; Parak, W. J. Photoactivated Release of Cargo from the Cavity of Polyelectrolyte Capsules to the Cytosol of Cells. *Langmuir* **2008**, *24*, 12517-12520.

Chapter 3

Dual pH- and Temperature-Responsive Protein Nanocapsules

3.1. Introduction

The development of stimuli-responsive nanoparticles is at the forefront of research in the diagnosis and treatment of tumors.[1-5] There have been numerous reports of nanoparticles engineered to respond to external stimuli such as temperature,[6-8] pH,[9-11] light,[12] magnetic field,[13,14] and reducing conditions.[15,16] Furthermore, therapeutic nanoparticles have been developed that respond to two or more of these stimuli.[17-24] In one example, Li and coworkers reported the development of doxorubicin loaded polymer nanoparticles and polymersomes, composed of a block copolymer containing segments of poly(ethylene oxide) and poly(*trans*-*N*-(2-ethoxy-1,3-dioxan-5-yl) acrylamide), which assemble at physiological temperatures and disassemble in acidic conditions.[23] Such acid-sensitive nanoparticles may be useful for applications in intracellular drug delivery due to acidic conditions found in endosomes and lysosomes. To date, all of the previously reported multiply stimuli responsive nanoparticles have been prepared by synthetic means, through the use of synthetic polymers and inorganic materials.

Naturally occurring protein cages, such as virus capsids, ferritin, and vault nanocapsules, can serve as scaffold for complex hybrid protein-polymer nanoparticles. Protein cages offer precise architectures, which can be genetically engineered and synthetically modified.[25-29] We, and others, have developed functionalized protein cages by modification with synthetic polymers.[28-38] For example, Xi and coworkers have modified ferritin with cell-binding RGD peptides and demonstrated the encapsulation of doxorubicin within these ferritin nanoparticles. Furthermore, these nanoparticles were shown to inhibit tumor growth in mouse models.[39] We have previously reported the preparation of vault-poly(*N*-isopropylacrylamide) (pNIPAAm) conjugates, which were shown to undergo a reversible thermally triggered aggregation at 35.9

°C.[38] Vault nanoparticles, first reported by Rome and coworkers in 1986, are stable non-immunogenic protein cages weighing 13 MDa and measuring 45 x 45 x 75 nm in dimension with a hollow interior measuring 5 x 10^7 $Å^3$.[40-44] Vaults are non-immunogenic, and are present in most eukaryotes, including humans.[41] Vaults are currently being pursued as templates for the development of drug delivery vehicles, have been engineered to target specific cell types and have been modified to encapsulate hydrophobic drugs.[45,46] Herein, we report the development of dual pH- and temperature-responsive vault nanoparticles (Figure 3.1**)**. These multiply responsive vault nanoparticles have been prepared through the conjugation of poly(*N*-isopropylacrylamide-*co*-acrylic acid) (pNIPAAm-*co*-AA) to human CP-H-MVP vaults.

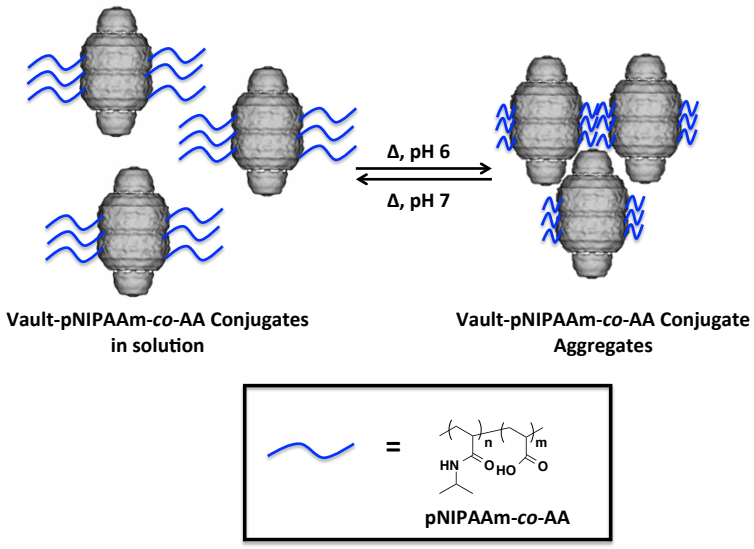

Figure 3.1. pH- and temperature-responsive vault-pNIPAAm-*co*-AA conjugates**.** The vault image was adapted from cryoEM reconstructions of recombinant vaults.

3.2. Results and Discussion

3.2.1. Polymer Synthesis

Temperature and pH responsive pNIPAAm-*co*-AA has been previously reported.[47,48,49] Compared to pNIPAAm, which has an LCST of approximately 32 °C, pNIPAAm-co-AA undergoes much higher LCST transitions in basic conditions and much lower LCST transitions in acidic conditions. This is due to the presence of the AA monomer units, which are deprotonated in basic and neutral conditions making the copolymer more soluble in water. In acidic conditions the AA monomer units are protonated, which makes the copolymer more hydrophobic. Our approach to developing a pH and temperature responsive vault nanoparticle is based on the conjugation of pNIPAAm-*co*-AA to human CP-H-MVP vaults. RAFT polymerization was used for the preparation of these polymers due to the precise level of control over polymer molecular weight and narrow molecular weight distribution afforded by this technique.[50]

A cysteine reactive pNIPAAm-*co*-AA was prepared *via* RAFT copolymerization of NIPAAm and AA in the presence of a pyridyl disulfide trithiocarbonate CTA **1** with AIBN (NIPAAm:AA:CTA:AIBN, 124:6:1:0.1) in DMF at 80 °C (Scheme 3.1). The polymerization was stopped after 1 h at 78% NIPAAm conversion and 88% AA conversion by ^{1}H NMR spectroscopy. The crude polymerization mixture was purified by extensive dialysis against MeOH to yield **polymer 1**. The number-average molecular weight (M_n) was determined by ^{1}H NMR to be 14.1 kDa and the polydispersity index (PDI) by GPC was 1.21. The overall monomer composition of **polymer 1** is approximately 97.7:5.3 NIPAAm:AA.

Scheme 3.1. RAFT copolymerization of NIPAAm and AA to yield **polymer 1**

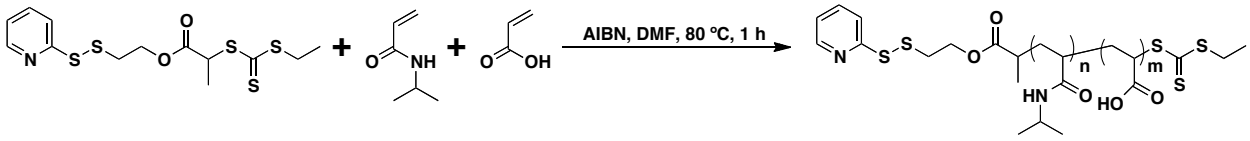

1 **Polymer 1**

In previous studies, we found the RAFT trithiocarbonate end-group to non-specifically react to thiols present on CP-MVP vaults. The trithiocarbonate end-group of **polymer 1** was therefore transformed into a non-reactive isobutylnitrile group by radical exchange with AIBN (Scheme 3.2).[51] After extensive dialysis against MeOH, **polymer 2** was obtained. Complete removal of the trithiocarbonate end-group was determined by the disappearance of the 305 nm trithiocarbonate absorption by UV-Vis. GPC analysis of **polymer 2** revealed a PDI of 1.25. End-group analysis by ^{1}H-NMR revealed a M_n(NMR) of 14.1 kDa. Radical exchange with AIBN did not significantly alter the polymer M_n and PDI.

Scheme 3.2. End-group modification of **polymer 1** by radical exchange with AIBN to yield **polymer 2.**

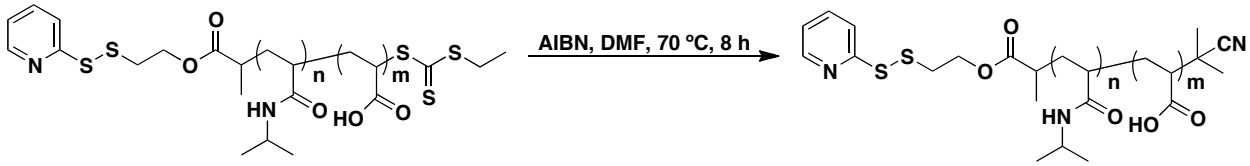

Polymer 1 **Polymer 2**

3.2.2. Polymer Turbidity Studies

The pH and temperature dependent thermal aggregation of **polymer 2** was evaluated by UV-Vis turbidity studies at pH 5.0, 6.0, and 7.0 (50 mM PB) (Figure 3.2). At pH 5.0 the LCST

was determined to be 31.9 °C. At pH 6.0 the LCST was determined to be 44.0 °C**.** At pH 7.0 there was no measureable LCST below 60 °C. As expected, the LCST of **polymer 2** increased as the pH level was increased.

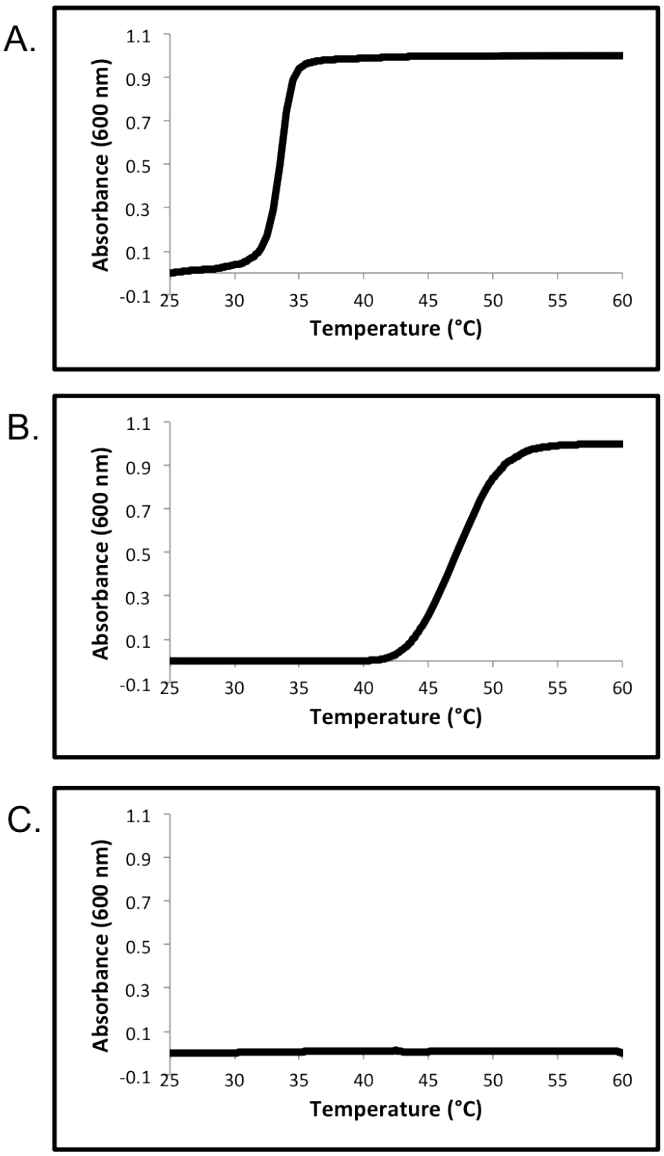

Figure 3.2. UV-Vis turbidity experiments of **polymer 2** in 50 mM PB at: (A) pH 5; (B) pH 6; (C) pH 7.

3.2.3. Vault pNIPAAm-*co*-AA Conjugation

Polymer 2 was conjugated to CP-H-MVP by incubation with CP-H-MVP Vaults at a ratio of 100 : 1 polymer : CP-H-MVP to yield **conjugate 1** (Scheme 3.3). The conjugate was analyzed by SDS-PAGE, to observe a shift in molecular weight of the CP-H-MVP-pNIPAAm-*co*-AA conjugates as compared to unmodified CP-H-MVP. Conjugation is apparent in the SDS-PAGE (Figure 3.3). Under non-reducing conditions, SDS-PAGE stained with Coomassie blue shows a shift to a higher molecular weight of the conjugate (Figure 3.3, Lane 5) when compared to the CP-H-MVP (~100 kDa) (Figure 3.3, Lane 4). The non-reduced conjugate appears (Figure 3.3, Lane 5) appears much fainter than the CP-H-MVP (Figure 3.3, Lane 4), which is a discreet band. This is because the conjugate is band is spread out due to multiple conjugations per protein This data shows that conjugation was highly efficient, as there is no free CP-H-MVP protein visible in the SDS-PAGE. Under reducing conditions with dithiothreitol (DTT), SDS-PAGE stained with Coomassie blue shows no difference in molecular weight of the conjugate compared to the unmodified CP-H-MVP due to the disulfide bond between the polymer and CP-H-MVP of the conjugate being reduced by DTT (Figure 3.3, Lane 3). The exact polymer conjugation sites on the vault structure are unknown. However, due to the presence of free cysteine residues on the vault interior and exterior, we expect that there is polymer conjugated on both the vault interior and exterior. We have previously conducted a number of experiments to determine precise conjugation sites, but these attempts were unsuccessful.[38]

Scheme 3.3. Conjugation of **Polymer 2** to CP-H-MVP

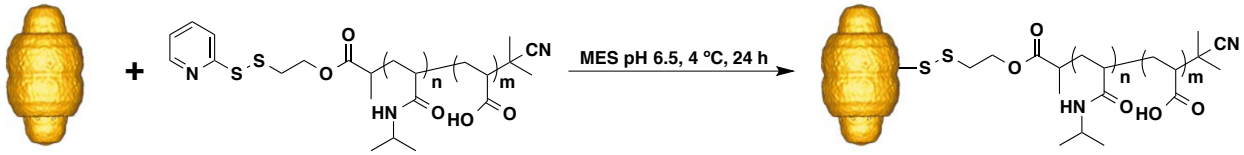

Polymer 2

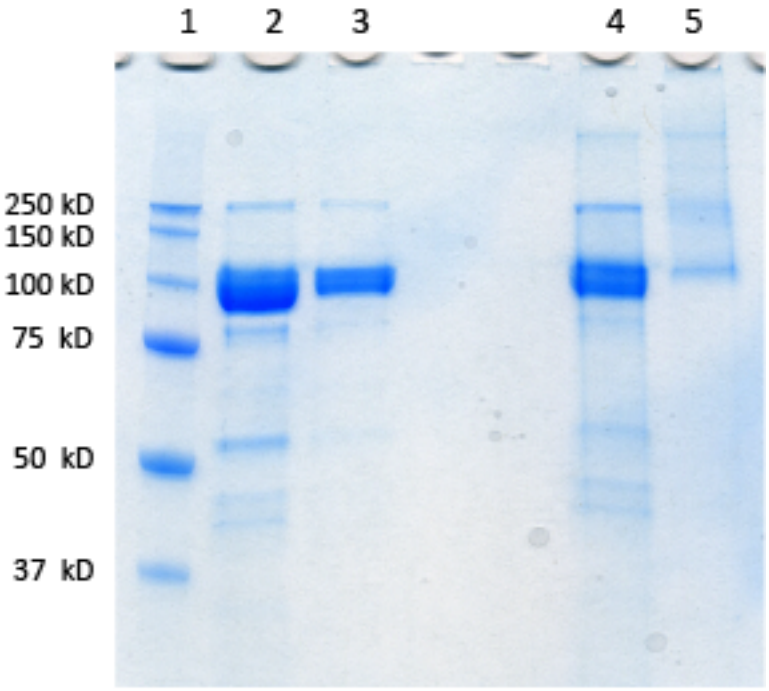

Figure 3.3. SDS-PAGE of CP-H-MVP vault and conjugate visualized by coomassie blue staining (Lane 1: protein marker; Lane 2: CP-H-MVP vault reducing conditions; Lane 3: conjugate reducing conditions; Lane 4: CP-H-MVP vault non-reducing conditions; Lane 5: conjugate non-reducing conditions)

3.2.4. pH- and Temperature Responsiveness of Vault-pNIPAAm-*co*-AA Conjugate

The pH and temperature responsive properties of the pNIPAAm-*co*-AA vault conjugates have been investigated by UV-Vis turbidity measurements at pH 6 and 7 (Figure 3.4). Below pH 6.0, vaults have been observed to be unstable. At pH 7.0 the conjugate did not display LCST behavior (Figure 3.4.C). However, at pH 6.0 the conjugate aggregated upon heating and was determined to have an LCST of 41.8 °C (Figure 3.4.D). At higher temperatures (>45 °C) at pH 6.0, the conjugate precipitated from solution to form macroscopic aggregates, this caused imprecise measurement of absorbance at 600 nm at high temperatures. Unmodified CP-H-MVP vaults did not exhibit LCST behavior at pH 7.0 or 6.0 **(**Figure 3.4. A-B). **Table 3.1** shows the LCSTs of **polymer 1**, **conjugate 2**, and CP-H-MVP vaults at pH 5, pH 6, and pH 7.

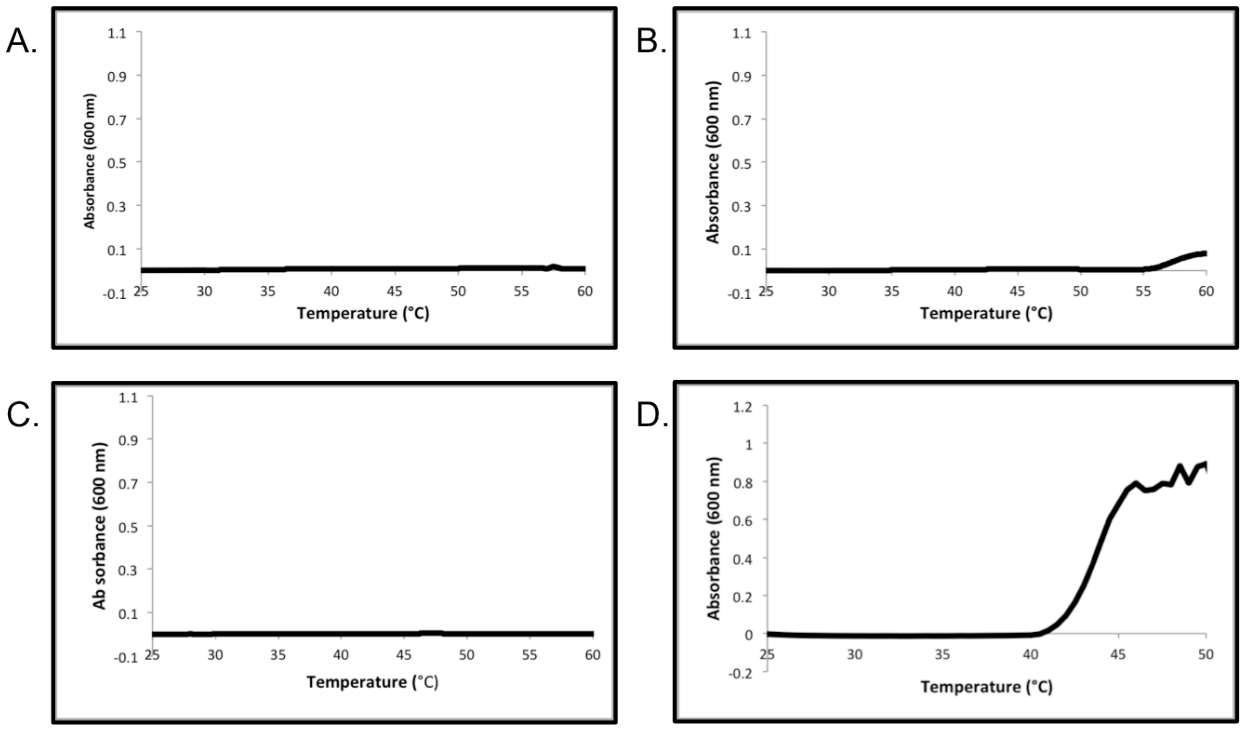

Figure 3.4. UV-Vis turbidity experiments of the CP-H-MVP vault at: (A) pH 7.0 and (B) pH 6.0 and of the pNIPAAm-*co*-AA-CP-H-MVP vault conjugate at (C**)** pH 7.0 and (D) pH 6.0.

	LCST (pH 7)	LCST (pH 6)	LCST (pH 7)
Polymer 2	31.9	44.0 °C	None Observed
Conjugate 1	N/A	41.8 °C	None Observed
CP-H-MVP Vault	N/A	None Observed	None Observed

Table 3.1. Calculated LCSTs for **polymer 2, conjugate 1**,and CP-H-MVP vaults at varying pH levels.

The pH and temperature dependent aggregation of the pNIPAAm-co-AA vault conjugates has been investigated by dynamic light scattering (DLS) (Figure 3.5). At pH 7.0, the

conjugate remains the same diameter at 25 (39.7 ± 13.7 nm) and 45 °C (40.4 ± 12.7 nm) (Figure 3.5.B). However, when the conjugate is at pH 6.0 there is a shift in conjugate size from 41.3 ± 11.6 nm at 25 °C to large aggregates (~300 nm) at 45 °C (Figure 3.5.B). The aggregation is reversible, and the conjugate returns to 39.3 ± 13.0 nm when cooled to 25 °C (Figure 3.5.B). At both pH 6.0 and 7.0 there was almost no change in the unmodified vault size when the temperature was elevated from 25 to 45 °C (Figure 3.5.A). Together, the UV-Vis turbidity studies, as well as the DLS size measurements indicate that the polymer is conjugated to the CP-H-MVP vaults and that pH- and temperature-responsiveness is due to the conjugated polymer. Unmodified CP-H-MVP vaults remain intact and in solution when heated up to 60 °C, suggesting that the pH- and temperature-responsiveness of the conjugate is solely due to the conjugated polymer.

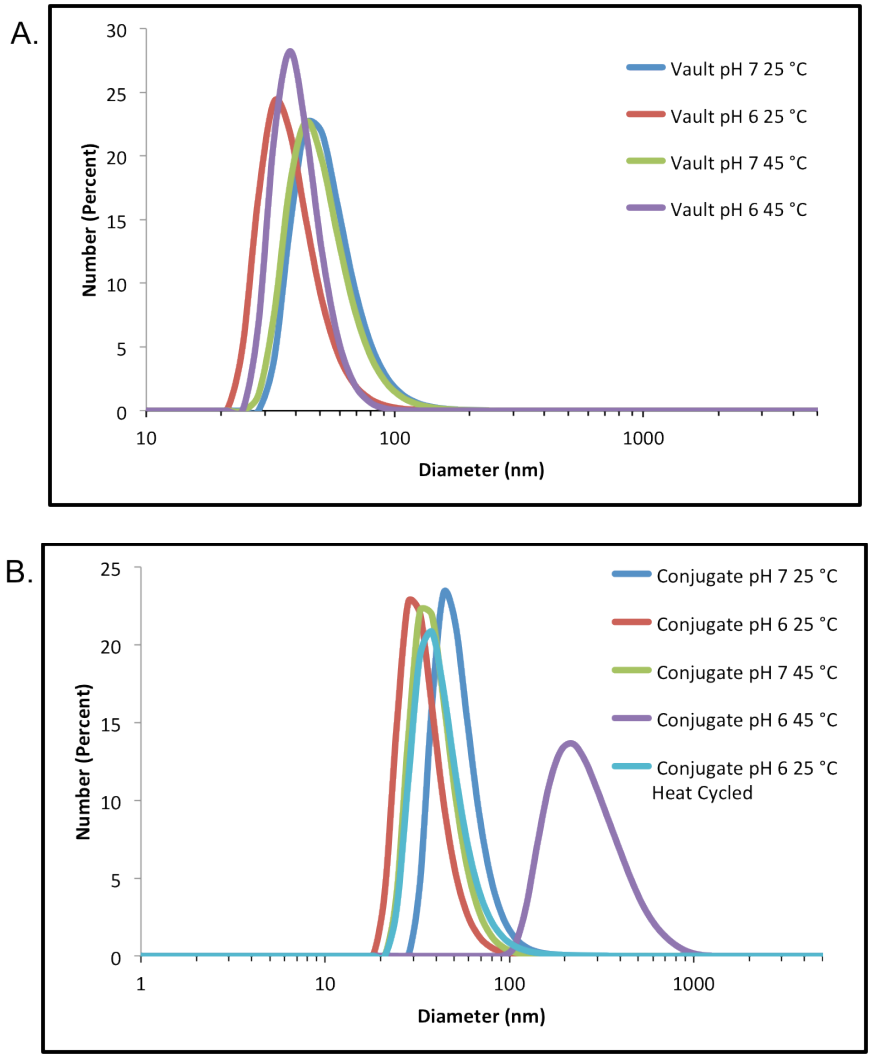

Figure 3.5. DLS measurements of: (A.) CP-H-MVP vaults; (B.) pNIPAAm-*co*-AA vault conjugates.

To determine the reversibility of the aggregation and the integrity of the vault structure through the pH and temperature dependent aggregation, CP-H-MVP vaults and the pNIPAAm-*co*-AA conjugates were visualized by electron microscopy before and after heating above 45 °C, which is above the LCST of the conjugate at pH 6.0 (Figure 3.6). At pH 6.0 the vault conjugate was found to remain intact throughout the thermally triggered aggregation process. At pH 6.5, The CP-H-MVP vaults, as well as the conjugate, were not damaged by heating. Furthermore, the conjugates were able to withstand three heating cycles without damaging the vault structure (Figure 3.6.H-I).

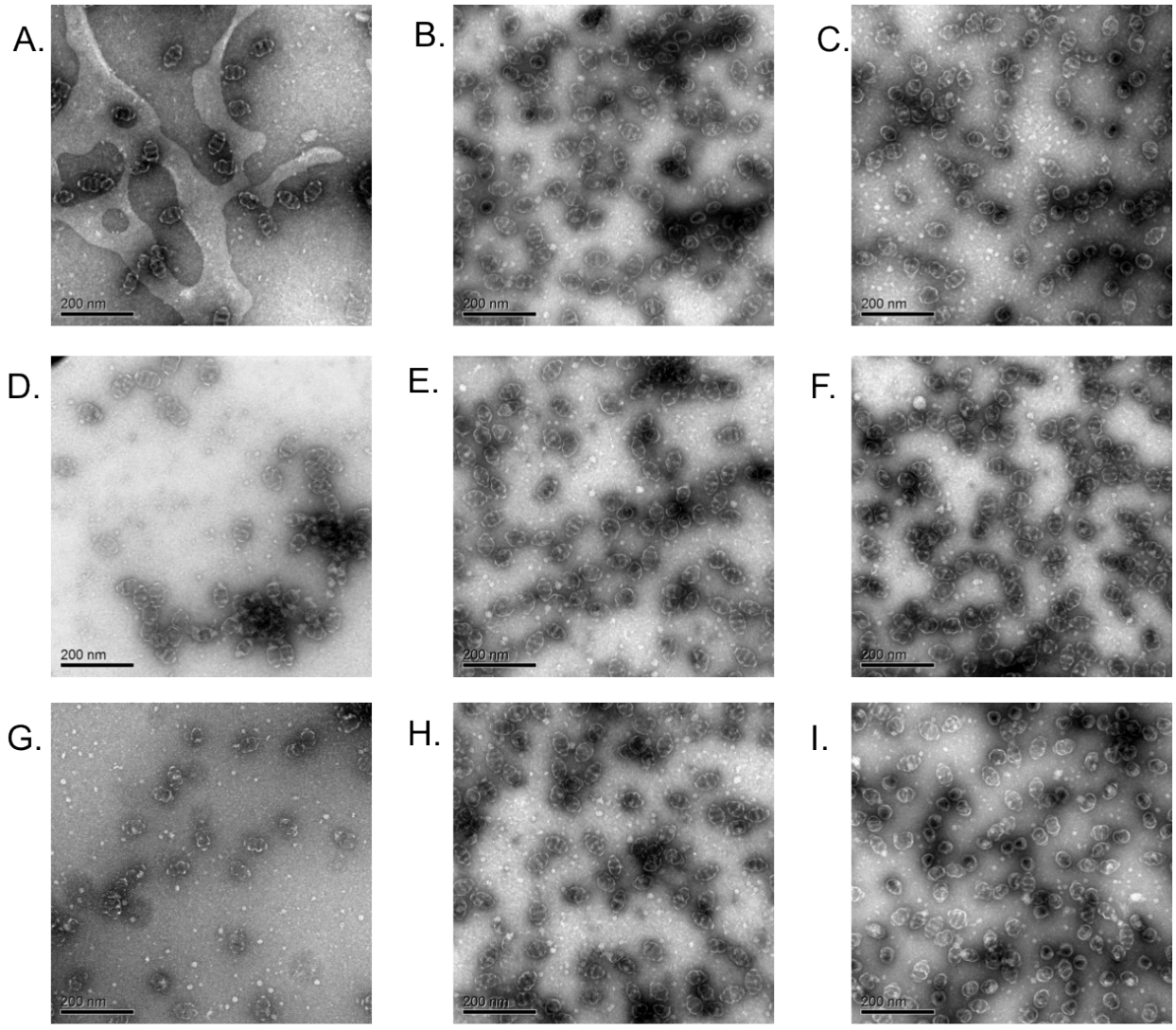

Figure 3.6. Negative stain TEM of (A.) CP-H-MVP vaults, pH 6.5 (in reaction buffer), 4 °C; (B.) Conjugate 1 pH 7.0; 4 °C (C.) Conjugate 1 pH 6.0, 4 °C; (D.) CP-H-MVP vaults heat cycled once (4 to 45 to 4 °C); (E.) Conjugate 1 pH 7.0 heat cycled once (4 to 45 to 4 °C); (F.) Conjugate pH 6.0 heat cycled once (4 to 45 to 4 °C); (G.) CP-H-MVP vaults heat cycled three times; (H.) Conjugate pH 7.0 heat cycled three times; (I.) Conjugate pH 6.0 heat cycled three times.

Together this data demonstrates the development of a dual pH- and temperature-responsive vault nanoparticle. These dual-responsive vault-pNIPAAm-*co*-AA conjugates are an improvement to our previously reported vault-pNIPAAm conjugates, which were shown to have an LCST of 35.9 °C. Furthermore, pNIPAAm-*co*-AA can be tuned to specific LCST values by the incorporation of more or less AA monomer units to the polymer.[49] This suggests that we will be able to tune the LCSTs of future vault-pNIPAAm-*co*-AA conjugates for applications such as intracellular drug delivery, where endosome and lysosome pH levels are known to be 5-6 and 4-5, respectively.[52] Furthermore, this technology may be applicable to solid tumor delivery as some tumors are known to have pH levels as low as 5.7.[53]

As previously demonstrated with the vault-pNIPAAm conjugates, conjugation of pNIPAAm-*co*-AA does not interfere with the vault structure, which is important for potential future applications of this pH- and temperature-responsive vault conjugate. The Rome group, has previously packaged hydrophobic molecules, chemotherapeutics, proteins, and inorganic nanoparticles into the vault interior.[46] These vault loading techniques should be compatible with polymer conjugation to the vault, resulting in multiple-responsive loaded vault conjugates

3.3. Experimental

3.3.1. Materials

Chemicals were purchased from Sigma-Aldrich, Fisher Scientific, and Acros. AIBN was recrystallized twice from acetone. NIPAAm was recrystallized twice from hexanes. The pyridyl disulfide trithiocarbonate CTA **1** was prepared according to previous literature.[54] Human CP-H-MVP vault was prepared and provided by George Buchman (C-PERL).

3.3.2. Analytical Techniques

NMR spectra were obtained on Bruker 500 MHz DRX spectrometer. Proton NMR spectra were acquired with a relaxation delay of 30 sec for all polymers. UV-Vis spectra were obtained on a Biomate 5 Thermo Spectronic UV-Vis spectrometer and a Hewlett-Packard HP8453 diode-array UV-Vis spectrophotometer with Peltier temperature control spectrometer with quartz cells. Gel Permeatinon Chromatography (GPC) was conducted on a Shimadzu HPLC system equipped with a refractive index detector (RID-10A), one Polymer Laboratories PLgel guard column, and two Polymer Laboratories PLgel 5 μm mixed D columns. LiBr (0.1 M) in DMF at 40 °C was used as an eluent (flow rate: 0.80 mL/min). Calibration was performed using near-monodisperse PMMA standards from Polymer Laboratories. SDS-PAGE was performed using Bio-Rad Any kD Mini-PROTEAN-TGX gels. TEM was conducted on a JEOL JEM1200-EX transmission electron microscope. Images were taken using a Gatan BioScan 600W 1x1K digital camera and Digital Micrograph acquisition software.

3.3.3. Methods

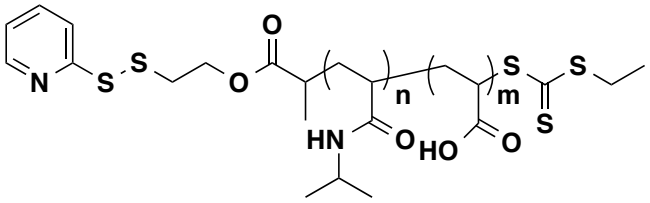

Copolymerization of NIPAAm and AA in the presence of pyridyl disulfide CTA to afford α-pyridyl disulfide pNIPAAm-*co*-AA (polymer 1): The pyridyl disulfide CTA **1** (45 mg, 0.11 mmol), NIPAAm (1.6 g, 14.1 mmol), AA (47 μL, 0.62 mmol), and AIBN (1.9 mg, 0.011 mmol), were added to a Schlenk tube containing a magnetic stir bar. DMF (2.28 mL) was added to dissolve the solids. Freeze-pump-thaw cycles were repeated four times and the reaction was performed at 80 ºC in an oil bath. The reaction was stopped after 1 h at 78% NIPAAm conversion and 88% AA conversion by cooling with liquid nitrogen and exposing the reaction to atmosphere. **Polymer 1** was purified by dialyzing against MeOH (MWCO 3,500 g/mol). ^{1}H NMR (500 MHz, MeOD) δ: 8.39 (m, Py), 8.18-7.25 (NH, pNIPAAm), 7.214 (m, Py), 7.26 (m) 4.27 (m), 4.12-3.73 (CH, pNIPAAm), 3.06 (s), 2.35-1.80 (CH_2, pNIPAAM), 1.79-1.45 (CH_2, pNIPAAm), 1.25-0.92 (NCH_3, pNIPAAm). The signals corresponding to AA are unidentifiable by ^{1}H NMR of the purified polymer. The incorporation of AA was calculated from the % conversion of the AA in the crude ^{1}NMR of the polymer at 1 h. M_n by ^{1}H NMR was 14,100 g/mol (targeted 12,000 g/mol). M_n(GPC) was 14,200 g/mol and the PDI was 1.21.

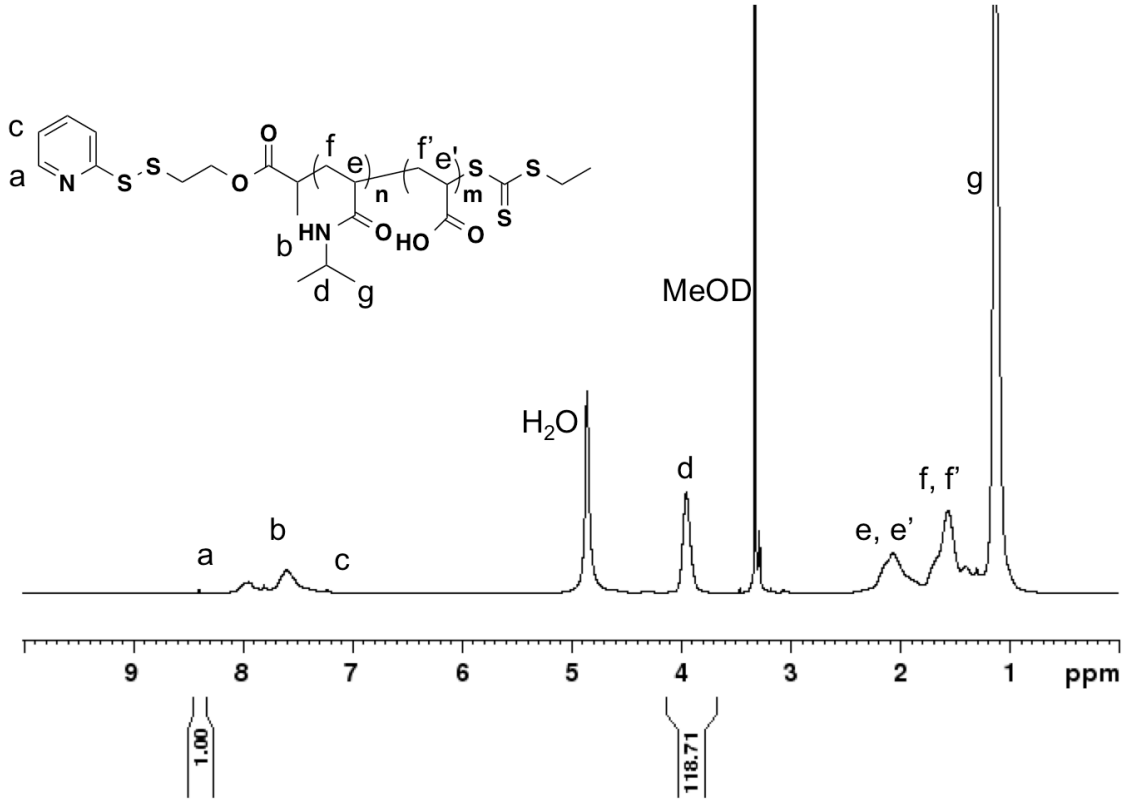

Figure 3.6. 1H NMR (500 MHz, MeOD) of polymer 1.

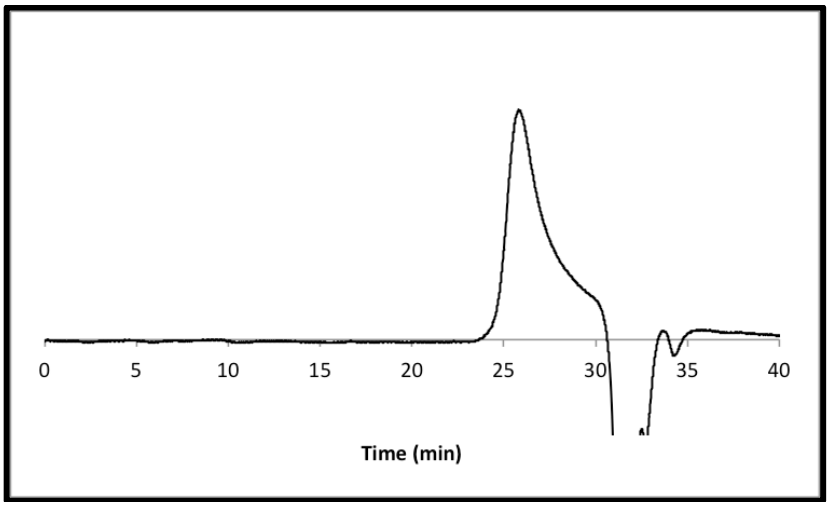

Figure 3.7. GPC chromatogram of **polymer 1,** normalized and analyzed by comparison with monodisperse PMMA standards.

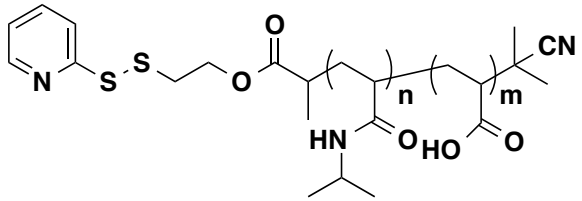

Trithiocarbonate endgroup removal by radical exchange with AIBN to yield polymer 2: **Polymer 1** (112 mg, 0.008 mmol) and AIBN (26.3 mg, 0.160 mmol) were added to a Schlenk tube containing a magnetic stir bar with DMF (1.56 mL). Freeze-pump-thaw cycles were repeated three times, and polymerization was then initiated by submerging the Schlenk tube in an oil bath at 80 °C. **Polymer 2** was obtained after dialyzing the crude reaction mixture against MeOH (MWCO 3,500 g/mol). Complete removal of the trithiocarbonate end group was observed by monitoring the UV-Vis abosorption at 305 nm. ^{1}H NMR (500 MHz, MeOD) δ: 8.39 (m, Py), 8.19-7.26 (NH, pNIPAAm), 7.23 (m, Py), 7.26 (d), 4.28 (m), 4.10-3.76 (CH, pNIPAAm), 3.06 (s), 2.48-1.79 (CH_2, pNIPAAM), 1.79-1.44 (CH_2, pNIPAAm), 1.32-0.92 (NCH_3, pNIPAAm). The signals corresponding to AA are unidentifiable by ^{1}H NMR. M_n by ^{1}H NMR was 14,100 g/mol (targeted 12,000 g/mol). M_n(GPC) was 14,200 g/mol and the PDI was 1.25.

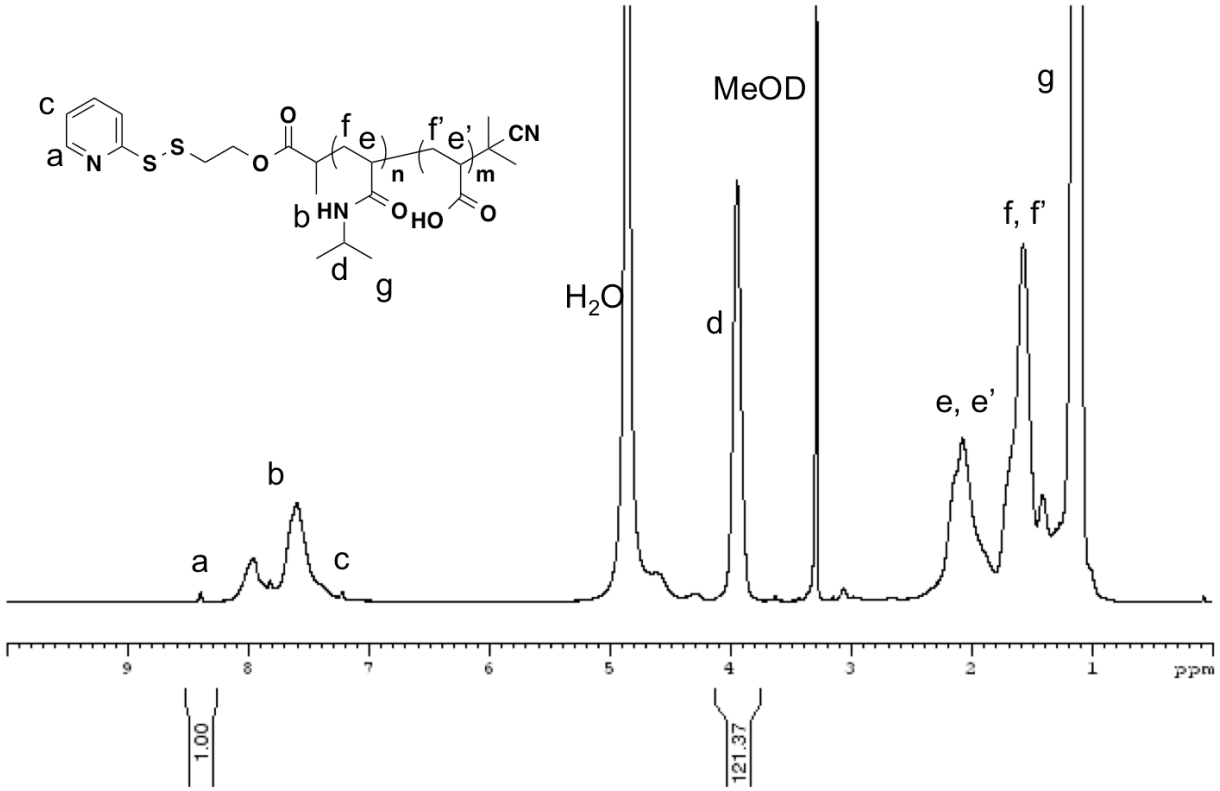

Figure 3.8. [1]H NMR (500 MHz, MeOD) of **polymer 2.**

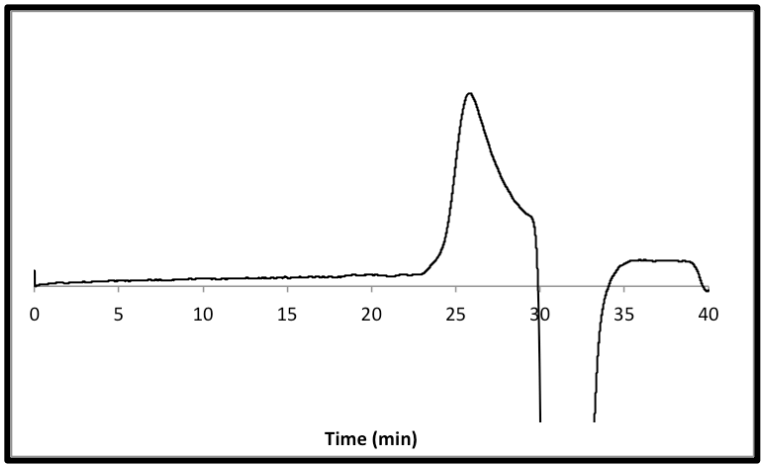

Figure 3.9. GPC chromatogram of **polymer 2,** normalized and analyzed by comparison with monodisperse PMMA standards.

pNIPAAm-*co*-AA conjugation to CP-H-MVP: A pH 6.5 20 mM 2-(*N*-morpholino) ethanesulfonic acid) (MES) buffer was degassed by bubbling argon gas through the buffer for 30 min. CP-H-MVP (0.50 mg, 0.05μmol) in 250 μL buffer was treated with triscarboxylethylphosphine (TCEP) resin for 2 h at 4 ºC, then filtered through a 0.22 μm syringe filter. **Polymer 2** (6.20 mg, 5.00 μmol) was dissolved in 250 μL of buffer. The filtered CP-H-MVP solution was added to the solution containing **polymer 2**. The reaction was incubated at 4 ºC for 24 h before purification by ultrafiltration (MWCO 100,000 g/mol) to give the conjugate.

LCST determination: A solution of **polymer 2**, conjugate, or unmodified vault at a concentration of 1.0 mg mL^{-1} in pH 5.0, 6.0, or 7.0 20 mM MES was placed in a 100 μL quartz cuvette. The cuvette was placed in a Hewlett-Packard HP8453 diode-array UV-Vis spectrophotometer with Peltier temperature control. The following temperature program was used: temperature was elevated at 0.5 ºC min^{-1} and held for 30 s prior to measuring the absorbance at 600 nm. The LCST was determined at 10% of the maximum absorbance.

Preparation of the TEM sample: A 40 μL aliquot of a 0.2 μg $μL^{-1}$ solution of CP-H-MVP-Vault-pNIPAAm conjugate in either pH 6.0 or 7.0 (50 mM PB) was warmed to 45 ºC incubated for 7 min then cooled to 4 °C. 20 μL of the solution was then pipetted onto an aluminum surface cooled to 4 °C. A carbon-coated EM grid was floated up-side down on the sample to allow the conjugate to adsorb to the grid surface. After 7 min, the grid was removed from the sample and blotted on filter paper to remove excess liquid. The grid was then floated up-side down in 500 μL of a 1% uranyl acetate solution at the 4 °C. After 7 min, the grid was removed from the uranyl acetate solution and blotted on filter paper. TEM was then conducted on a JEOL JEM1200-EX transmission electron microscope.

3.4. Conclusions

Dual pH- and temperature- responsive vault nanoparticles have been prepared through the conjugation of pNIPAAm-*co*-AA to CP-H-MVP vaults. This conjugate was shown to undergo a thermally triggered reversible aggregation at 41.8 °C in pH 6 buffer, while remaining stable in solution at pH 7. The dual-responsive properties of this conjugate are a significant improvement on our previously reported vault-pNIPAAm conjugate, which are only responsive to changes in temperature.[38] Furthermore, the pNIPAAm-*co*-AA conjugates exhibit sharper phase transitions than the vault-pNIPAAm conjugates. We believe that these vault-pNIPAAm-*co*-AA conjugates, in combination with reported vault loading strategies, may be useful for intracellular drug delivery and solid tumor drug delivery.

3.5. References

1. Peer, D.; Karp, J. M.; Hong, S.; FaroKhzad, O. C.; Margalit, R.; Langer, R. Nanocarriers as an Emerging Platform for Cancer Therapy. *Nat. Nanotechnol.* **2007**, *2*, 751-760.
2. Ferrari, M. Cancer Nanotechnology: Opportunities and Challenges. *Nat. Rev. Cancer* **2005**, *5*, 161-171.
3. Brigger, I.; Dubernet, C.; Couvreur, P. Nanoparticles in Cancer Therapy and Diagnosis. *Advanced Drug Delivery Reviews* **2002**, *54*, 631-651.
4. Davis, M. E.; Chen, Z.; Shin, D. M. Nanoparticle Therapeutics: An Emerging Treatment Modality for Cancer. *Nat. Rev. Drug Discov.* **2008**, *7*, 771-782.
5. Fonseca, N. A.; Gregorio, A. C.; Valerio-Fernandes, A.; Simoes, S.; Moreira, J. N. Bridging Cancer Biology and the Patients' Needs with Nanotechnology-Based Approaches. *Cancer Treat. Rev.* **2014**, *40*, 626-635.
6. Cammas, S.; Suzuki, K.; Sone, C.; Sakurai, Y.; Kataoka, K.; Okano, T. Thermo-Responsive Polymer Nanoparticles with a Core-Shell Micelle Structure as Site-Specific Drug Carriers. *J. Control. Release* **1997**, *48*, 157-164.
7. Berndt, I.; Pedersen, J. S.; Richtering, W. Temperature-Sensitive Core-Shell Microgel Particles with Dense Shell. *Angew. Chem.-Int. Edit.* **2006**, *45*, 1737-1741.
8. Hellweg, T.; Dewhurst, C. D.; Eimer, W.; Kratz, K. Pnipam-Co-Polystyrene Core-Shell Microgels: Structure, Swelling Behavior, and Crystallization. *Langmuir* **2004**, *20*, 4330-4335.
9. Soppimath, K. S.; Tan, D. C. W.; Yang, Y. Y. Ph-Triggered Thermally Responsive Polymer Core-Shell Nanoparticles for Drug Delivery. *Adv. Mater.* **2005**, *17*, 318-+.

10. Das, M.; Mardyani, S.; Chan, W. C. W.; Kumacheva, E. Biofunctionalized Ph-Responsive Microgels for Cancer Cell Targeting: Rational Design. *Adv. Mater.* **2006**, *18*, 80-83.

11. Dupin, D.; Fujii, S.; Armes, S. P.; Reeve, P.; Baxter, S. M. Efficient Synthesis of Sterically Stabilized Ph-Responsive Microgels of Controllable Particle Diameter by Emulsion Polymerization. *Langmuir* **2006**, *22*, 3381-3387.

12. Angelatos, A. S.; Radt, B.; Caruso, F. Light-Responsive Polyelectrolyte/Gold Nanoparticle Microcapsules. *J. Phys. Chem. B* 2005, ***109***, 3071-3076.

13. Pankhurst, Q. A.; Connolly, J.; Jones, S. K.; Dobson, J. Applications of Magnetic Nanoparticles in Biomedicine. *J. Phys. D-Appl. Phys.* **2003**, *36*, R167-R181.

14. Lu, A. H.; Salabas, E. L.; Schuth, F. Magnetic Nanoparticles: Synthesis, Protection, Functionalization, and Application. *Angew. Chem.-Int. Edit.* **2007**, *46*, 1222-1244.

15. Ryu, J.-H.; Chacko, R. T.; Jiwpanich, S.; Bickerton, S.; Babu, R. P.; Thayumanavan, S. Self-Cross-Linked Polymer Nanogels: A Versatile Nanoscopic Drug Delivery Platform. *J. Am. Chem. Soc.* **2010**, *132*, 17227-17235.

16. Ryu, J. H.; Jiwpanich, S.; Chacko, R.; Bickerton, S.; Thayumanavan, S. Surface-Functionalizable Polymer Nanogels with Facile Hydrophobic Guest Encapsulation Capabilities. *J. Am. Chem. Soc.* **2010**, *132*, 8246-8247.

17. Jaiswal, M. K.; Pradhan, A.; Banerjee, R.; Bahadur, D. Dual Ph and Temperature Stimuli-Responsive Magnetic Nanohydrogels for Thermo-Chemotherapy. *J. Nanosci. Nanotechnol.* **2014**, *14*, 4082-4089.

18. Hoare, T.; Pelton, R. Highly Ph and Temperature Responsive Microgels Functionalized with Vinylacetic Acid. *Macromolecules* **2004**, *37*, 2544-2550.

19. Kuckling, D.; Vo, C. D.; Wohlrab, S. E. Preparation of Nanogels with Temperature-Responsive Core and Ph-Responsive Arms by Photo-Cross-Linking. *Langmuir* **2002**, *18*, 4263-4269.

20. Isojima, T.; Lattuada, M.; Vander Sande, J. B.; Hatton, T. A. Reversible Clustering of Ph- and Temperature-Responsive Janus Magnetic Nanoparticles. *ACS Nano* **2008**, *2*, 1799-1806.

21. Cheng, R.; Meng, F. H.; Deng, C.; Klok, H. A.; Zhong, Z. Y. Dual and Multi-Stimuli Responsive Polymeric Nanoparticles for Programmed Site-Specific Drug Delivery. *Biomaterials* **2013**, *34*, 3647-3657.

22. Kang, S. I.; Na, K.; Bae, Y. H. Physicochemical Characteristics and Doxorubicin-Release Behaviors of Ph/Temperature-Sensitive Polymeric Nanoparticles. *Colloid Surf. A-Physicochem. Eng. Asp.* **2003**, *231*, 103-112.

23. Qiao, Z. Y.; Ji, R.; Huang, X. N.; Du, F. S.; Zhang, R.; Liang, D. H.; Li, Z. C. Polymersomes from Dual Responsive Block Copolymers: Drug Encapsulation by Heating and Acid-Triggered Release. *Biomacromolecules* **2013**, *14*, 1555-1563.

24. Wang, A. N.; Gao, H.; Sun, Y. F.; Sun, Y. L.; Yang, Y. W.; Wu, G. L.; Wang, Y. N.; Fan, Y. G.; Ma, J. B. Temperature- and Ph-Responsive Nanoparticles of Biocompatible Polyurethanes for Doxorubicin Delivery. *Int. J. Pharm.* **2013**, *441*, 30-39.

25. Douglas, T.; Young, M. Virus Particles as Templates for Materials Synthesis. *Adv. Mater.* **1999**, *11*, 679-681.

26. Witus, L. S.; Francis, M. B. Using Synthetically Modified Proteins to Make New Materials. *Acc. Chem. Res.* **2011**, *44*, 774-783.

27. Lee, L. A.; Niu, Z. W.; Wang, Q. Viruses and Virus-Like Protein Assemblies-Chemically Programmable Nanoscale Building Blocks. *Nano Res.* **2009**, *2*, 349-364.

28. Uchida, M.; Klem, M. T.; Allen, M.; Suci, P.; Flenniken, M.; Gillitzer, E.; Varpness, Z.; Liepold, L. O.; Young, M.; Douglas, T. Biological Containers: Protein Cages as Multifunctional Nanoplatforms. *Adv. Mater.* **2007**, *19*, 1025-1042.

29. Soto, C. M.; Ratna, B. R. Virus Hybrids as Nanomaterials for Biotechnology. *Curr. Opin. Biotechnol.* **2010**, *21*, 426-438.

30. MaHam, A.; Tang, Z. W.; Wu, H.; Wang, J.; Lin, Y. H. Protein-Based Nanomedicine Platforms for Drug Delivery. *Small* **2009**, *5*, 1706-1721.

31. Manchester, M.; Singh, P. Virus-Based Nanoparticles (Vnps): Platform Technologies for Diagnostic Imaging. *Adv. Drug Delivery Rev.* **2006**, *58*, 1505-1522.

32. Ma, Y. J.; Nolte, R. J. M.; Cornelissen, J. Virus-Based Nanocarriers for Drug Delivery. *Adv. Drug Delivery Rev.* **2012**, *64*, 811-825.

33. Garcea, R. L.; Gissmann, L. Virus-Like Particles as Vaccines and Vessels for the Delivery of Small Molecules. *Curr. Opin. Biotechnol.* 2**004**, *15*, 513-517.

34. Nam, K. T.; Kim, D.-W.; Yoo, P. J.; Chiang, C.-Y.; Meethong, N.; Hammond, P. T.; Chiang, Y.-M.; Belcher, A. M. Virus-Enabled Synthesis and Assembly of Nanowires for Lithium Ion Battery Electrodes. *Science* **2006**, *312*, 885-888.

35. Jutz, G.; Boker, A. Bionanoparticles as Functional Macromolecular Building Blocks - a New Class of Nanomaterials. *Polymer* **2011**, *52*, 211-232.

36. Steinmetz, N. F.; Evans, D. J. Utilisation of Plant Viruses in Bionanotechnology. *Org. Biomol. Chem.* **2007**, *5*, 2891-2902.

37. Endo, M.; Fujitsuka, M.; Majima, T. Porphyrin Light-Harvesting Arrays Constructed in the Recombinant Tobacco Mosaic Virus Scaffold. *Chem.-Eur. J.* **2007**, *13*, 8660-8666.

38. Matsumoto, N. M.; Prabhakaran, P.; Rome, L. H.; Maynard, H. D. Smart Vaults: Thermally-Responsive Protein Nanocapsules. *ACS Nano* **2013**, *7*, 867-874.

39. Zhen, Z. P.; Tang, W.; Chen, H. M.; Lin, X.; Todd, T.; Wang, G.; Cowger, T.; Chen, X. Y.; Xie, J. Rgd-Modified Apoferritin Nanoparticles for Efficient Drug Delivery to Tumors. *ACS Nano* **2013**, *7*, 4830-4837.

40. Kedersha, N. L.; Rome, L. H. Isolation and Characterization of a Novel Ribonucleoprotein Particle - Large Structures Contain a Single Species of Small Rna. *J. Cell Biol.* **1986**, *103*, 699-709.

41. Kedersha, N. L.; Miquel, M. C.; Bittner, D.; Rome, L. H. Vaults .2. Ribonucleoprotein Structures Are Highly Conserved among Higher and Lower Eukaryotes. *J. Cell Biol.* **1990**, *110*, 895-901.

42. Suprenant, K. A. Vault Ribonucleoprotein Particles: Sarcophagi, Gondolas, or Safety Deposit Boxes? *Biochemistry* **2002**, *41*, 14447-14454.

43. Kong, L. B.; Siva, A. C.; Rome, L. H.; Stewart, P. L. Structure of the Vault, a Ubiquitous Cellular Component. *Structure with Folding & Design* **1999**, *7*, 371-379.

44. Kedersha, N. L.; Heuser, J. E.; Chugani, D. C.; Rome, L. H. Vaults .3. Vault Ribonucleoprotein-Particles Open into Flower-Like Structures with Octagonal Symmetry. *J. Cell Biol.* **1991**, *112*, 225-235.

45. Kickhoefer, V. A.; Han, M.; Raval-Fernandes, S.; Poderycki, M. J.; Moniz, R. J.; Vaccari, D.; Silvestry, M.; Stewart, P. L.; Kelly, K. A.; Rome, L. H. Targeting Vault Nanoparticles to Specific Cell Surface Receptors. *ACS Nano* **2009**, *3*, 27-36.

46. Buehler, D. C.; Toso, D. B.; Kickhoefer, V. A.; Zhou, Z. H.; Rome, L. H. Vaults Engineered for Hydrophobic Drug Delivery. *Small* **2011**, *7*, 1432-1439.

47. Chen, G.; Hoffman, A. S. Temperature-inudced Phase Transition Behaviours of Random vs. Graft Copolymers of *N*-Isopropylacrylamide and Acrylic Acid. *Macromol. Rapid Commun.* **1995**, *16,* 175-182.

48. Dong, L.C.; Hoffman, A. S. A Novel Approach for Preparation of pH-Sensitive Hydrogels for Enteric Drug Delivery. *J. Control. Release* **1991**, *15*, 141-152.

49. Yin, X.; Hoffman, A. S.; Stayton, P. S. Poly(*N*-isopropylacrylamide-*co*-Acrylic Acid) Copolymers that Respond Sharply to Temperature and pH. *Biomacromolecules* **2006**, *7*, 1381-1385.

50. Moad, G.; Rizzardo, E.; Thang, S. H. Living Radical Polymerization by the Raft Process - a Third Update. *Aust. J. Chem.* **2012**, *65*, 985-1076.

51. Perrier, S.; Takolpuckdee, P.; Mars, C. A. Reversible Addition-Fragmentation Chain Transfer Polymerization: End Group Modification for Functionalized Polymers and Chain Transfer Agent Recovery. *Macromolecules* **2005**, *38*, 2033-2036.

52. Duncan, R. Drug Polymer Conjugates - Potential for Improved Chemotherapy. *Anti-Cancer Drugs* **1992**, *3*, 175-210.

53. Soppimath, K. S.; Tan, D. C. W.; Yang, Y. Y. Ph-Triggered Thermally Responsive Polymer Core–Shell Nanoparticles for Drug Delivery. *Adv. Mater.* **2005**, *17*, 318-323.

54. Mancini, R. J.; Lee, J.; Maynard, H. D. Trehalose Glycopolymers for Stabilization of Protein Conjugates to Environmental Stressors. *J. Am. Chem. Soc.* **2012**, *134*, 8474-8479.

Chapter 4

Synthesis of Nanogel-Protein Conjugates[‡]

4.1. Introduction

The development of therapeutic encapsulated nanomaterials is critical for the delivery of therapeutic agents.[1,2] "Smart" or stimuli-responsive materials have been synthesized which encapsulate lipophilic small molecules and release them in response to external triggers for various applications.[3] Furthermore, incorporation of multiple molecules into a single carrier is of great interest in areas such as theranostics and combinatorial therapy.[4,5] Conjugation of synthetic polymers to therapeutic proteins has significant advantages over unmodified counterparts, because the resulting nanomaterials often exhibit improved therapeutic activity.[6]

Due to their size, physical properties, and high degree of functionality, polymeric nanogels are ideal materials for drug delivery.[7-10] Synthesis of nanogels and similar polymeric nanomaterials has been achieved by a variety of methods including micromolding techniques,[11] emulsion methods,[12,13] dispersion polymerizations,[14,15] and crosslinking of polymeric starting materials.[16-19] Thayumanavan and co-workers have previously reported polymeric nanogels, which demonstrated excellent stability and encapsulation capabilities.[20-23] These nanogels can be assembled in aqueous solution by a simple self-crosslinking reaction from random copolymer precursors in which the template structure contains a hydrophilic monomer, poly(ethylene glycol) methyl ether methacrylate (PEGMA), and a hydrophobic monomer, pyridyl disulfide methacrylate (PDSMA), that is also used as the cross-linker. This self-crosslinking strategy avoids the harsh conditions of microemulsion polymerization that would be incompatible for encapsulation of sensitive therapeutic peptides. Manipulation of the polymeric structure affords control over encapsulation of hydrophilic/hydrophobic molecules as well as ligand incorporation. This system provides for well defined nanogels with sizes ranging from 10 to 200 nm, such that

nanogels could be designed to take advantage of the enhanced permeation and retention (EPR) effect.[24] These nanogels have been shown to successfully encapsulate lipophilic small molecules such as 1,1'-dioctadecyl-3,3,3',3'-tetramethylindocarbocyanine perchlorate (DiI), a lipophilic carbocyanide dye, and doxorubicin. The gels were also easily surface-modified by thiol-containing ligands such as cysteine-modified folic acid.[20-23] Thayumanavan and co-workers have also reported a drug delivery system based on this nanogel technology that concurrently encapsulates lipophilic small molecules within the interior of a nanoassembly and complexes negatively charged proteins at the positively charged nanogel surface.[23] Although this non-covalent electrostatic interaction is a simple way to modify hydrogels, it is less robust and therefore may not be suitable for some applications. Covalent conjugation of proteins to the nanogel surface is an alternative to physical adsorption. By covalently conjugating proteins to the nanogel surface, the proteins will remain bound to the nanogel in complex biological environments such as blood for longer periods of time than if the protein and nanogel were bound by electrostatic interactions.

A wide variety of materials have been conjugated to proteins such as small molecules, polymers, and nanoparticles.[25-27] Protein PEGylation, pioneered by Abuchowski and co-workers,[28,29] has proven to effectively stabilize proteins *in vivo*,[30] and this strategy is currently used in several protein-based therapeutics.[31] Controlled radical polymerization techniques (CRP) have been employed for the preparation of protein-polymer conjugates due to its tolerance of various monomer types, control of molecular weight distributions, and the ease of introducing protein reactive end-group functionality.[27,32,33] End-groups such as amine-reactive aldehydes[34] as well as cysteine-reactive maleimides[35,36] and pyridyl disulfides[37,38] are typically used in the

formation of protein-polymer conjugates. Proteins can be conjugated to polymeric nanomaterials such as polymersomes[39] and micelles.[40] For example, Lu and co-workers have conjugated BSA to the exterior of self-assembled glycopolymer micelles.[40]

The disulfide cross-linked pPEGMA nanogel system, developed by Thayumanavan and co-workers, is a simple and effective platform for the construction of multi-functional drug delivery vehicles. In collaboration with the Thayumanavan group, we have developed the methodology for the covalent conjugation of proteins to nanogels. Herein we report the conjugation of bovine serum albumin (BSA) to the surface of DiI encapsulated nanogels.

4.2. Results and Discussion

4.2.1. Disulfide Cross-linked Nanogel Formation

Nanogels were prepared by the Thayumanavan research group, according to previously reported literature procedures (Figure 4.1).[8] The nanogel random copolymer precursor contained 29% PEGMA and 71% PDSMA. PDSMA serves as a cross-linker for the nanogel formation and as a reactive handle on the surface of the nanogel, and also increases the hydrophobicity of the nanogel interior.

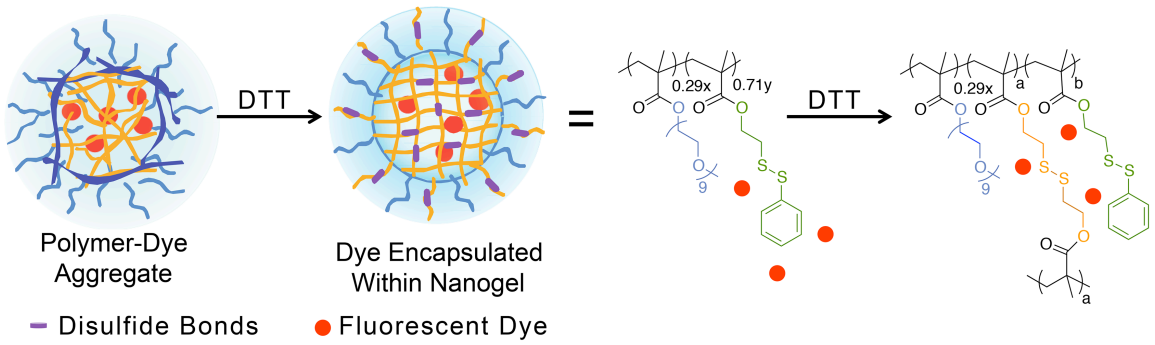

Figure 4.1. Nanogel formation and polymeric precursors.

4.2.2. Conjugation and Purification of BSA to Nanogels

We used BSA as a model protein to demonstrate the conjugation of proteins to the DiI loaded nanogels (NG-DiI). BSA is a 66.5 kDa protein which contains a surface exposed free cysteine residue (Cys34). The conjugation was expected to proceed through a simple thiol-disulfide exchange reaction between the free cysteine of BSA and the PDS moieties present on the nanogel surface. Although the BSA Cys 34 has been successfully used for polymer conjugation,[37] direct conjugation to the nanogel surface was not successful. We believe this is

due to the size of the nanogels, which are much larger and have a bulkier structure than the linear and comb type polymers previously conjugated to BSA.

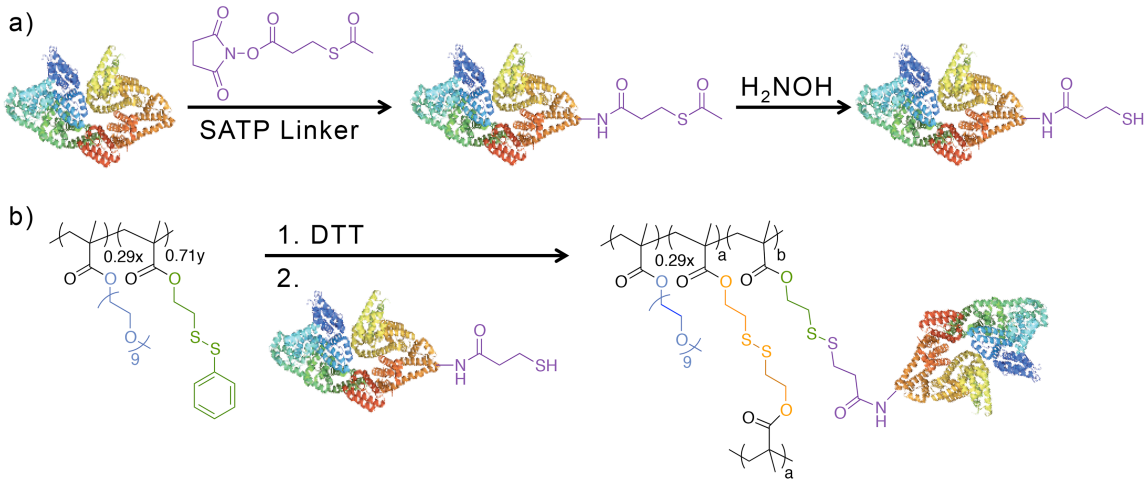

Scheme 4.1. (a) addition of free thiols to BSA, (b) NG-DiI-BSA conjugate formation.

To overcome this obstacle, extended thiol groups were introduced to BSA by modification with the well-known thiolating agent SATP (Scheme 4.1.a). The resulting thiolated-BSA contained three additional thiol groups ([BSA]:[Thiol] = [1]:[4]). Nanogel conjugation was then conducted by incubating the thiolated-BSA with the nanogels in a ratio of [NG-DiI]:[BSA] = [1]:[2] in a pH 7.5 50mM phosphate buffer (Scheme 4.2.b). The crude conjugation mixture was then purified and analyzed by size exclusion chromatography (SEC) (Figure 4.2). In SEC, larger macromolecules elute from the column faster than smaller macromolecules. Unreacted BSA and NG-DiI have retention times of 60 and 55 minutes, respectively. Conjugation is evident due to the appearance of the NG-DiI-BSA conjugate peak at a retention time of ~46 min. A high molecular weight aggregate, with a retention time ~30 min, was also observed; this aggregate was also present in the unmodified nanogels. Fractions containing this aggregate were not collected with the purified nanogel conjugates.

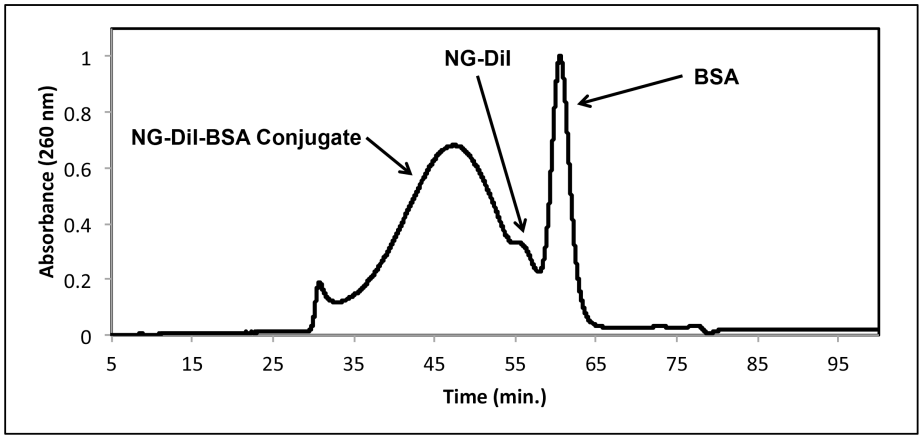

Figure 4.2. Normalized SEC chromatogram of the nanogel conjugation mixture.

4.2.3. Analysis of Nanogel-BSA Conjugate Size by Dynamic Light Scattering

Next, differences in size between NG-DiI, BSA and the NG-DiI-BSA conjugates were measured by dynamic light scattering (DLS). The hydrodynamic diameter of the NG-DiI was measured to be 14 nm, and the thiolated-BSA was measured to be 8 nm. The purified NG-DiI-BSA conjugates were found to have a hydrodynamic radius of 25.5 nm, which indicates protein conjugation to the NG-DiI nanogels (Figure 4.3).

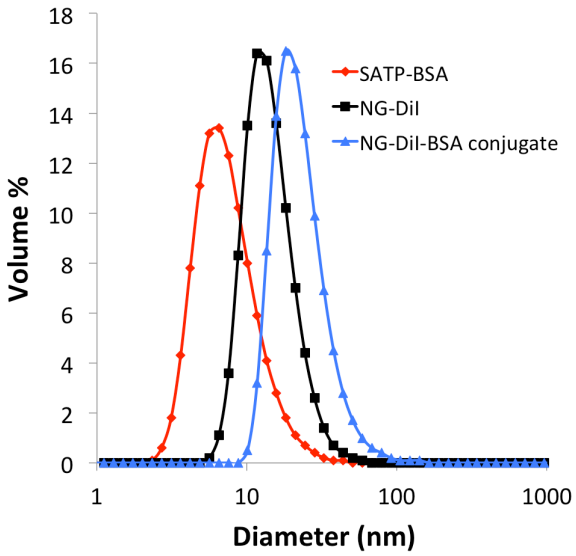

Figure 4.3. DLS size measurements of thiolated-BSA (8 nm, red trace), NG-DiI (14 nm, black trace), and NG-DiI-BSA conjugates (25.5 nm, blue trace).

4.2.4. Analysis of Nanogel-BSA Conjugate Agarose Gel Electrophoresis

Conjugation of thiolated-BSA to the DiI-NG nanogels was analyzed by agarose gel electrophoresis (Figure 4.4). In order to visualize the co-localization of the DiI-NG and the thiolated-BSA, the thiolated-BSA was labeled with an AlexaFluor 488 (AF488) fluorophore and conjugated to the DiI as described earlier. The unmodified NG-DiI (Figure 4.4**,** lane 1) appears red and at the top of the gel. The thiolated-AF488-BSA appears as a green band at the bottom of the gel (Figure 4.4, lane 4). Conjugation is evident by the shift in the band corresponding to the NG-DiI-AF488-BSA conjugate towards the cathode (Figure 4.4, lane 2). Furthermore, the band appears orange as a result of the co-localization of the red DiI and green AF488 fluorophores present on the nanogels and protein, respectively.

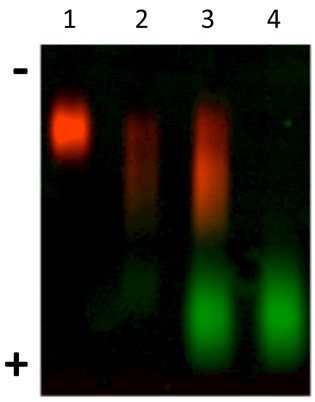

Figure 4.4. Agarose electrophoresis gel of unmodified NG-DiI, NG-DiI-AF-488 BSA conjugate, crude NG-DiI-AF488-BSA, and AF488-BSA visualized on a fluorescent gel imager (lane 1 = NG-DiI; lane 2 = NG-DiI-BSA conjugate; lane 3 = crude NG-DiI-BSA; lane 4 = AF488-BSA).

4.2.5. Analysis of Nanogel-BSA Conjugate by SDS-PAGE

The NG-DiI-AF488 conjugates were also analyzed by sodium dodecyl sulfate polyacrylamide gel electrophoresis (SDS-PAGE) and visualized on a fluorescence gel imager. Free BSA (Figure 4.5, lanes 1 and 4) can be seen as a green band and free NG-DiI as a red band (Figure 4.5, lanes 2 and 5). When the DiI-NG nanogel and the AF488-BSA are conjugated, the color is observed as yellow under non-reducing conditions (Figure 4.5, lane 6), demonstrating co-localization of the two fluorophores. Once the samples are subjected to reducing conditions release of the protein is evidenced by the appearance of green color again (Figure 4.5, lane 3) and disappearance of the red color from the release of DiI dye upon dissolution of the nanogel. Interesting, the band for the unconjugated nanogel (Figure 4.5, lane 2) did show the red fluorescence of the DiI under reducing conditions; however, the intensity was decreased. This indicated that the unmodified nanogel cleaved to some extent, but did not completely degrade during the short exposure time to DTT. It may be that the presence of the protein facilitates reduction of the nanogel because of its hydrophilic nature or that residual pyridyl disulfides on

the unmodified gels cause reoxidation of the material. This is interesting because it suggests that nanogel degradation may be tunable depending on what is conjugated to the outer surface.

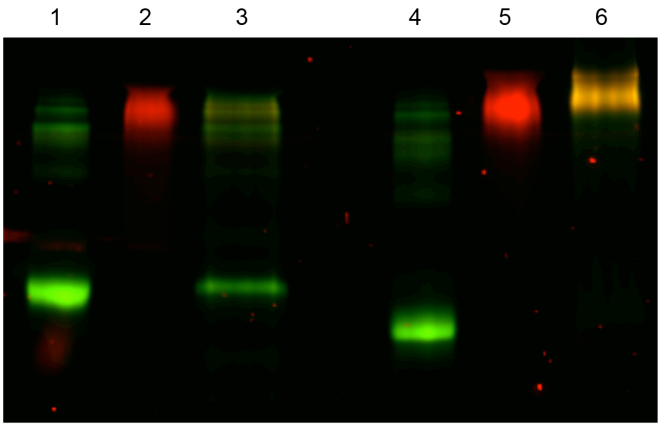

Figure 4.5. SDS-PAGE visualized on a fluorescence gel imager (Lane 1: BSA reducing conditions; Lane 2: NG-DiI reducing conditions; Lane 3: NG-DiI-BSA conjugate reducing conditions; Lane 4: BSA non-reducing conditions; Lane 5: NG-DiI non- reducing conditions; Lane 6: NG-DiI-BSA conjugate non-reducing conditions).

Together, this data demonstrates that proteins can be successfully conjugated to nanogels loaded with hydrophobic molecules. Development of such nanogel-protein conjugates provides a tool for the incorporation of imaging agents and therapeutic proteins for theranostic or combinatorial therapy applications. The use of nanocarriers for theranostics provides the opportunity for image-guided therapy. This ability to monitor treatment in real time enhances the probability of providing a more accurate disease treatment by allowing physicians to detect and treat simultaneously. In addition to this, combination of several therapeutics in a single carrier, especially if incorporation of therapeutics with different characteristics is facilitated, may

enhance the effectiveness of the therapy by providing a synergistic therapeutic effect. Importantly the data show that proteins can be attached to these nanogels, suggesting that targeting proteins or antibodies may be conjugated to the nanogels to increase effectiveness of therapeutic treatments. Investigation into some of these applications is currently underway.

4.3 Experimental

4.3.1 Materials

The nanogels were provided by the Thayumanavan research group (UMass Amherst) according to previous literature.[21] Bovine serum albumin (BSA), UltraPure Agarose and buffer materials were purchased from commercial sources (Fischer, Sigma-Aldrich or Invitrogen) and were used as received. Pre-cast Any-kD Mini-PROTEAN-TGX gels and 10x Tris/Glycine/SDS buffer solution for SDS-PAGE studies were purchased from Bio-Rad. All buffers for protein conjugations were degassed by bubbling with argon for 30 min, and filtered through a 0.22 micron filter. *N*-Succinimidyl-*S*-acetylthiopropionate (SATP) was synthesized according to previous literature.[41]

4.3.2 Analytical Techniques

Dynamic light scattering (DLS) measurements were performed using a Malvern Nanozetasizer. UV-Visible spectroscopy was conducted on Thermo Scientific NanoDrop 2000 and Biomate 5 spectrophotometers. Fast protein liquid chromatography (FPLC) with SEC columns was performed on a Bio-Rad BioLogic DuoFlow chromatography system equipped with a GE Healthcare Life Sciences Superose 6 10/300 column. A 50 mM sodium phosphate (pH 7.5) buffer containing 15 mM NaCl at 4 °C was used as the solvent (flow rate: 0.3 mL/min). Fluorescent gel images were obtained on a Bio-Rad FX Pro Plus Fluorimager/PhosphorImager.

4.3.3 Methods

Preparation of Thiolated-AlexaFluor 488-BSA: Thiol enriched AlexaFluor 488 labeled BSA was prepared by modifying a literature procedure.[42] BSA (5 mg) was dissolved in 0.5 mL of 50 mM sodium phosphate (pH 7.5) containing 1 mM ethylenediaminetetraacetic acid (EDTA). Then, 5 μL of SATP in DMF (16 mg/mL) was added to the BSA solution, and the mixture was incubated for 1 h at 20 °C. To the BSA solution, 1.75 mL of the EDTA in 50 mM sodium phosphate pH 7.5 buffer was added, followed by 250 μL of AlexaFluor 488 carboxylic acid succinimidyl ester in DMF (2 mg/mL). This solution was incubated for 1 h at 20 °C. The SATP and AlexaFluor 488 modified BSA was then purified by ultrafiltration (Amicon Ultra, 30 kDa MWCO). After purification, SATP-AlexaFluor 488-BSA was diluted in 50 mM sodium phosphate buffer (pH 7.5) containing 1 mM EDTA up to a total volume of 0.5 mL and 10 mg/mL concentration. To deprotect the acetylated thiols, 50 μL of a solution containing 0.5 M hydroxyl amine hydrochloride in 50 mM sodium phosphate buffer (pH 7.5) containing 25 mM EDTA was then added to the SATP-AlexaFluor 488-BSA solution and incubated for 2 hours at 20 °C. Following deprotection with hydroxylamine, the thiolated-AlexaFluor 488-BSA was purified by FPLC and concentrated to a final concentration of 2 mg/mL by ultrafiltration. Ellman's assay was used to determine the extent of the thiol-modification (BSA: free thiol; 1:4.1). UV-Vis spectroscopy was used to determine the extent of AlexaFluor 488 labeling of BSA (BSA: AlexaFluor 488; 1:1.7).

Conjugation of Thiolated-AlexaFluor 488-BSA to DiI Nanogels: A solution of 6% cross-linked, 2 wt% DiI encapsulated nanogels (0.50 mg) in 250 μL 50 mM sodium phosphate (pH 7.5) with 1 mM EDTA was added to a 250 μL solution of thiolated-AlexaFluor 488-BSA (1 mg) in the same buffer. The solution was then agitated for 24 hours at 4 °C on a thermo-shaker (TSZ Scientific). The resulting conjugates were purified by SEC.

4.4. Conclusions

We have demonstrated the versatility of this disulfide cross-linked polymeric nanogel system to encapsulate lipophilic small molecules on the interior and conjugate proteins at the nanogel exterior. BSA was modified with a thiol linker, and was readily conjugated to the nanogels *via* disulfide exchange reactions with pyridyl disulfide moieties at the nanogel exterior. The results suggest that this nanogel system is a simple and effective platform for development of sophisticated drug delivery systems. This work provides the groundwork for successful application of therapeutic proteins and antibodies to the nanogels, which would be important for selective targeting of the nanogels.

4.5 References

‡Portions of Chapter 4 have been published as: Matsumoto, N. M.; Gonzalez-Toro, D. C.; Chacko, R. T.; Maynard, H. D.; Thayumanavan, S. Synthesis of Nanogel-Protein Conjugates. *Polymer Chem.* **2013**, *4*, 2464-2469.

1. Baldwin, S. P.; Saltzman, W. M. Materials for Protein Delivery in Tissue Engineering. *Adv. Drug Delivery Rev.* **1998**, *33*, 71-86.
2. Avichezer, D.; Schechter, B.; Arnon, R. Functional Polymers in Drug Delivery: Carrier-Supported Cddp (Cis-Platin) Complexes of Polycarboxylates - Effect on Human Ovarian Carcinoma. *React Funct Polym* **1998**, *36*, 59-69.
3. Zha, L.; Banik, B.; Alexis, F. Stimulus Responsive Nanogels for Drug Delivery. *Soft Matter* **2011**, *7*, 5908-5916.
4. Agrawal, V.; Paul, M. K.; Mukhopadhyay, A. K. 6-Mercaptopurine and Daunorubicin Double Drug Liposomes - Preparation, Drug-Drug Interaction and Characterization. *J. Liposome R.* **2005**, *15*, 141-155.
5. Hoffmann, S.; Vystrcilova, L.; Ulbrich, K.; Etrych, T.; Caysa, H.; Mueller, T.; Maeder, K. Dual Fluorescent Hpma Copolymers for Passive Tumor Targeting with Ph-Sensitive Drug Release: Synthesis and Characterization of Distribution and Tumor Accumulation in Mice by Noninvasive Multispectral Optical Imaging. *Biomacromolecules* **2012**, *13*, 652-663.
6. Broyer, R. M.; Grover, G. N.; Maynard, H. D. Emerging Synthetic Approaches for Protein-Polymer Conjugations. *Chem. Commun.* **2011**, *47*, 2212-2226.

7. Asadian-Birjand, M.; Sousa-Herves, A.; Steinhilber, D.; Cuggino, J. C.; Calderon, M. Functional Nanogels for Biomedical Applications. *Curr. Med. Chem.* **2012**, *19*, 5029-5043.

8. Raemdonck, K.; Demeester, J.; De Smedt, S. Advanced Nanogel Engineering for Drug Delivery. *Soft Matter* **2009**, *5*, 707-715.

9. Oh, J. K.; Drumright, R.; Siegwart, D. J.; Matyjaszewski, K. The Development of Microgels/Nanogels for Drug Delivery Applications. *Prog. Polym. Sci.* **2008**, *33*, 448-477.

10. Yallapu, M. M.; Jaggi, M.; Chauhan, S. C. Design and Engineering of Nanogels for Cancer Treatment. *Drug Discov. Today* **2011**, *16*, 457-463.

11. Rolland, J. P.; Maynor, B. W.; Euliss, L. E.; Exner, A. E.; Denison, G. M.; DeSimone, J. M. Direct Fabrication and Harvesting of Monodisperse, Shape-Specific Nanobiomaterials. *J. Am. Chem. Soc.* **2005**, *127*, 10096-10100.

12. Mitra, S.; Gaur, U.; Ghosh, P. C.; Maitra, A. N. Tumour Targeted Delivery of Encapsulated Dextran-Doxorubicin Conjugate Using Chitosan Nanoparticles as Carrier. *J. Control. Release* **2001**, *74*, 317-323.

13. Lee, H.; Mok, H.; Lee, S.; Oh, Y. K.; Park, T. G. Target-Specific Intracellular Delivery of Sirna Using Degradable Hyaluronic Acid Nanogels. *J. Control. Release* **2007**, *119*, 245-252.

14. Rieger, J.; Grazon, C.; Charleux, B.; Alaimo, D.; Jerome, C. Pegylated Thermally Responsive Block Copolymer Micelles and Nanogels Via in Situ Raft Aqueous Dispersion Polymerization. *J. Polym. Sci., Part A: Polym. Chem. Chemistry* **2009**, *47*, 2373-2390.

15. Shen, W. Q.; Chang, Y. L.; Liu, G. Y.; Wang, H. F.; Cao, A. N.; An, Z. S. Biocompatible, Antifouling, and Thermosensitive Core-Shell Nanogels Synthesized by Raft Aqueous Dispersion Polymerization. *Macromolecules* **2011**, *44*, 2524-2530.

16. Thurmond, K. B.; Kowalewski, T.; Wooley, K. L. Water-Soluble Knedel-Like Structures: The Preparation of Shell-Cross-Linked Small Particles. *J. Am. Chem. Soc.* **1996**, *118*, 7239-7240.

17. Rijcken, C. J.; Snel, C. J.; Schiffelers, R. M.; van Nostrum, C. F.; Hennink, W. E. Hydrolysable Core-Crosslinked Thermosensitive Polymeric Micelles: Synthesis, Characterisation and in Vivo Studies. *Biomaterials* **2007**, *28*, 5581-5593.

18. Liu, S. Y.; Weaver, J. V. M.; Tang, Y. Q.; Billingham, N. C.; Armes, S. P.; Tribe, K. Synthesis of Shell Cross-Linked Micelles with Ph-Responsive Cores Using Abc Triblock Copolymers. *Macromolecules* **2002**, *35*, 6121-6131.

19. Cheng, C.; Qi, K.; Germack, D. S.; Khoshdel, E.; Wooley, K. L. Synthesis of Core-Crosslinked Nanoparticles with Controlled Cylindrical Shape and Narrowly-Dispersed Size Via Core-Shell Brush Block Copolymer Templates. *Adv. Mater.* **2007**, *19*, 2830-2835.

20. Ryu, J.-H.; Bickerton, S.; Zhuang, J.; Thayumanavan, S. Ligand-Decorated Nanogels: Fast One-Pot Synthesis and Cellular Targeting. *Biomacromolecules* **2012**, *13*, 1515-1522.

21. Ryu, J.-H.; Chacko, R. T.; Jiwpanich, S.; Bickerton, S.; Babu, R. P.; Thayumanavan, S. Self-Cross-Linked Polymer Nanogels: A Versatile Nanoscopic Drug Delivery Platform. *J. Am. Chem. Soc.* **2010**, *132*, 17227-17235.

22. Ryu, J. H.; Jiwpanich, S.; Chacko, R.; Bickerton, S.; Thayumanavan, S. Surface-Functionalizable Polymer Nanogels with Facile Hydrophobic Guest Encapsulation Capabilities. *J. Am. Chem. Soc.* **2010**, *132*, 8246-8247.

23. Gonzalez-Toro, D. C.; Ryu, J.-H.; Chacko, R. T.; Zhuang, J.; Thayumanavan, S. Concurrent Binding and Delivery of Proteins and Lipophilic Small Molecules Using Polymeric Nanogels. *J. Am. Chem. Soc.* **2012**, *134*, 6964-6967.

24. Savic, R.; Eisenberg, A.; Maysinger, D. Block Copolymer Micelles as Delivery Vehicles of Hydrophobic Drugs: Micelle-Cell Interactions. *J. of Drug Targeting* **2006**, *14*, 343-355.

25. Rana, S.; Yeh, Y.-C.; Rotello, V. M. Engineering the Nanoparticle-Protein Interface: Applications and Possibilities. *Curr. Opin. Chem. Biol.* **2010**, *14*, 828-834.

26. Thompson, S.; Walker, J. M., Ed.; Humana Press: 2009, p 1715-1726.

27. Grover, G. N.; Maynard, H. D. Protein–Polymer Conjugates: Synthetic Approaches by Controlled Radical Polymerizations and Interesting Applications. *Curr. Opin. Chem. Biol.* **2010**, *14*, 818-827.

28. Abuchowski, A.; Vanes, T.; Palczuk, N. C.; Davis, F. F. Alteration of Immunological Properties of Bovine Serum-Albumin by Covalent Attachment of Polyethylene-Glycol. *J. Biol. Chem.* **1977**, *252*, 3578-3581.

29. Pasut, G.; Veronese, F. In *Polymer Therapeutics I*; Satchi-Fainaro, R., Duncan, R., Eds.; Springer Berlin Heidelberg: 2006; Vol. 192, p 95-134.

30. Joralemon, M. J.; McRae, S.; Emrick, T. Pegylated Polymers for Medicine: From Conjugation to Self-Assembled Systems. *Chem. Commun.* **2010**, *46*, 1377-1393.

31. Alconcel, S. N. S.; Baas, A. S.; Maynard, H. D. Fda-Approved Poly(Ethylene Glycol)-Protein Conjugate Drugs. *Polym. Chem.* **2011**, *2*, 1442-1448.

32. Le Droumaguet, B.; Nicolas, J. Recent Advances in the Design of Bioconjugates from Controlled/Living Radical Polymerization. *Polym. Chem.* **2010**, *1*, 563-598.

33. Sumerlin, B. S. Proteins as Initiators of Controlled Radical Polymerization: Grafting-from Via Atrp and Raft. *ACS Macro Letters* **2011**, *1*, 141-145.

34. Tao, L.; Mantovani, G.; Lecolley, F.; Haddleton, D. M. A-Aldehyde Terminally Functional Methacrylic Polymers from Living Radical Polymerization: Application in Protein Conjugation "Pegylation". *J. Am. Chem. Soc.* **2004**, *126*, 13220-13221.

35. Velonia, K.; Rowan, A. E.; Nolte, R. J. M. Lipase Polystyrene Giant Amphiphiles. *J. Am. Chem. Soc.* **2002**, *124*, 4224-4225.

36. De, P.; Li, M.; Gondi, S. R.; Sumerlin, B. S. Temperature-Regulated Activity of Responsive Polymer−Protein Conjugates Prepared by Grafting-from Via Raft Polymerization. *J. Am. Chem. Soc.* **2008**, *130*, 11288-11289.

37. Bontempo, D.; Heredia, K. L.; Fish, B. A.; Maynard, H. D. Cysteine-Reactive Polymers Synthesized by Atom Transfer Radical Polymerization for Conjugation to Proteins. *J. Am. Chem. Soc.* **2004**, *126*, 15372-15373.

38. Liu, J. Q.; Bulmus, V.; Herlambang, D. L.; Barner-Kowollik, C.; Stenzel, M. H.; Davis, T. P. In Situ Formation of Protein-Polymer Conjugates through Reversible Addition Fragmentation Chain Transfer Polymerization. *Angew. Chem.-Int. Edit.* **2007**, *46*, 3099-3103.

39. van Dongen, S. F. M.; Nallani, M.; Cornelissen, J. J. L. M.; Nolte, R. J. M.; van Hest, J. C. M. A Three-Enzyme Cascade Reaction through Positional Assembly of Enzymes in a Polymersome Nanoreactor. *Chem.--Eur. J.* **2009**, *15*, 1107-1114.

40. Xiao, N.-Y.; Li, A.-L.; Liang, H.; Lu, J. A Well-Defined Novel Aldehyde-Functionalized Glycopolymer: Synthesis, Micelle Formation, and Its Protein Immobilization. *Macromolecules* **2008**, *41*, 2374-2380.

41. Liu, L.; Rozenman, M.; Breslow, R. Hydrophobic Effects on Rates and Substrate Selectivities in Polymeric Transaminase Mimics. *Journal of the American Chemical Society* **2002**, *124*, 12660-12661.

42. Hermanson, G. T. *Bioconjugate Techniques*; 2nd ed.; Elsevier: San Diego, 2008.

Chapter 5

Protein Reactive Unsaturated Poly(Ethylene Glycol) Analogs by Ring Opening Metathesis Polymerization

5.1. Introduction

Covalent conjugation of poly(ethylene glycol) (PEG) to proteins, or protein PEGylation, is known to increase stability, solubility, and *in vivo* circulation lifetimes of proteins.[1,2] This strategy has been employed in the development of PEGylated protein therapeutics, which display superior pharmacokinetic properties compared to unmodified proteins. Currently there are 10 such PEGylated protein therapeutics approved for use in the United States.[3]

The activity of PEGylated proteins is highly dependent on the conjugation site. Conjugation of linear PEG and other synthetic polymers, such as poly(oligo PEG) and poly(*N*-isopropylacrylamide), near the protein active site can greatly diminish protein activity. In one example, Greenwald and coworkers reported the complete loss of enzymatic activity after the conjugation of a single PEG to lysozyme.[4] In another example, Haddleton and coworkers reported the conjugation of poly(oligo PEG) to lysozyme, which resulted in the complete loss of lysozyme activity.[5] This apparent drawback to PEGylation and polymer conjugation can be used to modulate protein activity. For example, Roberts and Harris have reported the preparation of hydrolytically degradable ester-containing PEG-lysozyme conjugates that exhibited no bioactivity until the conjugated PEG polymers were cleaved by degradation of the ester group.[6] The authors proposed that this technology could be applied to therapeutic proteins.

Another class of polymers that have been employed to modulate protein activity are stimuli-responsive polymers. Hoffman, Stayton, and others have employed thermo-responsive polymers such as poly(*N*-isopropylacrylamide) (pNIPAAm) to effectively control protein bioactivity. Such protein-pNIPAAm conjugates become inactive at elevated temperatures due to the thermally induced aggregation of the protein-pNIPAAm conjugates. Other thermo-responsive smart polymers have been employed, such as poly(oligo(ethylene glycol)) copolymers used by

Lutz and coworkers for the modification of trypsin.[7] In 2013, Liu and coworkers reported the modulation of glucose oxidase (GOx) activity by the conjugation of poly(oligo PEG)s through disulfide bonds.[8] Conjugation of the polymers greatly diminished GOx activity, and enzyme activity recovered upon cleavage of the polymers with dithiothreitol (DTT).[8] Liu and coworkers noted that loss of enzyme activity of the reduced conjugate may be attributed to denaturation of the protein by DTT.[8] To date, all of the examples of modulating protein activity through polymer conjugation rely on polymer cleavage to return activity to the conjugated protein. There are no examples of degrading the polymer backbone to reestablish protein activity.

To our knowledge, reversibly inactivatable protein-enzyme conjugates that respond to bio-orthogonal chemoselective triggers such as transition metal catalysts have not been reported. Transition metal catalysts including ruthenium-based Grubbs' type olefin metathesis catalysts have been successfully employed for metathesis in aqueous conditions as well as for the synthetic modification of proteins. There are many reports, from the Grubbs groups as well as others, of the development of water-soluble ruthenium metathesis catalysts; however, none of these catalysts are currently commercially available.[9-14] Olefin metathesis has also been conducted in the presence of proteins. Davis and coworkers have demonstrated the utility of the commercially available Hoveyda-Grubbs 2nd generation catalyst (Hoveyda-Grubbs II) for cross-metathesis on proteins functionalized with allylic sulfides. This reaction allowed for cross metathesis with a number of terminal olefin-containing partners, including sugars, lipids, and PEG.[15-19] In another example, Ward and coworkers developed artificial metalloenzymes by incorporating a Hoveyda-Grubbs catalyst onto streptavidin. The artificial metalloenzyme was shown to be highly efficient for ring closing metathesis on small molecules.[20,21]

ROMP is a well established method for the development of bioactive polymers. Kiessling and coworkers have reported the ROMP derived glycopolymers, which were capable of binding proteins.[22-30] In an early example a sulfated neoglycopolymer was prepared *via* ROMP, which was capable of binding P-selectin.[23] In another example ROMP was used for the preparation of glycopolymers capable of binding the lectin Concanavalin A.[22]

There are only several examples of the development of ROMP polymers for protein polymer conjugation.[31] Kane and coworkers, reported the preparation of ROMP polymers containing multiple pendant 2-chloromethylester functionality, which is reactive towards free thiols on cysteine residues at pH 8.0 through a displacement reaction of the chloride.[31] Reaction of this cysteine reactive polymer resulted in protein multimers.[31] In another example, Sleiman and coworkers reported the preparation of block co-polymers with biotin-end-group functionality, capable of binding the protein SAv. Biotin functionality was installed by terminating the ROMP reaction with biotin functionalized vinyl ethers. In aqueous conditions, the biotin-functionalized block co-polymers assembled into micelles, which could be crosslinked *via* the addition of SAv tetramers. To our knowledge, there are no examples of end-functionalized ROMP polymers for the preparation of covalent protein-polymer conjugates.

Grubbs, Marsella, and Maynard have previously reported the ring opening metathesis polymerization (ROMP) of unsaturated crown ether analogs, producing water-soluble unsaturated PEG analogs (Scheme 5.1).[32,33] Polymers ranging from 10 to 200 kDa could be prepared in good yield. Investigations into the cytotoxicity of this polymer with human dermal fibroblasts (HDF) showed the polymer to be non-toxic up to 0.1 mg/mL.[34] Furthermore, treating dilute solutions of this polymer with LiCl and Grubbs 1st generation catalyst (Grubbs I) resulted in a back-biting reaction which yielded the original unsaturated crown ether monomer.

Scheme 5.1. (A.) Lithium templated ring closing metathesis of diallyl triethylene glycol to yield an unsaturated crown ether analog, (B.) ROMP of the unsaturated crown ether to yield an unsaturated PEG analog, (C.) Depolymerization of the unsaturated PEG analog.[32,33]

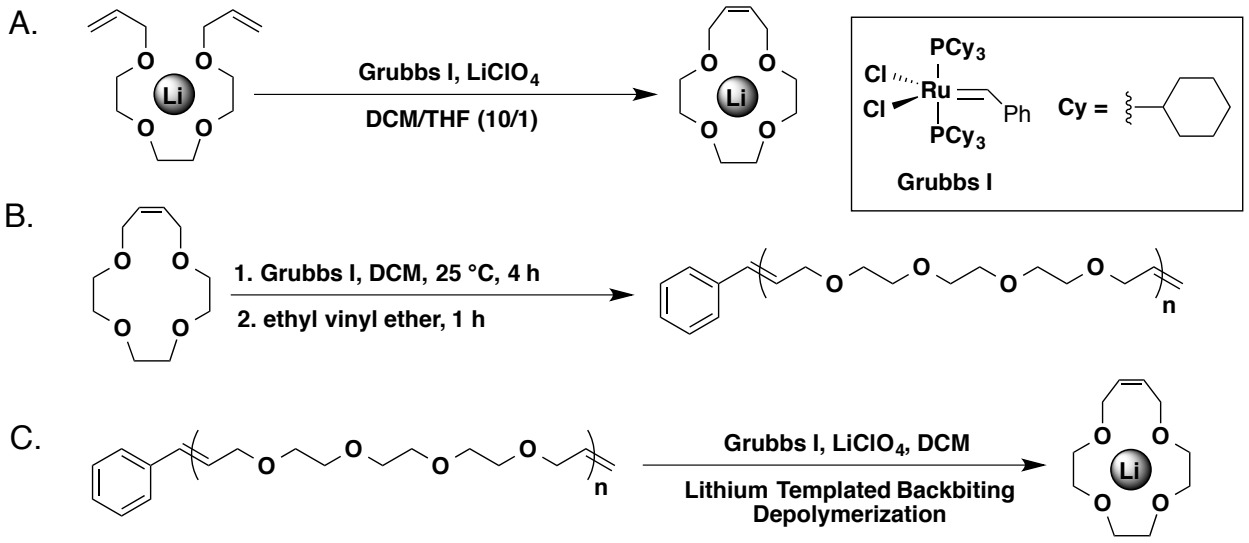

We have expanded on this work by preparing protein reactive unsaturated PEG analogs, *via* ROMP, for conjugation to proteins. Alkenes present in the polymer backbone can be cleaved by reaction with ruthenium metathesis catalysts in aqueous conditions to yield degraded conjugates. We are currently investigating depolymerization of the polymer from the conjugate, as a method to modulate protein activity.

5.2. Results and Discussion

5.2.1. Polymer Synthesis

Aldehyde functionalized PEGs are commonly used for conjugation to surface exposed amines on proteins. **Polymers 1-7** were prepared by ROMP of the unsaturated crown ether monomer **1** (Scheme 5.2), which was prepared according to literature procedure.[32,33] Aldehyde ω-end-group functionality was installed by terminating the ROMP reaction with vinylene carbonate, as previously reported by Kilbinger and coworkers.[35] The polymerizations were carried out under argon atmosphere at 20 °C with a ratio of [Grubbs I]:[monomer **1**] = [1]:[35-175]. After 4 h, the polymerization was terminated by the addition of an excess of vinylene carbonate (>100 eq). The crude polymer was then purified by precipitation from cold diethylether. The resulting polymers were analyzed by ^{1}H NMR and gel permeation chromatography (GPC) to determine the molecular weight (M_n) and polydispersity index (PDI). A total of seven polymers were prepared with varying degrees of polymerization (DP). Polymer PDIs were high (PDI >1.4), which was expected for the polymerization of unstrained monomer **1**. Table 5.1, lists the polymers prepared with degree of polymerization (DP), M_n, and PDI.

Scheme 5.2. ROMP of unsaturated crown ether **1**, to produce **polymers 1-7**.

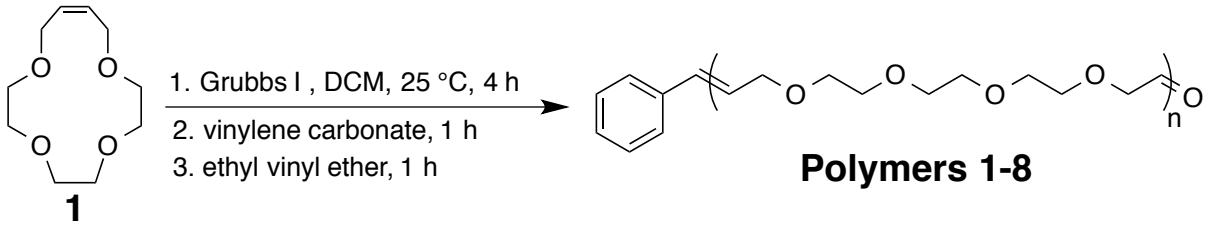

	DP (NMR)	M_n (NMR) (kDa)	PDI (GPC)
Polymer 1	198	40.0	2.88
Polymer 2	175	35.4	1.54
Polymer 3	119	24.1	1.97
Polymer 4	101	20.4	1.39
Polymer 5	60	12.2	1.61
Polymer 6	56	11.5	1.89
Polymer 7	35	7	3.51

Table 5.1. Characterization data (DP, M_n, and PDI) for **polymers 1-7**.

5.2.2. Polymer Degradation in Aqueous Conditions

We have studied the depolymerization of polymer **3** in aqueous conditions. In a typical depolymerization, polymer **3** (3 mg/ml) was dissolved in a phosphate buffer containing 20% *t*-BuOH, 100 mM $MgCl_2$, 100 mM LiCl and 5 mM of Grubbs III (dichloro[1,3-bis(2,4,6-trimethylphenyl)-2-imidazolidinylidene](benzylidene)bis(3-bromopyridine)ruthenium(II)) (Scheme 5.2). The reaction was also conducted without LiCl. After incubating the solution for 18 h at 20 °C, the reaction was stopped *via* the addition of ethyl vinyl ether. The solvent and volatile components were removed by rotary evaporation, followed by lyophilization. The crude reaction mixture was then dissolved in DMF and analyzed by GPC (Figure 5.1) Comparison of the GPC

chromatograms of the polymer and depolymerized products shows major degradation of the polymer when exposed to Grubbs type catalysts in aqueous solution. In organic solvent, lithium ions are necessary for depolymerization of similar unsaturated PEG polymers. However, lithium ions are not necessary for the depolymerization of the conjugated polymer.

Scheme 5.3. Aqueous depolymerization of polymer **3**.

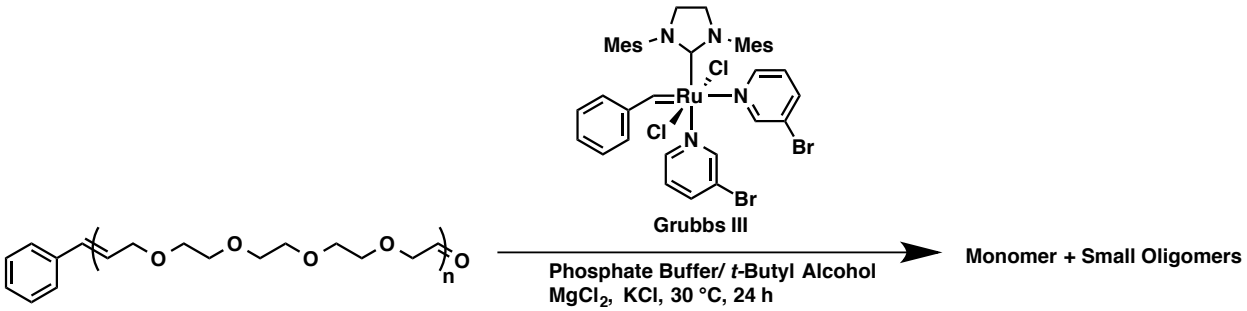

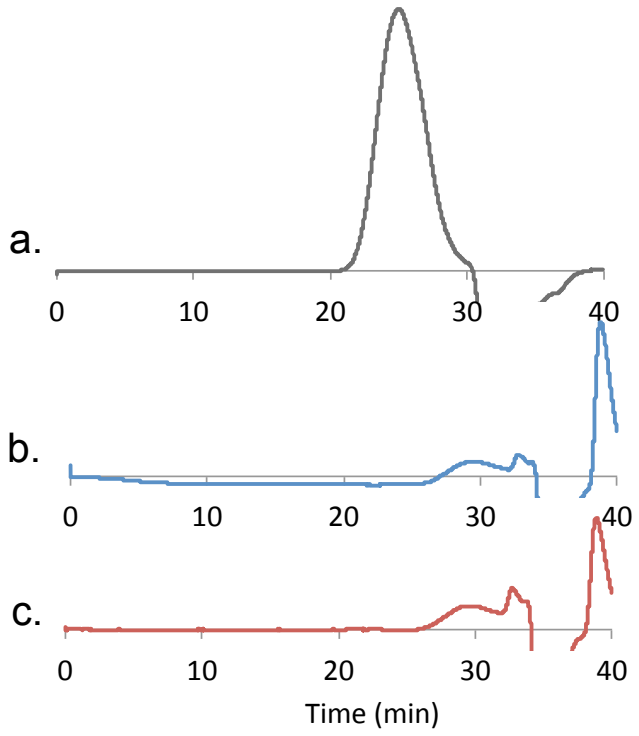

Figure 5.1. GPC chromatograms of (a.) polymer **3** (b.) polymer **3** degraded in the presence of LiCl and (c.) polymer **3** degraded without LiCl.

5.2.3. Polymer Cytotoxicity

Cytotoxicity of the unsaturated PEG analog **polymer 3** and the degraded polymer were evaluated through a LIVE/DEAD viability/cytotoxicity assay using human dermal fibroblasts (HDFs) (Figure 5.2). We found that the polymer is non-toxic up to concentrations of 1 mg/mL. The degraded polymer shows no toxicity to HDFs at 0.5 mg/mL, however the degraded polymer shows slight toxicity at concentrations of 1 mg/mL, with cell viabilities of approximately 90%. Fresh polymer samples were used for these toxicity studies. In previous toxicity studies by Grubbs and Maynard these unsaturated PEG polymers were toxic at 1 mg/mL, this toxicity may have been due to degradation of the polymer after long-term storage.

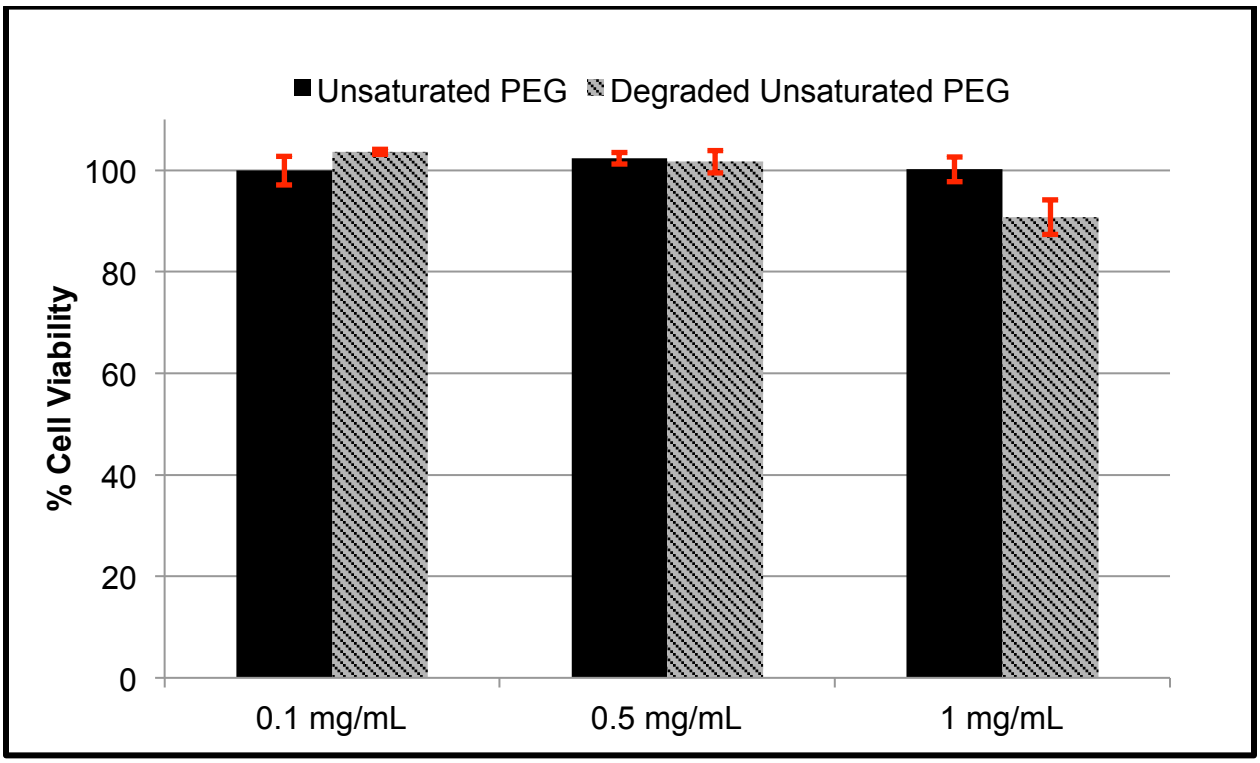

Figure 5.2. Live/Dead viability/cytotoxicity assay of the unsaturated PEG **polymer 3** and the degradation products of **polymer 3** on HDF cells.

5.2.4. Conjugation to Lysozyme

Scheme 5.4. Conjugation of **polymer 2** to Lysozyme by reductive amination.

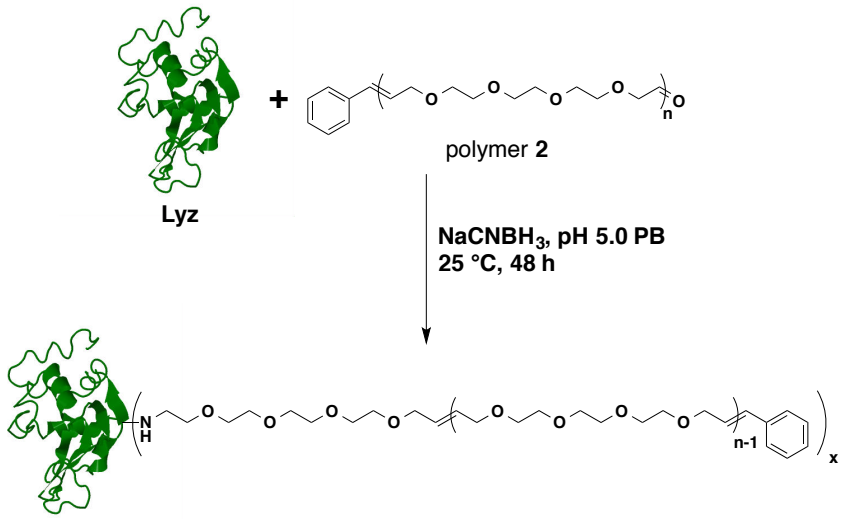

The ω-aldehyde unsaturated PEG polymer **5** was conjugated to lysozyme (Lyz) *via* reductive amination (Scheme 5.4). Lyz and polymer **5** were incubated in a pH 6.0 100 mM phosphate buffer (PB) at 25 °C using a ratio [lysozyme]:[polymer **5**] = 1:50. After 30 min, sodium cyanoborohydride was added to a final concentration of 20 mM in the reaction solution. The conjugation mixture was allowed to incubate for 48 h at 25 °C, before purification by ultracentrifugation. As previously observed by Haddleton and coworkers,[5] long reaction times were necessary to achieve full conjugation of the polymer to the protein. The resulting Lyz-polymer **5** conjugate was analyzed by sodium dodecyl sulfate polyacrylamide gel electrophoresis (SDS-PAGE) (Figure 5.3). Conjugation was evident by a high molecular weight smeared band (Figure 5.3, lane 3), which corresponded to a higher molecular weight than the unmodified Lyz (Figure 5.3, lane 2) The conjugate was also be purified and analyzed *via* size exclusion chromatography (SEC) (Figure 5.4). The increased size of the conjugate was also apparent by

SEC, due to the decreased retention time of the conjugate compared to unmodified Lyz. Based on the SDS-PAGE and SEC results, it is apparent that the lysozyme has been highly conjugated.

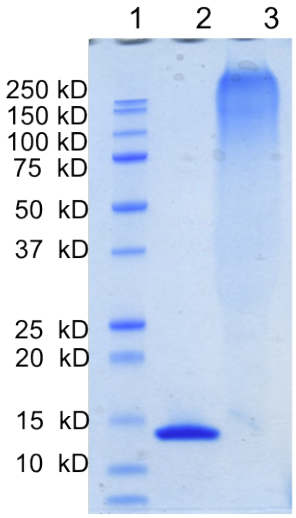

Figure 5.3. SDS-PAGE of Lyz and Lyz-**polymer 5 conjugate (**lane 1: protein marker; lane 2: Lyz; lane 3: Lyz-**polymer 5** conjugate**).**

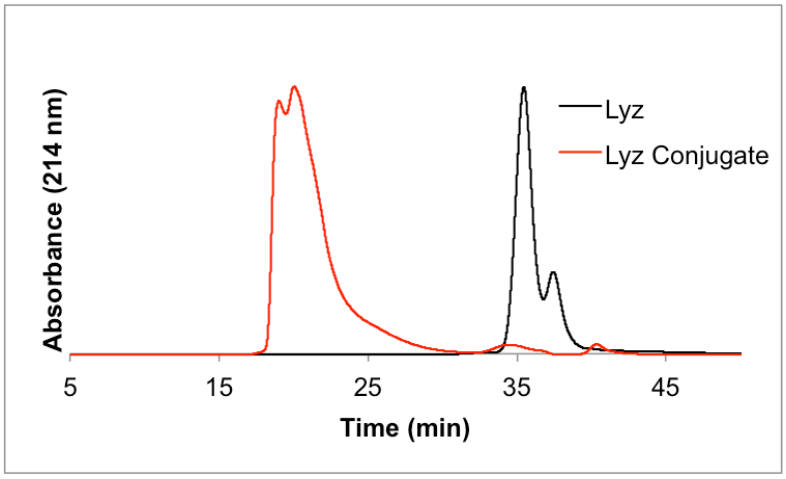

Figure 5.4. SEC chromatogram of Lyz (black trace) and Lyz-**polymer 5** conjugate (red trace).

5.2.5. Depolymerization of Lysozyme Conjugates

Following successful conjugation, depolymerization of the Lyz conjugates with Grubbs 3rd generation catalyst was studied (Scheme 5.5.). Optimal results were obtained using freshly conjugated material with $MgCl_2$ as an additive and *tert*-butyl alcohol as a cosolvent. $MgCl_2$ is often used as an additive in aqueous metathesis because it is a weak Lewis-acid,[36] which inhibits the formation of metathesis inactive catalyst-heteroatom chelates.[36] *Tert*-butyl alcohol has previously been used as a cosolvent to solubilize the ruthenium metathesis catalysts. The Lyz-polymer 1 conjugate was incubated with 5 mM Grubbs III in buffer solution containing 100 mM $MgCl_2$ and 20% *tert*-butyl alcohol. The solution was allowed to incubate at 25 °C for 12 h, after which the catalyst could be removed by pelleting *via* centrifugation. The depolymerized conjugate was analyzed by SDS-PAGE (Figure 5.5). Depolymerization is evident by the decrease in the weight of the depolymerized conjugate (Figure 5.5, lane 4) compared to the conjugate (Figure 5.5, lane 3). Reproducing depolymerization with different conjugate samples has been difficult, fresh samples of polymer and conjugate yielded ideal results. This could be due to isomerization of the polymer backbone from allyl ether to vinyl ether, Ruthenium metathesis catalysts react with vinyl ethers to form metathesis inactive complexes.

Scheme 5.5. Depolymerization of Lyz-**polymer 1** conjugate.

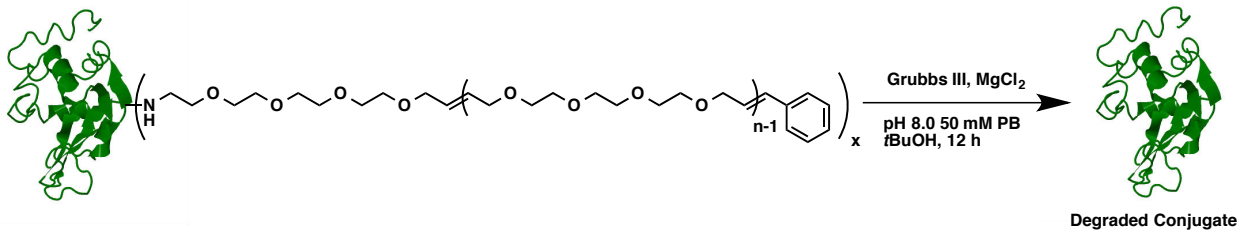

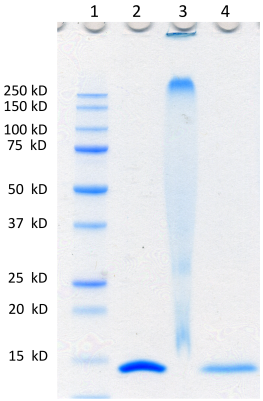

Figure 5.5. SDS-PAGE of Lyz, Lyz-**polymer 1** conjugate, and depolymerized Lyz-**polymer 1** conjugate (lane 1: protein marker; lane 2: Lyz; lane 3: Lyz-**polymer 1** conjugate; depolymerized Lyz-**polymer 1** conjugate).

5.2.6. Bovine Serum Albumin Conjugations and Depolymerizations

Scheme 5.6. Conjugation of **polymer 2** to BSA *via* reductive amination.

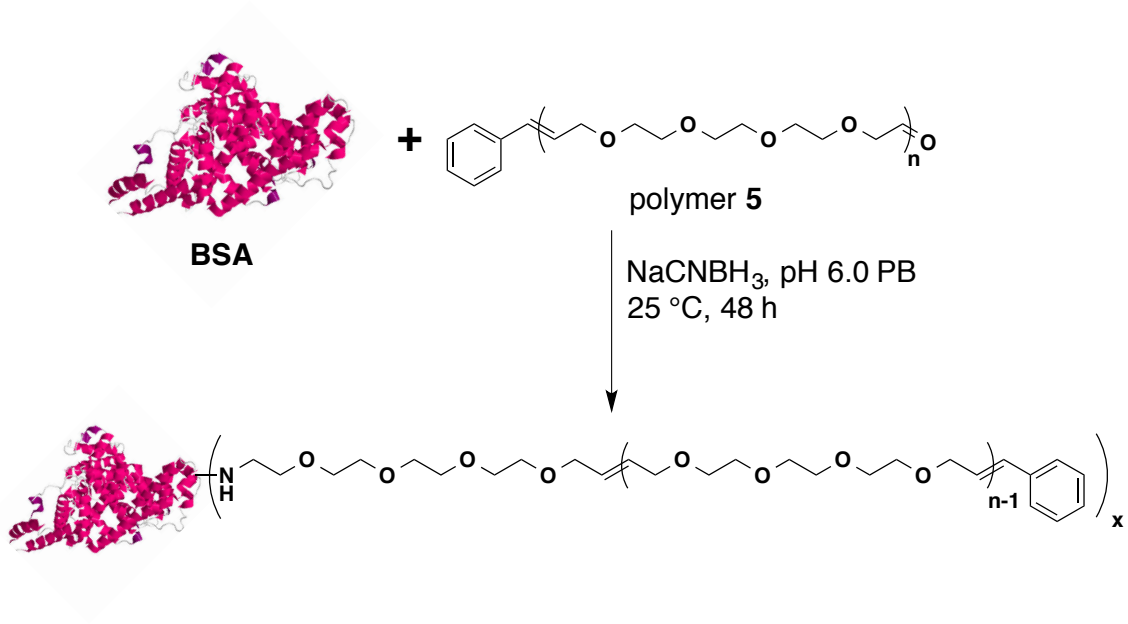

Polymer 5 was conjugated to BSA *via* reductive amination (Scheme 5.6). BSA and 20 molar equivalents of polymer 5 were incubated in a pH 6.0 100 mM PB for 30 min. After 30 min, Sodium cyanoborohydride was then added to achieve a final concentration of 20 mM. The conjugation was incubated for 48 h at 25 °C followed by purification by ultracentrifugation or SEC. SDS-PAGE shows the conjugate (Figure 5.6, lane 3) shifted to a higher molecular weight than the unmodified protein (Figure 5.6, lane 2). BSA is known to oliomerize, these high molecular weight oligomers can be seen on the SDS-PAGE (**Figure 5.6**, lane 2). Analysis of the SEC chromatogram shows the conjugates shifted to a lower retention time than unmodified BSA, indicating that the conjugates are larger in size (Figure 5.7). In the SEC chromatogram of BSA, the BSA can be seen eluting from the column at 23 min and the dimer peak can be seen at 20

min. The conjugate peak is shifted to 19 min and is clearly larger than the BSA dimer. The number of conjugated polymers to BSA is unknown.

Scheme 5.7. Depolymerization of the BSA-**polymer 5** conjugate.

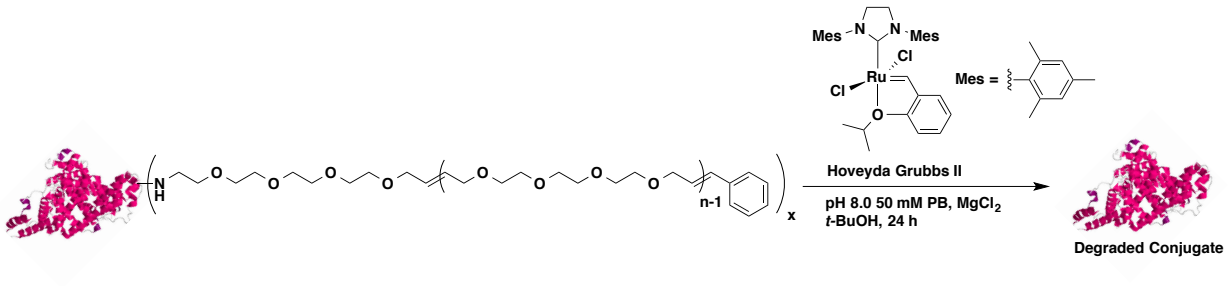

Hoveyda-Grubbs type catalysts have been utilized successfully in aqueous environments and are known to perform well on sterically hindered substrates.[20,21,36] Following successful conjugation, the polymer of the BSA conjugate was depolymerized with Hoveyda-Grubbs II catalyst (Scheme 5.7). The BSA-polymer 5 conjugate was incubated with 2 mM Hoveyda-Grubbs II in buffer solution containing 190 mM $MgCl_2$ and 30% *tert*-butyl alcohol. The solution was allowed to incubate at 35 °C for 3 h followed by purification by ultracentrifugation. Depolymerization was analyzed by SDS-PAGE (Figure 5.6). The depolymerized conjugate (Figure 5.6, lane 4) shifted to a lower molecular weight compared to the conjugate (Figure 5.6, lane 3). Unlike the depolymerization of the Lyz conjugates, the depolymerized BSA conjugate appeared as a faint smeared band on the SDS-PAGE that is lower in molecular weight that the original conjugate. This is most likely due to incomplete depolymerization and the presence of low molecular weight unsaturated PEG oligomers retained on BSA.

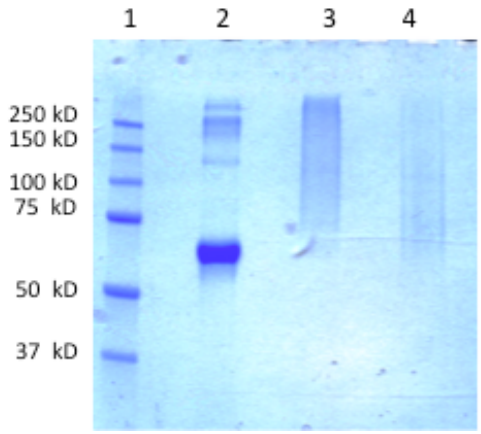

Figure 5.6. SDS-PAGE of BSA, BSA-**polymer 5** conjugate, and depolymerized BSA-**polymer 5** conjugate (lane 1: protein marker; lane 2: BSA; lane 3: BSA-**polymer 5** conjugate; lane 4: depolymerized BSA-**polymer 5** conjugate).

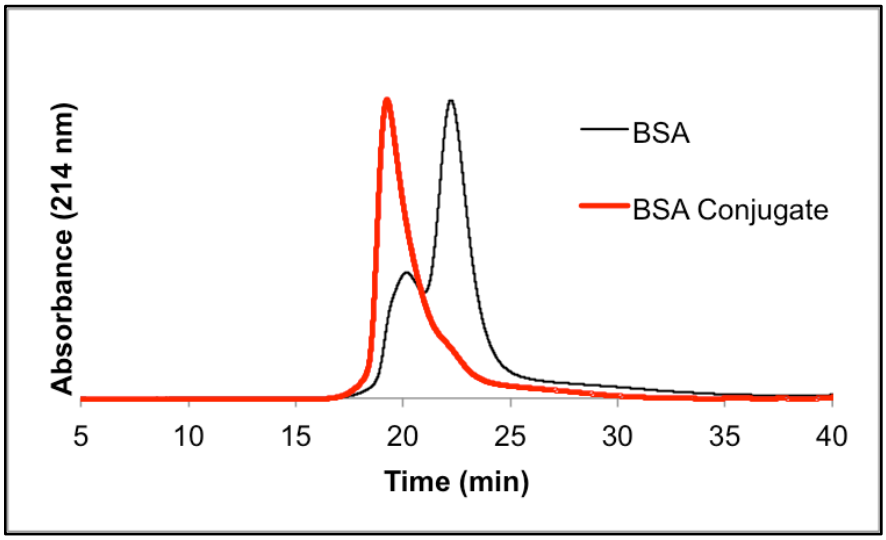

Figure 5.7. SEC chromatogram of BSA (black trace) and BSA-**polymer 5** conjugate (red trace).

This data together shows that ROMP derived polymers can be applied to the preparation of covalent protein-polymer conjugates. Aldehyde-functionalized unsaturated PEG analogs were readily prepared *via* ROMP and conjugated to free-amines present on Lyz and BSA by reductive amination. Reductive amination is a non-specific conjugation technique. It is clear that a high degree of conjugation to Lyz and BSA has been achieved through this route, but the exact number of conjugations per protein has been difficult to quantify. To quantify the extent of conjugation, matrix-assisted laser desorption/ionization time-of-flight (MALDI-TOF) mass spectrometry has been attempted to determine molecular weight of the conjugate, however this was unsuccessful. Site-specific conjugation methods may be necessary to determine exact number of conjugations per protein.

Depolymerization of the unsaturated PEG polymer backbone can be accomplished through the use of Grubbs III and Hoveyda-Grubbs II catalysts with the use of an organic co-solvent. Depolymerization can be achieved on the polymer alone and with the protein-polymer conjugate. Activity of the depolymerized conjugates has been studied, but the results so far are inconclusive. Due to the hydrophobic nature of the catalysts, they may be noncovalently interacting with hydrophobic domains of BSA and Lyz altering protein structure or occupying binding sites. Although ruthenium metathesis catalysts have been used in the presence of proteins, there are no examples of active proteins that have been exposed to ruthenium metathesis catalysts. Work is currently underway to remove residual catalyst from proteins and to determine enzymatic activity of the depolymerized Lyz and BSA unsaturated PEG conjugates. If enzymatic activity can be restored after depolymerization this technology may be applicable to modulating protein activity by sterically inactivating a protein with unsaturated PEGs followed by reactivation by depolymerization. This strategy may be beneficial for biotechnology

applications where it is important to control enzymatic activity, such as enzyme catalysis and point-of-care diagnostics. Due to the use of ruthenium catalysts, this conjugation/depolymerization technology is not amenable to *in vivo* applications.

5.3. Experimental

5.3.1. Materials

All chemicals were purchased from Sigma-Aldrich, Fisher Scientific, and Acros and used as received unless otherwise noted. The proteins BSA and Lyz were obtained from Sigma-Aldrich and used as received. CH_2Cl_2 over CaH_2 and stored under argon. THF was distilled over sodium/benzophenone and stored under argon. Unsaturated crown ether **1** was prepared according to a modified literature procedure.[33]

5.3.2. Analytical Techniques

NMR spectra were obtained on a Bruker 600 MHZ ARX spectrometer. Proton NMR spectra were acquired with a relaxation delay of 2 sec for small molecules and 30 sec for all polymers. Infrared absorption spectra were recorded using a PerkinElmer FT-IR equipped with an ATR accessory. GPC was conducted on a Shimadzu HPLC system equipped with a refractive index detector RID-10A, one Polymer Laboratories PLgel guard column, and two Polymer Laboratories PLgel 5 μm mixed D columns. LiBr (0.1 M) in dimethylformamide (DMF) at 40 °C was used as an eluent (flow rate: 0.60 mL/min). Calibration was performed using near-monodisperse PMMA standards from Polymer Laboratories. SDS-PAGE was performed using Bio-Rad Any kD Mini-PROTEAN-TGX gels. SDS-PAGE protein standards were obtained from Bio-Rad (Precision Plus Protein Pre-stained Standards). For SDS-PAGE analysis, approximately 5 μg of protein was loaded into each lane. Fast protein liquid chromatography (FPLC) was performed on a Bio-Rad BioLogic DuoFlow chromatography system equipped with a GE Healthcare Life Sciences Superdex 75 10/300 column. For BSA and BSA conjugates, a 25 mM sodium phosphate (pH 8.0) buffer containing 400 mM NaCl at 4 °C was used as the solvent

(flow rate: 0.5 mL/min). For Lyz and Lyz conjugates, a 200 mM sodium phosphate (pH 7.0) buffer containing 300 mM NaCl or a 25 mM sodium phosphate (pH 8.0) buffer containing 400 mM NaCl at 4 °C was used as the solvent (flow rate: 0.5 mL/min).

5.3.3. Methods

A typical ROMP of unsaturated crown ether monomer 1 to yield polymer 5: The unsaturated crown ether **1** (278.0 mg, 1.37 mmol) was added to a Schlenk tube containing a magnetic stir bar. The Schlenk tube was subjected to high vacuum for 15 minutes and then refilled with argon gas. Grubbs I (45.1 mg, 0.05 mmol) was added to a second Schlenk tube containing a magnetic stir bar. Dry DCM (0.60 mL) was added to dissolve the solid catalyst and the Schlenk tube was subjected to four freeze-pump-thaw cycles. The polymerization was initiated by transferring the catalyst solution into the Schlenk tube containing monomer **1** *via* syringe. The reaction was stirred for 4 h at 20 °C under argon. After 4 h, the polymerization was terminated by the addition of vinylene carbonate (0.50 mL) and allowed to stir for 45 min, followed by the addition of ethyl vinyl ether (0.50 mL) and then allowed to stir for 30 min. Solvent and volatiles were then removed by high vacuum. The crude reaction mixture was then dissolved in a minimal amount of MeOH and precipitated from diethyl ether 5 times to yield **polymer 5**. ^{1}H NMR (600 MHz, MeOD) δ: 9.79 (s, Aldehyde), 7.37 (m, Ar), 7.30 (t, Ar), 6.60 (d, CH), 6.29 (m, CH), 5.60-5.75 (m, E-alkene), 5.74-5.65 (m, Z-alkene), 5.27 (d), 5.17 (m), 4.17-3.94 (m, OCH_2), 3.76-3.52 (m, OCH_2). M_n by ^{1}H NMR = 12,200 g/mol (targeted 20,100 g/mol). M_n(GPC) = 14,200 g/mol, and PDI = 1.61.

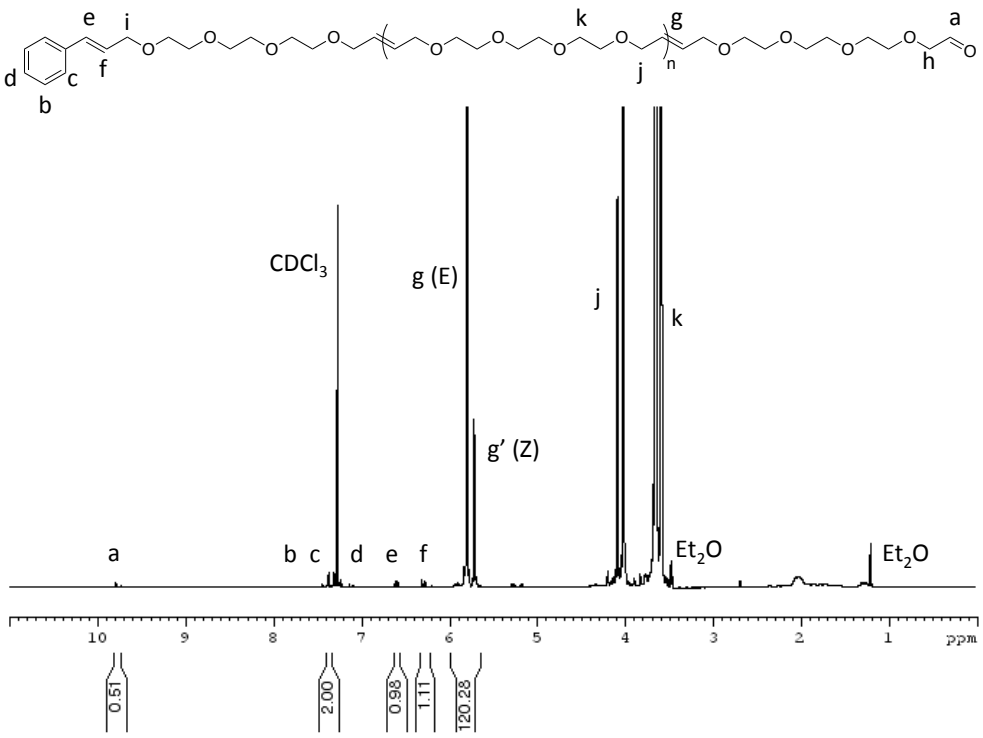

Figure 5.8. ^{1}H NMR (600 MHz, $CDCl_3$) of **polymer 5**.

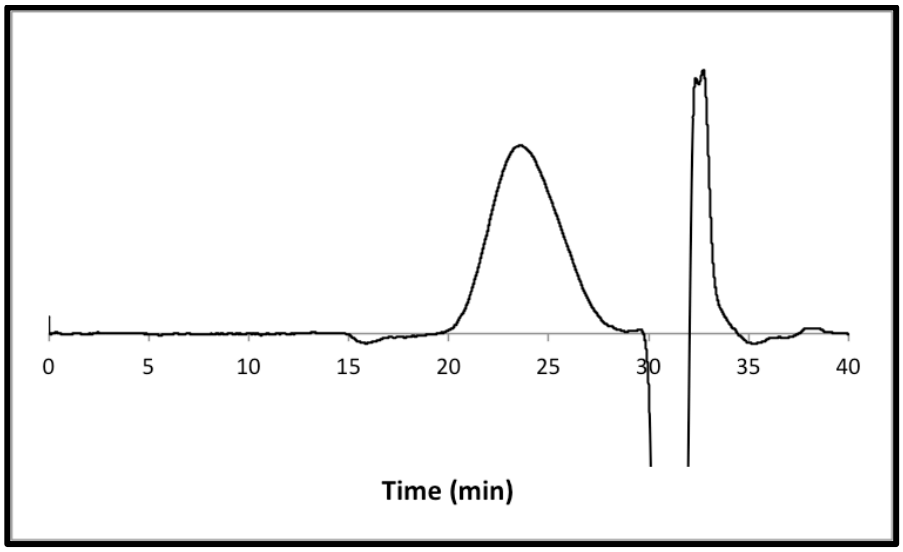

Figure 5.9. GPC chromatogram of **polymer 5,** normalized and analyzed by comparison with monodisperse PMMA standards.

Aqueous depolymerization of Polymer 2: Polymer 2 (3.0 mg, 0.12 μmol) was weighed into a 2 mL vial and dissolved in pH 8.0 50 mM PB containing 100 mM $MgCl_2$ (0.80 mL). A 50 mM stock solution of Grubbs III was prepared in *tert*-butyl alcohol and 0.20 mL of the catalyst solution was added to the polymer solution. The total concentration of catalyst in the reaction was 5 mM. A magnetic stir bar was added and the reaction was sealed under argon. The reaction was stirred for 20 h at 20 °C. After 20 h, the reaction was stopped with the addition of ethyl vinyl ether (0.10 mL) and stirred for 30 min. The ethyl vinyl ether was removed by rotary evaporation, and the crude reaction was lyophilized to remove water. After the water was removed, the remaining solids and oils were redissolved in DMF and analyzed by GPC.

A typical conjugation of Polymer 5 to Lyz: Lyz (1.0 mg, 0.07 μmol) was dissolved in pH 6.0 100 mM PB. **Polymer 5** (42.3 mg, 3.47 μmol) was dissolved in pH 6.0 100 mM PB (0.40 mL). The polymer solution was then added to the Lyz solution and agitated on a temperature controlled thermoshaker at 1250 rpm for 1 h at 25 °C. A 200 mM stock solution of sodium cyanoborohydride was prepared in pH 6.0 100 mM PB, 0.10 mL of the sodium cyanoborohydride solution was added to the solution containing Lyz and the polymer. The reaction was agitated at 1250 rpm for 48 h at 25 °C. The crude reaction was then purified by ultrafiltration (MWCO 10,000 g/mol) or by FPLC, to obtain the conjugate.

A typical conjugation of Polymer 5 to BSA: BSA (1.0 mg, 0.02 μmol) was dissolved in pH 6.0 100 mM PB. **Polymer 5** (3.70 mg, 0.30 μmol) was dissolved in pH 6.0 100 mM PB (0.40 mL). The polymer solution was then added to the BSA solution and agitated on a temperature controlled thermoshaker at 1250 rpm for 1 h at 25 °C. A 200 mM stock solution of sodium

cyanoborohydride was prepared in pH 6.0 100 mM PB, 0.10 mL of the sodium cyanoborohydride solution was added to the solution containing BSA and the polymer. The reaction was agitated at 1250 rpm for 48 h at 25 °C. The crude reaction was then purified by ultrafiltration (MWCO 30,000 g/mol) or by FPLC, to obtain the conjugate.

A typical depolymerization of Lyz-polymer 1 conjugate: An equal volume of a 200 mM $MgCl_2$ solution adjusted to pH 8.0 (50 μL) was added to a solution of Lyz-**polymer 1** (50 μL) conjugate containing 1 mg/mL Lyz. A 25 mM stock solution of Grubbs III degassed *tert*-butyl alcohol was prepared fresh. Stock solution (25 μL) was added to bring the total concentration of catalyst to 5 mM and the total volume percent of *tert*-butyl alcohol to 30%. The reaction mixture was then incubated for 12 h at 25 °C. After 12 h, any precipitate in the solution was pelleted by centrifugation and discarded. The crude mixture was then analyzed by SDS-PAGE.

A typical depolymerization of BSA-polymer 5 conjugate: Magnesium chloride hexahydrate (0.90 mg, 4.44 μmol) was dissolved in a 20 μL of a 1 μg/μL solution of the BSA-**polymer 2** conjugate in pH 8.0 100 mM PB (concentration based on amount of protein). A stock solution of Hoveyda-Grubbs II in degassed *tert*-butyl alcohol was prepared with a catalyst concentration of 5.0 mM. Catalyst stock solution (13.3 μL) was added to bring the final concentration of catalyst to 2 mM and the total volume of *tert*-butyl alcohol to 30%**.** The reaction mixture was incubated at 35 °C for 2 h. SDS-PAGE was conducted on the crude reaction mixture.

Polymer cytotoxicity studies: Cytotoxicity of the unsaturated PEG and degraded products toward human dermal fibroblasts (HDFs, Promocell GmbH) was evaluated using a LIVE/DEAD

viability/cytotoxicity assay (Invitrogen). HDF cells were cultured in fibroblast growth medium containing 2% fetal calf serum (FCS), 1 ng/mL basic fibroblast growth factor, 5 μg/mL insulin, and 1% penicillin-streptomycin. The cells were seeded in 48-well plates at a density of 6 x 10^3 cells per well and incubated at 37 °C and 5% CO_2. After 24 h, the culture media was replaced with 200 μL of the working medium containing the polymers at concentrations of 0.1, 0.5 and 1 mg/mL. After incubation for 24 h, the cells were gently washed with pre-warmed Dulbecco's phosphate buffered saline (D-PBS), and stained with the LIVE/DEAD reagent (2 μM calcein AM and 4 μM ethidium homodimer-1). Fluorescent images of each well were captured on an Axiovert 200 microscope with an AxioCam MRm camera and FluoArc mercury lamp. The number of live and dead cells were counted, and percent cell viability was calculated by dividing the number of live cells by the total number of cells. Percent viability was determined using the formula 100 x (number of live cells / total number of cells). All experiments were conducted in quadruplicate. Each experimental set was normalized to a control of blank medium.

5.4. Conclusions

We have prepared a series of unsaturated PEG analogs with protein-reactive aldehyde ω-end-group functionality and demonstrated conjugation to Lyz and BSA. These polymers as well as the polymers on the protein conjugates can be depolymerized in the presence of ruthenium metathesis catalysts in aqueous conditions. We are currently investigating the modulation of enzymatic activity through conjugation and depolymerization of these conjugates. Due to the necessity for ruthenium catalysts for depolymerization, this technology is not applicable for therapeutic applications. However, we envision that such materials would be valuable for use in a variety of biotechnology applications such as enzymatic catalysis, biosensing applications, and point-of-care diagnostics.

5.5. References

1. Abuchowski, A.; McCoy, J. R.; Palczuk, N. C.; Vanes, T.; Davis, F. F. Effect of Covalent Attachment of Polyethylene-Glycol on Immunogenicity and Circulating Life of Bovine Liver Catalase. *J. Biol. Chem.* **1977**, *252*, 3582-3586.
2. Abuchowski, A.; Vanes, T.; Palczuk, N. C.; Davis, F. F. Alteration of Immunological Properties of Bovine Serum-Albumin by Covalent Attachment of Polyethylene-Glycol. *J. Biol. Chem.* **1977**, *252*, 3578-3581.
3. Alconcel, S. N. S.; Baas, A. S.; Maynard, H. D. Fda-Approved Poly(Ethylene Glycol)-Protein Conjugate Drugs. *Polym. Chem.* **2011**, *2*, 1442-1448.
4. Greenwald, R. B.; Yang, K.; Zhao, H.; Conover, C. D.; Lee, S.; Filpula, D. Controlled Release of Proteins from Their Poly(Ethylene Glycol) Conjugates: Drug Delivery Systems Employing 1,6-Elimination. *Bioconjugate Chem.* **2003**, *14*, 395-403.
5. Tao, L.; Mantovani, G.; Lecolley, F.; Haddleton, D. M. Alpha-Aldehyde Terminally Functional Methacrylic Polymers from Living Radical Polymerization: Application in Protein Conjugation "Pegylation". *J. Am. Chem. Soc.* **2004**, *126*, 13220-13221.
6. Roberts, M. J.; Harris, J. M. Attachment of Degradable Poly(Ethylene Glycol) to Proteins Has the Potential to Increase Therapeutic Efficacy. *J. Pharm. Sci.* **1998**, *87*, 1440-1445.
7. Zarafshani, Z.; Obata, T.; Lutz, J.-F. o. Smart Pegylation of Trypsin. *Biomacromolecules* **2010**, *11*, 2130-2135.
8. Liu, H. H.; Zhang, J. Z.; Luo, X.; Kong, N.; Cui, L.; Liu, J. Q. Preparation of Biodegradable and Thermoresponsive Enzyme-Polymer Conjugates with Controllable Bioactivity Via Raft Polymerization. *Eur. Polym. J.* **2013**, *49*, 2949-2960.

9. Gallivan, J. P.; Jordan, J. P.; Grubbs, R. H. A Neutral, Water-Soluble Olefin Metathesis Catalyst Based on an N-Heterocyclic Carbene Ligand. *Tetrahedron Lett.* **2005**, *46*, 2577-2580.

10. Hong, S. H.; Grubbs, R. H. Highly Active Water-Soluble Olefin Metathesis Catalyst. *J. Am. Chem. Soc.* **2006**, *128*, 3508-3509.

11. Lynn, D. M.; Mohr, B.; Grubbs, R. H. Living Ring-Opening Metathesis Polymerization in Water. *J. Am. Chem. Soc.* **1998**, *120*, 1627-1628.

12. Lynn, D. M.; Mohr, B.; Grubbs, R. H.; Henling, L. M.; Day, M. W. Water-Soluble Ruthenium Alkylidenes: Synthesis, Characterization, and Application to Olefin Metathesis in Protic Solvents. *J. Am. Chem. Soc.* **2000**, *122*, 6601-6609.

13. Mohr, B.; Lynn, D. M.; Grubbs, R. H. Synthesis of Water-Soluble, Aliphatic Phosphines and Their Application to Well-Defined Ruthenium Olefin Metathesis Catalysts. *Organometallics* **1996**, *15*, 4317-4325.

14. Quemener, D.; Heroguez, V.; Gnanou, Y. Design of Peo-Based Ruthenium Carbene for Aqueous Metathesis Polymerization. Synthesis by the "Macromonomer Method" and Application in the Miniemulsion Metathesis Polymerization of Norbornene. *J. Polym. Sci. Pol. Chem.* **2006**, *44*, 2784-2793.

15. Chalker, J. M.; Lin, Y. A.; Boutureira, O.; Davis, B. G. Enabling Olefin Metathesis on Proteins: Chemical Methods for Installation of S-Allyl Cysteine. *Chem. Comm.* **2009**, 3714-3716.

16. Lin, Y. A.; Chalker, J. M.; Davis, B. G. Olefin Cross-Metathesis on Proteins: Investigation of Allylic Chalcogen Effects and Guiding Principles in Metathesis Partner Selection. *J. Am. Chem. Soc.* **2010**, *132*, 16805-16811.

17. Li, M.; De, P.; Gondi, S. R.; Sumerlin, B. S. Responsive Polymer-Protein Bioconjugates Prepared by Raft Polymerization and Copper-Catalyzed Azide-Alkyne Click Chemistry. *Macromol. Rapid Commun.* **2008**, *29*, 1172-1176.

18. Li, M.; De, P.; Li, H. M.; Sumerlin, B. S. Conjugation of Raft-Generated Polymers to Proteins by Two Consecutive Thiol-Ene Reactions. *Polym. Chem.* **2010**, *1*, 854-859.

19. Lin, Y. Y. A.; Chalker, J. M.; Davis, B. G. Olefin Metathesis for Site-Selective Protein Modification. *ChemBioChem* **2009**, *10*, 959-969.

20. Lo, C.; Ringenberg, M. R.; Gnandt, D.; Wilson, Y.; Ward, T. R. Artificial Metalloenzymes for Olefin Metathesis Based on the Biotin-(Strept)Avidin Technology. *Chem. Commun.* **2011**, *47*, 12065-12067.

21. Kajetanowicz, A.; Chatterjee, A.; Reuter, R.; Ward, T. R. Biotinylated Metathesis Catalysts: Synthesis and Performance in Ring Closing Metathesis. *Catal. Lett.* **2014**, *144*, 373-379.

22. Marsella, M. J.; Maynard, H. D.; Grubbs, R. H. Template-Directed Ring-Closing Metathesis: Synthesis and Polymerization of Unsaturated Crown Ether Analogs. *Angew. Chem.-Int. Edit. Engl.* **1997**, *36*, 1101-1103.

23. Maynard, H. D.; Grubbs, R. H. Synthesis of Functionalized Polyethers by Ring-Opening Metathesis Polymerization of Unsaturated Crown Ethers. *Macromolecules* **1999**, *32*, 6917-6924.

24. Maynard, H. D., New materials for biological applications prepared by olefin metathesis reactions. PhD Disseratation, California Institute of Technology, Pasadena, CA, 2000.

25. Hilf, S.; Grubbs, R. H.; Kilbinger, A. F. M. End Capping Ring-Opening Olefin Metathesis Polymerization Polymers with Vinyl Lactones. *Journal of the American Chemical Society* **2008**, *130*, 11040-11048.

Chapter 6

Grafting From Proteins *via* Ring Opening Metathesis Polymerization

6.1. Introduction

Conjugation of synthetic polymers to proteins results in materials with enhanced physical properties while retaining the activity of the native protein.[1-4] The simplest and most widely used technique for the preparation of protein-polymer conjugates is the so called *grafting to*.[1-4] This strategy involves the synthesis of a protein-reactive polymer, which is then conjugated to a protein. This method often requires the use of a large excess of polymer to overcome low concentrations of protein and the steric difficulties of reacting proteins and polymers. Furthermore, modern biomolecule purification techniques, such as gel filtration, dialysis, and ultracentrifugation, are optimized for the removal of small molecules from large biomacromolecules. Purification of conjugates from unreacted polymer and protein, all of which are high molecular weight macromolecules, is often a challenging process.

Grafting from techniques have been developed whereby polymer chains are grown directly from functionalized proteins. This approach to protein-polymer conjugation is more amenable to common protein purification techniques. Grafting from proteins has been achieved through the use of controlled radical polymerization (CRP) techniques, such as atom transfer radical polymerization (ATRP)[5-9] and reversible addition-fragmentation chain transfer (RAFT) polymerization.[10-12] In the first example of *grafting from* proteins *via* ATRP, our group reported the preparation of a biotinylated ATRP initiator, which was then bound to a streptavidin tetramer to form a SAv ATRP macro-initiator.[5] The SAv macro-initiator was then used in the polymerization of *N*-isopropylacrylamide (NIPAAm) and poly(ethylene glycol) methyl ether methacrylate (PEGMA) to yield well-defined protein-polymer conjugates.[5]

Ring opening metathesis polymerization (ROMP) is the polymerization of cyclic olefins through the use of transition metal catalysts.[13,14] Unlike CRPs, ROMP can be a true living

polymerization, devoid of chain transfer and termination events. Strained cyclic monomers, such as norbornenes, are necessary for a living ROMP.[14] ROMP as well as other olefin metathesis reactions, such as ring closing metathesis (RCM), cross metathesis (CM), and acyclic diene metathesis (ADMET), are commonly catalyzed by commercially available Grubbs type ruthenium catalysts.[13] These versatile catalysts are highly selective towards alkene/alkynyl substrates and are tolerant of a broad range of functional groups, water, and air.[13]

Aqueous metathesis is often limited by catalyst solubility. To overcome these solubility issues, surfactants and emulsions have been utilized.[15-28] Solubilizing ligands have been incorporated onto ruthenium metathesis catalysts, including charged ligands as well as water-soluble poly(ethylene glycol) based polymeric ligands, however none of these catalysts are commercially available.[29-35]

Due to the selectivity for alkene/alkynyl substrates ruthenium catalyzed olefin metathesis has been investigated for use in the selective modification of biomolecules, such as proteins, in aqueous conditions. Davis and coworkers reported the use of Hoveyda-Grubbs 2nd generation catalyst for the selective modification of allyl sulfides on proteins by CM using a mixed aqueous and organic solvent system.[36-39] There have been several reports of highly active protein-bound ruthenium macro-catalysts. In one example, Ward and coworkers have demonstrated the development of artificial metalloenzymes by binding biotin-modified Hoveyda-Grubbs catalysts to the protein SAv for RCM of small molecules in aqueous media.[40,41]

To date there are only several reports of the use of ROMP polymers for the preparation of protein-polymer conjugates *via* a *grafting to* approach,[42,43] and to our knowledge there are no examples of *grafting from* proteins by ROMP. Herein we report the first example of *grafting from* a protein *via* ROMP. Our approach to grafting from the protein SAv *via* ROMP is based on

the development of a SAv macro-catalyst prepared from SAv and a biotinylated Grubbs catalyst. Biotin has a strong affinity for the tetramer SAv, with a dissociation constant of $K_d = 10^{-15}$ M.[44] A biotinylated Grubbs 2nd generation catalyst (Grubbs II) analog was bound to SAv, and the resulting macro-catalyst was utilized in the ROMP of a tetraethyleneglycol modified norbornene monomer.

6.2. Results and Discussion

6.2.1 Small Molecule Synthesis

Scheme 6.1. (a.) Synthesis of vinylbenzyl-TEG **1** (b.) Synthesis of vinylbenzyl-TEG-biotin **2.**

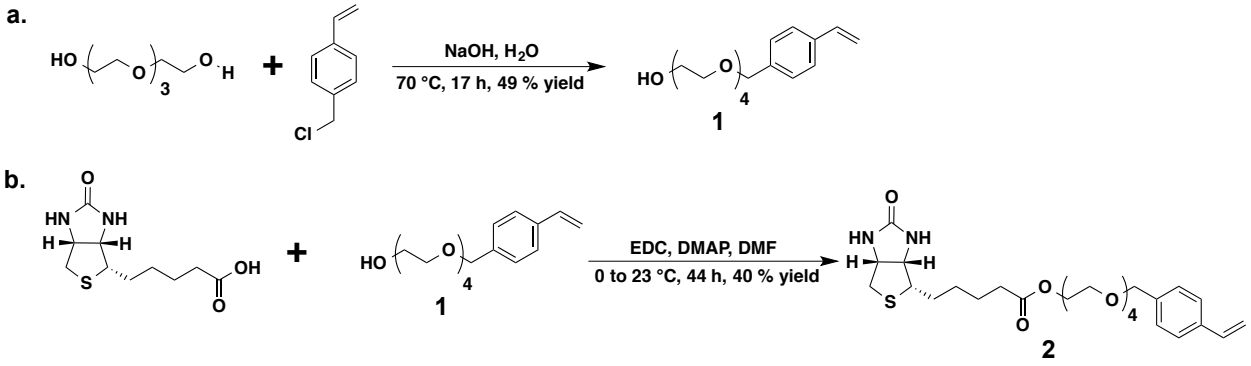

Our approach to the development of a SAv macro-catalyst for ROMP began with the preparation of a biotinylated styrene containing a tetra(ethylene glycol) (TEG) spacer between the Biotin and styrene. This was accomplished through a simple two-step synthesis. First, vinylbenzyl-TEG, **1,** was prepared by reaction of vinylbenzylchloride with TEG in the presence of NaOH in 49% yield (Scheme 6.1.a). Next, vinylbenzyl-TEG-biotin, **2,** was prepared through carbodiimide coupling of **1** with biotin in 40% yield (Scheme 6.1.b).

6.2.2. Biotinylated-TEG-Styrene Ligand Exchange

Scheme 6.2. Benzylidene exchange of Grubbs II and **2**, to yield the biotin-functionalized catalyst **3**.

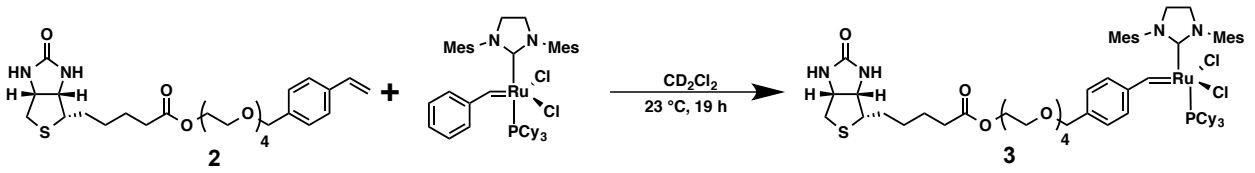

A biotin-functionalized ruthenium metathesis catalyst was prepared by ligand exchange of the Grubbs II benzylidene ligand with styrenyl-TEG-biotin, **2,** by modifying a procedure reported by Lamaty and coworkers (Scheme 6.2).[45] A 1:1 ratio Grubbs II and **2** were dissolved in degassed deuterated-DCM and allowed to react in a vial sealed under argon at 23 °C. Progress of the reaction was monitored by ^{1}H NMR. After 19 h, the complete disappearance of the signal corresponding to the Grubbs II benzylidene at 19.1 ppm and the appearance of a new alkylidene signal at 17.74 ppm was observed (for spectra see section 6.3.3, Figure 6.7). The solvent and styrene by-product were then removed under high vacuum to obtain the biotin-functionalized catalyst **3**, which was then dissolved in *tert*-butyl alcohol and used without further purification.

6.2.3. Polymerization from SAv

Scheme 6.3. Conjugation of biotinylated catalyst **3** to SAv, followed by *in situ* polymerization of monomer **4**.

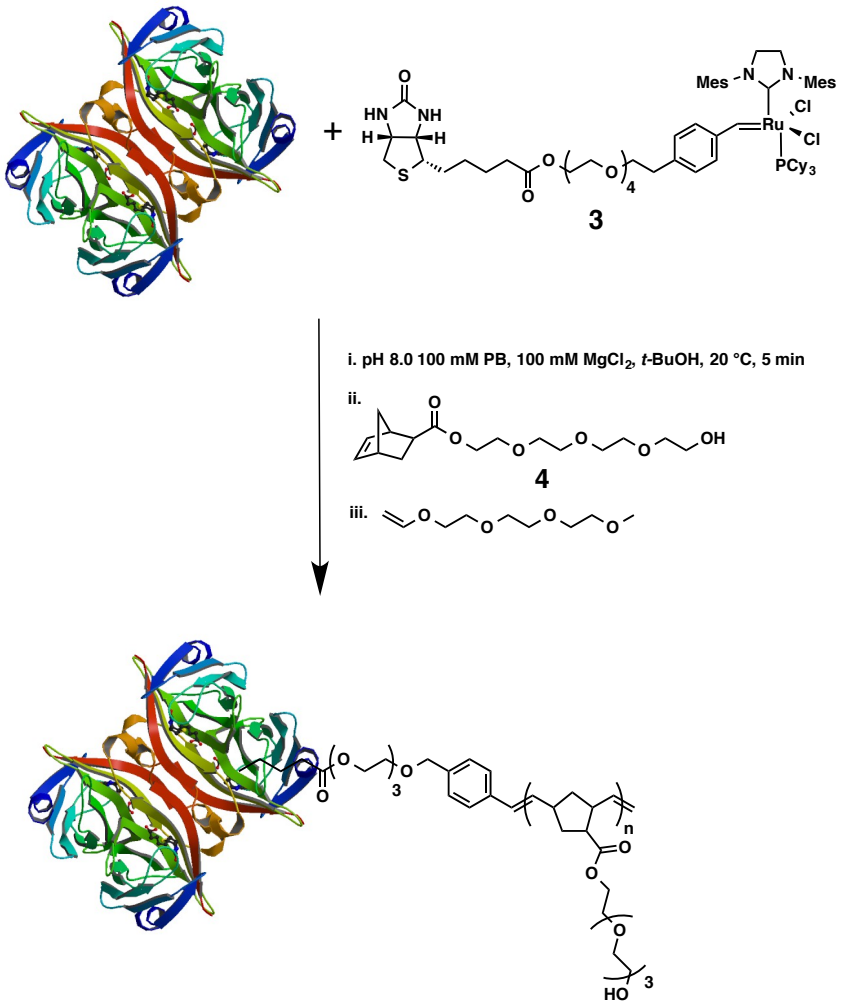

A SAv macro-catalyst was prepared by incubating the biotinylated catalyst **3** with SAv (Scheme 6.3), containing ~1.5 biotin binding sites by HABA assay, in a sodium phosphate buffer (PB) containing 100 mM $MgCl_2$ and 20% *tert*-butyl alcohol. After five minutes, the SAv macro-catalyst solution was added to a 1.5 mL centrifuge tube containing the norbornenyl TEG

monomer **4**, which was then sealed under argon and agitated at 30 °C. After 12 h, the reaction was stopped *via* the addition of triethylene glycol vinyl ether.

A *grafting from* polymerization was evident by sodium dodecyl sulfate polyacrylamide gel electrophoresis (SDS-PAGE) analysis. The resulting SAv-polymer conjugate (Figure 6.1, lane 4) was shifted to a higher molecular weight than the macro-catalyst (Figure 6.1, Lane 3), which was shifted to a slightly higher molecular weight compared to unmodified SAv (Figure 6.1**,** Lane 2). Denaturation of the conjugate (Figure 6.1, lane 7) with concentrated urea resulted in free SAv monomer, which runs at the same molecular weight as denatured macrocatalyst (Figure 6.1, lane 6), and the denatured unmodified SAv monomer (Figure 6.1, lane 5).

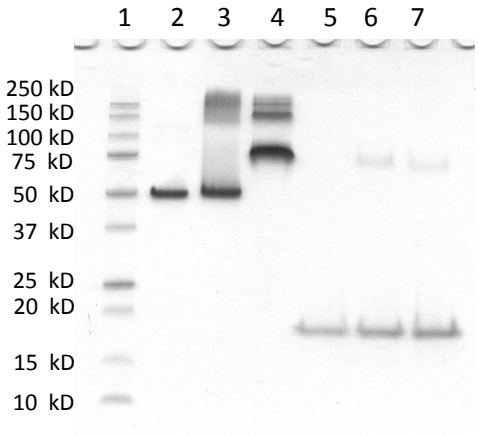

Figure 6.1. SDS-PAGE of SAv, SAv macro-catalyst, and SAv-polymer conjugate under non-denaturing and denaturing conditions visualized by Coomassie blue staining (lane 1: protein marker; lane 2: SAv; lane 3: SAv macro-catalyst; lane 4: SAv-polymer conjugate; lane 5: SAv (denatured); lane 6: SAv macro-catalyst (denatured); lane 7: SAv-polymer conjugate (denatured)).

The increase in molecular weight was also observed by size exclusion chromatography (SEC) (Figure 6.2), where the conjugate had a lower retention time than the macrocatalyst and the unmodified SAv. By both SDS-PAGE and SEC analysis, high molecular weight impurities

were present in the macrocatalyst and the conjugate. The high molecular weight impurities are likely SAv multimers, which formed due to the CM product of **2.**

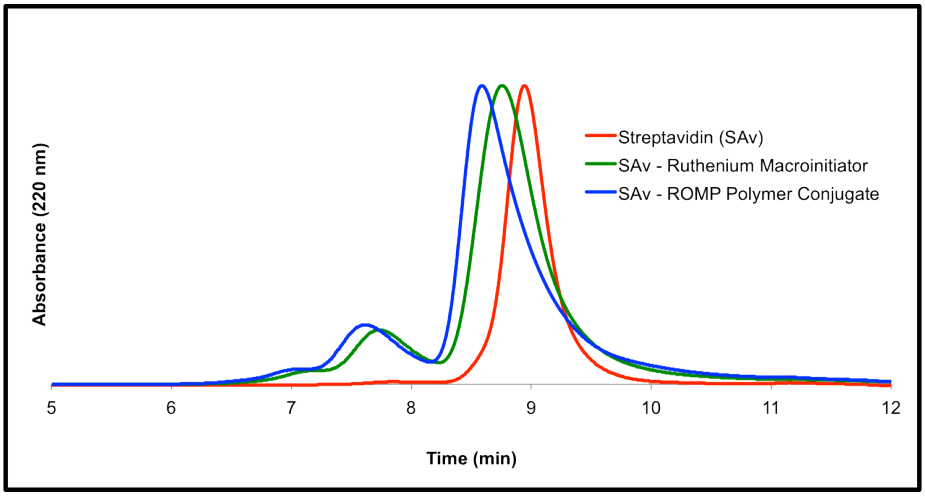

Figure 6.2. Normalized SEC chromatograms of SAv (red trace), SAv macro-catalyst (green trace), and SAv-polymer conjugate (blue trace).

The poly(norbornenyl TEG) was isolated from the conjugate by precipitation of the conjugate in deuterated acetonitrile. Isolated polymer was analyzed by ^{1}H NMR and gel permeation chromatography (GPC). By NMR, polymer formation is evident due to the cis/trans alkene polymer backbone peaks (5.1-5.5 ppm) present in the ^{1}H NMR spectrum. Furthermore, a molecular weight can be calculated by end-group analysis of the polymer, by comparing the integrations for the aromatic end-group (7.54 and 7.35 ppm) to the polymer backbone peaks (5.1-5.5 ppm) a molecular weight of 38.2 kDa was calculated for the isolated polymer. GPC analysis of the polymer showed a polydispersity index (PDI) of 1.40.

To date, the use of metathesis catalysts in the presence of proteins and for the synthetic modification of proteins has been limited to CM and RCM.[37,38,40,41] This data together suggests

that the conjugation of a biotinylated Grubbs catalyst to SAv, followed by the *in situ* polymerization of a water-soluble TEG functionalized norbornene results in well-defined protein-polymer conjugates. This is the first example of *grafting from via* ROMP, and only the second example of ROMP in the presence of proteins. This technique opens *grafting from* techniques to a wider variety of monomers than is currently available for CRP-based *grafting from* methods. *Grafting from* SAv is the first advancement in ROMP from proteins, however for this technique to be applicable to most proteins covalent methods must be developed. Ruthenium metathesis catalysts are known to degrade in the presence of alcohols and in aqueous environments.[46] Covalent *grafting from via* ROMP requires functionalized metathesis catalysts that can be covalently conjugated to proteins quickly and efficiently in order for polymerization to occur before catalyst degradation. Investigation of covalent ROMP *grafting from* techniques is under way.

6.3. Experimental

6.3.1. Materials

All chemicals were purchased from Sigma-Aldrich, Fisher Scientific, and Acros and used as received unless otherwise noted. SAv (~1.5 biotin binding sites by HABA assay) was purchased from Prof. T. Ward (University of Basel). CH_2Cl_2 was distilled after stirring with CaH_2 and stored under argon. THF was distilled over sodium/benzophenone and stored under argon. Endo/exo mixture of (1S,2R,4S)-2-(2-(2-(2-hydroxyethoxy)ethoxy)ethoxy)ethyl bicyclo[2.2.1]hept-5-ene-2-carboxylate (**4**) was prepared according to a previously reported protocol.[47]

6.3.2. Analytical Techniques

NMR spectra were obtained on Bruker 600 or 500 MHZ AV spectrometers. Proton NMR spectra were acquired with a relaxation delay of 2 sec for small molecules. Proton NMR spectra were acquired with a relaxation delay of 30 sec for all polymers. Infrared absorption spectra were recorded using a PerkinElmer FT-IR equipped with an ATR accessory. Mass spectra were obtained on Thermo Fisher Scientific Exactive Plus with IonSense ID-CUBE DART source. GPC was conducted on a Shimadzu HPLC system equipped with a refractive index detector RID-10A, one Polymer Laboratories PLgel guard column, and two Polymer Laboratories PLgel 5 μm mixed D columns. LiBr (0.1 M) in *N,N*-dimethylformamide (DMF) at 40 °C was used as an eluent (flow rate: 0.80 mL/min). Calibration was performed using near-monodisperse PMMA standards from Polymer Laboratories. Aqueous SEC was conducted on a Shimadzu HPLC system equipped with a UV-Vis detector, one Phenomenex SecurityGuard guard filter, and one

Phenomenex BioSep-SEC-S 2000 column. A pH 7.0 200 mM sodium phosphate buffer containing 300 mM NaCl at 20 °C was used as the eluent (flow rate: 1.0 mL/min). SDS-PAGE was performed using Bio-Rad Any kD Mini-PROTEAN-TGX gels. SDS-PAGE protein standards were obtained from Bio-Rad (Precision Plus Protein Prestained Standards). For SDS-PAGE analysis, approximately 5 μg of protein was loaded into each lane.

6.3.3. Methods

Synthesis of styrenyl tetraethyleneglycol *1*. NaOH (0.31 g, 7.7 mmol) and water (0.14 mL) were added to a round bottom flask equipped with a magnetic stir bar and a reflux condenser. TEG (33.6 g, 173.0 mmol) was added to the reaction vessel and the mixture was heated to 70 °C and allowed to stir until all of the solids were dissolved. Vinyl benzylchloride (1 g, 6.4 mmol) was then slowly added to the TEG/NaOH solution and allowed to stir under reflux. After 17 h, water (100 mL) was added to the reaction and the reaction was extracted with diethyl ether (3 x 100 mL). The diethyl ether layers were combined and dried with $MgSO_4$, and then concentrated by rotary evaporation. The crude reaction was then purified by silica gel chromatography using diethyl ether as the eluent. Fractions containing the product were combined and concentrated by rotary evaporation followed by high vacuum to yield **1** as a light yellow liquid in (1.17 g, 49% yield). ^{1}H NMR (600 MHz, $CDCl_3$) δ: 7.38 (d, J = 7.9 Hz, 2H), 7.30 (d, J = 7.9 Hz, 2H), 6.70 (dd, J = 17.0, 10.5 Hz, 1H), 5.74 (d, J = 17.6 Hz, 1H), 5.23 (d, J = 10.7 Hz, 1H), 4.55 (s, 2H), 3.73-3.57 (m, 16H). ^{13}C NMR (500 MHz, $CDCl_3$) δ: 137.82, 136.97, 136.54, 127.98, 126.21, 113.7693, 72.95, 70.64, 70.61, 70.58, 70.55, 69.99, 61.58. HRMS expected (observed) [MH+]: 311.185 (311.184). IR (neat): 3434, 2921, 2853, 1743, 1457, 1376, 1348, 1259, 1240, 1097, 1064, 935, 886, 827 cm^{-1}.

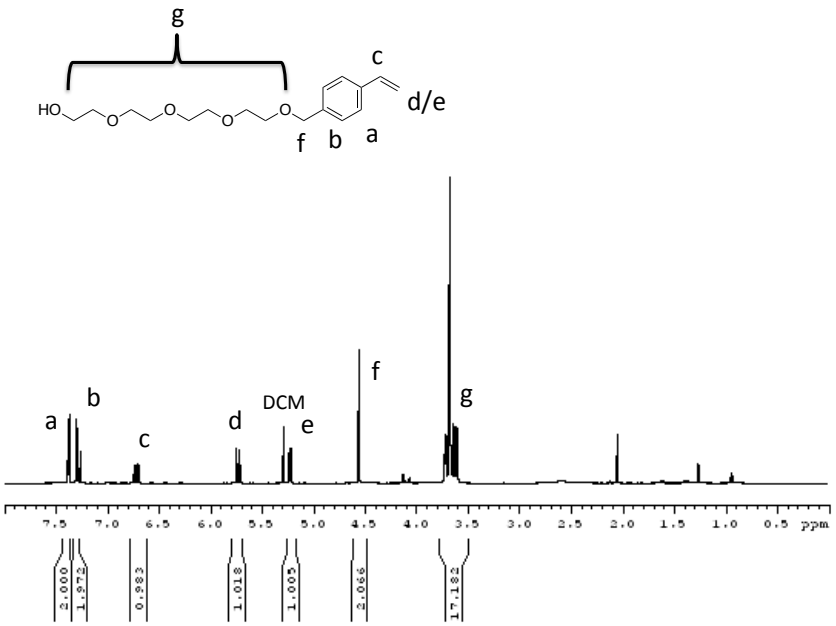

Figure 6.3. ^{1}H NMR (600 MHz, $CDCl_3$) of **1**.

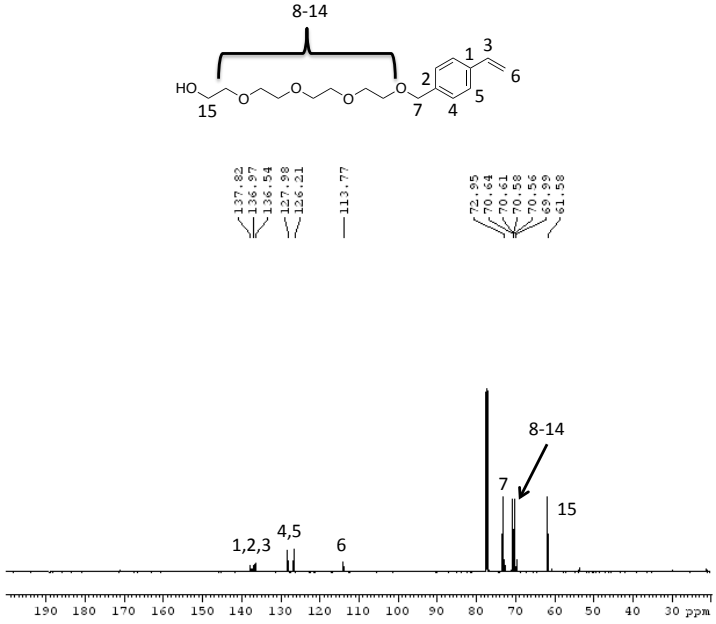

Figure 6.4. ^{13}C NMR (500 MHz, $CDCl_3$) of **1**.

Synthesis of styrenyl-TEG-biotin *2*. Biotin (213 mg, 0.87 mmol) and **1** (405 mg, 1.30 mmol) were added to a flame dried round bottom flask equipped with a magnetic stir bar and dissolved in DMF (35 mL). The reaction vessel was then cooled to 0 °C. N-(3-Dimethylaminopropyl)-N′-ethylcarbodiimide hydrochloride (EDC) (500 mg, 2.61 mmol) and then 4-(Dimethylamino)pyridine (DMAP) (32 mg, 0.26 mmol) were added to the reaction vessel. The reaction was then allowed to stir under argon and warm to 23 °C. After 44 h, the solvent was removed by heating the reaction to 45 °C under high vacuum. The crude reaction was purified by silica gel chromatography, diethyl ether was used as the eluent until all of the unreacted starting material **1** was eluted from the column, the eluent was then switched to 9:1 EtOAc:MeOH to obtain **2** as a viscous yellow oil (187 mg, 40% yield). %). ^{1}H NMR (600 MHz, $CDCl_3$) δ: 7.38 (d, J = 7.7 Hz, 2H), 7.30 (d, *J* = 7.7, 2H), 6.71 (m, 1H), 5.76 (m, 2H), 5.21 (m, 2H), 4.55 (s, 2H), 4.48 (m, 1H), 4.29 (m, 1H), 4.21 (m, 2H), 3.70-3.58 (m, 16H), 3.13 (m, 1H), 2.89 (m, 1H), 2.72 (m, 1H), 1.67 (m, 4H), 1.44 (m, 2H). ^{13}C NMR (500 MHz, $CDCl_3$) δ: 173.68, 163.53, 137.86, 136.98, 136.53, 128.02, 126.21, 113.89, 72.95, 70.64, 70.57, 70.52, 69.98, 69.42, 69.39, 69.16, 64.44, 61.96, 61.56, 60.14, 55.45, 40.51, 33.76, 28.29, 28.21, 24.71. HRMS expected (observed) [MH+]: 537.263 (537.261). IR (neat): 3242, 2912, 2864, 1729, 1698, 1629, 1512, 1457, 1349, 1251, 1096, 992, 855, 827 cm^{-1}.

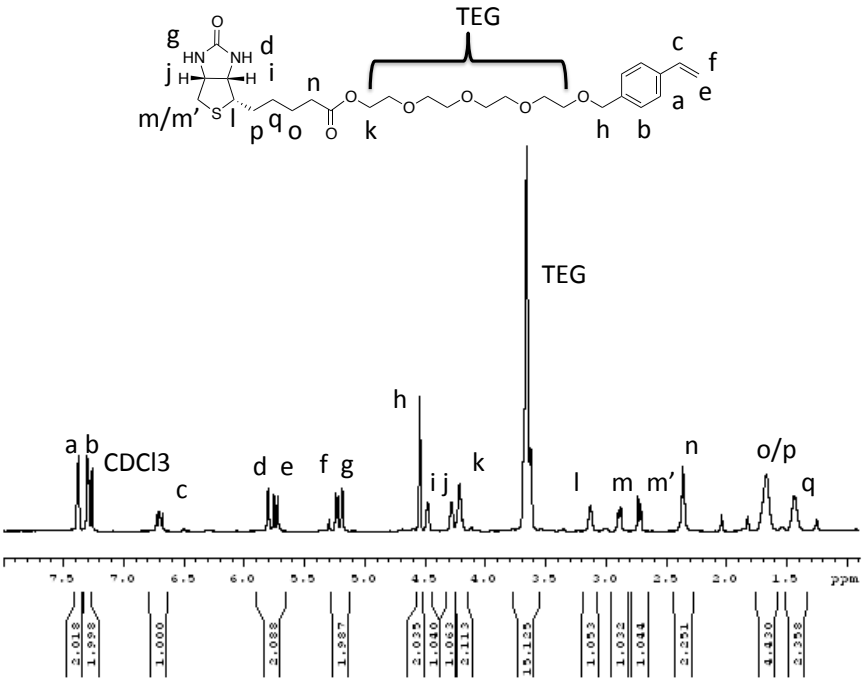

Figure 6.5. ^{1}H NMR (600 MHz, $CDCl_3$) of **2**.

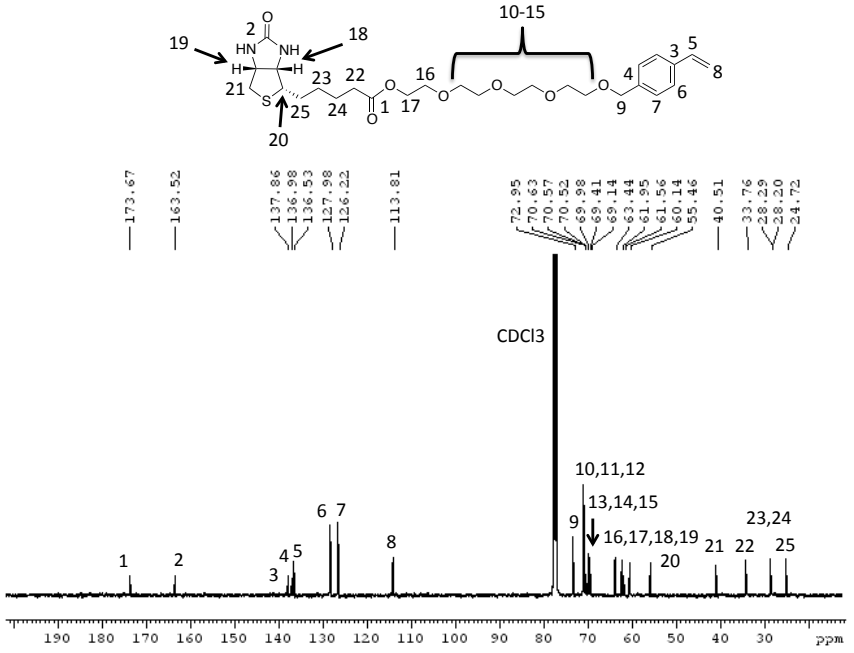

Figure 6.6. ^{13}C NMR (500 MHz, $CDCl_3$) of **2**.

Benzylidne ligand exchange on Grubbs 2nd generation catalyst to yield catalyst *3*. Styrenyl-TEG-biotin **2** (2.7 mg, 5.03 μmol) was weighed into a 2 mL vial and a magnetic stir bar was added. In a separate vial, Grubbs 2nd generation catalyst (4.7, 5.34 μmol) was dissolved in degassed CD_2Cl_2 (314 μL). The catalyst solution was transferred to the vial containing compound **2**, the vial was sealed under argon and allowed to stir at 23 °C. After 19 h, an additional 350 uL of CD_2Cl_2 was added and the extent of the reaction was analyzed by ^{1}H NMR. The solvent was then removed *in vacuo* and *tert*-butyl alcohol (167 uL) was added to the biotinylated Grubbs catalyst **3** (32 mM catalyst concentration). The solution was used without further purification**.** ^{1}H NMR (600 MHz, CD_2Cl_2) δ: 19.1 (Grubbs II Benzylidene), 17.7 (Biotinylated-Grubbs II Benzylidene), 4.2-3.7 (NHC -NC**H2**C**H2**N-).

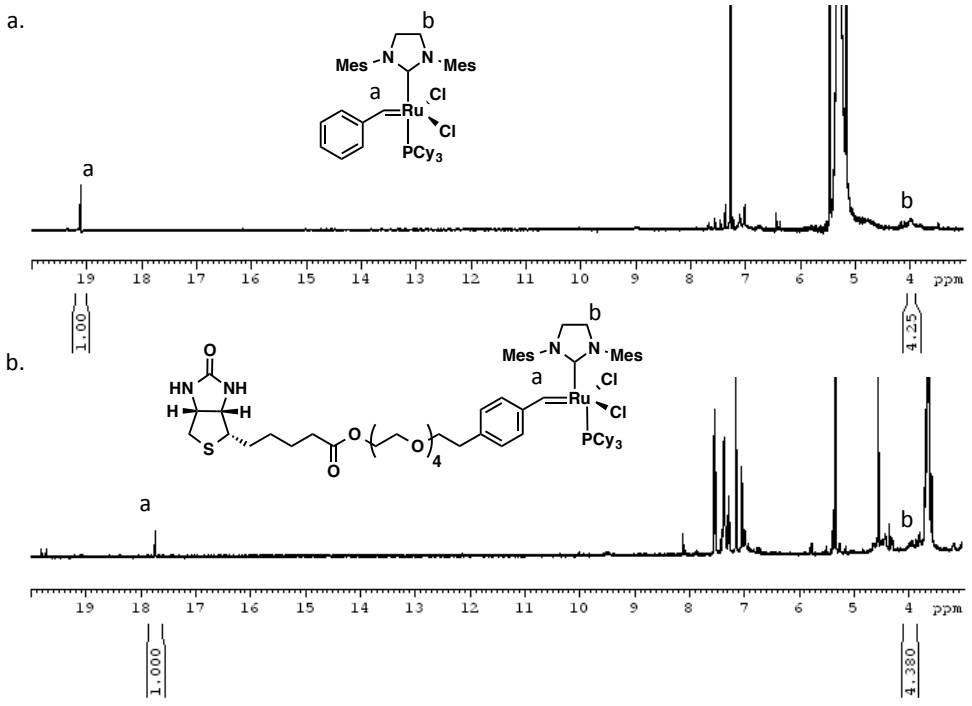

Figure 6.7. ^{1}H NMR (600 MHz, CD_2Cl_2) overlays of (a.) Grubbs 2nd gen. catalyst and (b.) biotinylated catalyst **3**.

Typical conjugation of SAv to catalyst *3* and *in situ* ROMP of norbornenyl-TEG 4. SAv (5 mg, 0.08 μmol) was weighed into a 1.5 mL centrifuge tube and dissolved with 200 μL of a pH 8.0 100 mM PB containing 100 mM $MgCl_2$. 50 μL of the catalyst in *tert*-butyl alcohol was added. The reaction solution was sealed under argon and incubated for 5 min. The catalyst/SAv solution was then transferred to a 1.5 mL centrifuge tube containing the norbornene-TEG monomer **4** (12.0 mg, 38.17 μmol). The reaction vessel was sealed under argon, and incubated for 12 h on a temperature controlled shaker at 30 °C and shaking at 1250 rpm. After 12 h, ethylene glycol vinyl ether (50 μL) was added, and reaction buffer was added to a total protein concentration of 1 mg/mL.

Denaturation of SAv conjugate for SDS PAGE. 10 μL of the crude polymerization mixture was added to 90 μL of saturated urea solution in a 1.5 mL centrifuge tube and heated to 80 °C for 1 h on a dry bath.

Denaturation of SAv Conjugate for NMR and GPC. 100 μL of the crude reaction solution was added to 900 μL of deuterated acetonitrile and vortexed. A solid precipitate was observed. The supernatant was then analyzed by ^{1}H NMR followed by GPC.

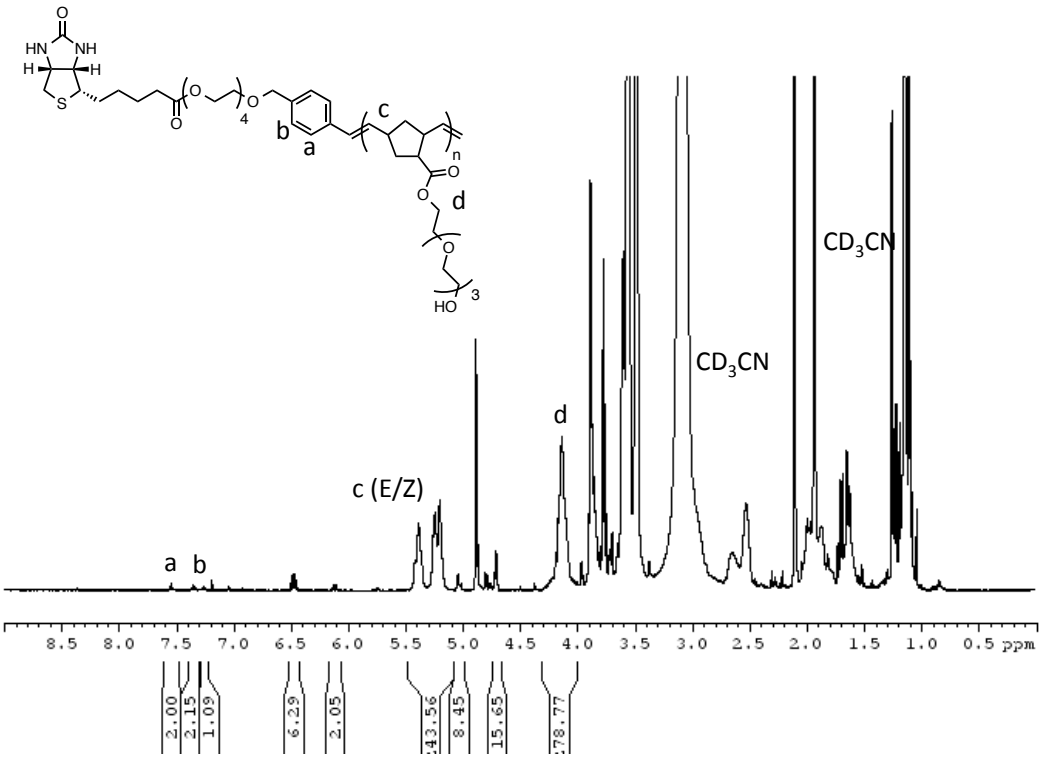

Figure 6.8. ^{1}H NMR (600 MHz, CD_3CN) of the isolated ROMP polymer.

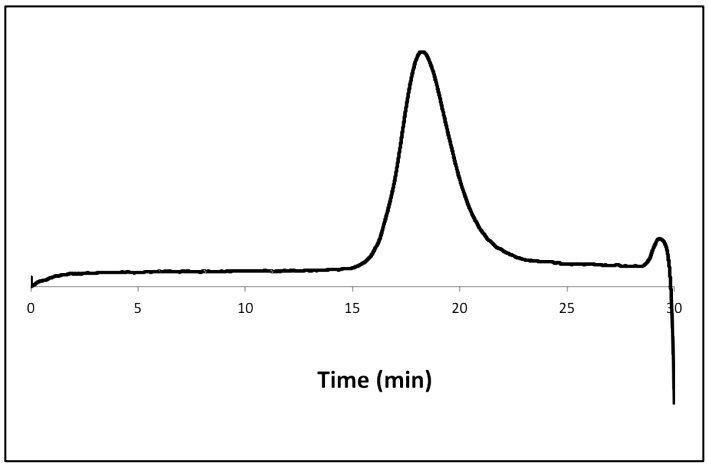

Figure 6.9. GPC chromatogram of isolated ROMP polymer**,** normalized and analyzed by comparison with monodisperse PMMA standards.

6.4. Conclusions

We have successfully demonstrated the direct polymerization of a TEG modified norbornenyl monomer from a SAv macro-catalyst by ROMP in aqueous media. To our knowledge, this is the first example of the use of ROMP for *grafting from* proteins. Grubbs II was modified with a biotin-functionalized benzylidene ligand. The biotinylated Grubbs catalyst was then bound to SAv. The resulting SAv macro-catalyst was then used to initiate ROMP of a norbornenyl monomer. Polymerization resulted in a well-defined conjugate. This work expands the utility of ruthenium catalyzed olefin metathesis chemistry to ROMP in complex protein solutions, and widens the current monomer scope available for *grafting from* proteins. Currently the development of methods for the ROMP from proteins resulting in covalent protein-polymer conjugates is under way.

6.5. References

1. Broyer, R. M.; Grover, G. N.; Maynard, H. D. Emerging Synthetic Approaches for Protein-Polymer Conjugations. *Chem. Commun.* **2011**, *47*, 2212-2226.
2. Grover, G. N.; Maynard, H. D. Protein-Polymer Conjugates: Synthetic Approaches by Controlled Radical Polymerizations and Interesting Applications. *Curr. Opin. Chem. Biol.* **2010**, *14*, 818-827.
3. Jung, B.; Theato, P. In *Bio-Synthetic Polymer Conjugates*; Schlaad, H., Ed.; Springer-Verlag Berlin: Berlin, 2013; Vol. 253, p 37-70.
4. Le Droumaguet, B.; Nicolas, J. Recent Advances in the Design of Bioconjugates from Controlled/Living Radical Polymerization. *Polym. Chem.* **2010**, *1*, 563-598.
5. Bontempo, D.; Maynard, H. D. Streptavidin as a Macroinitiator for Polymerization: In Situ Protein-Polymer Conjugate Formation. *J. Am. Chem. Soc.* **2005**, *127*, 6508-6509.
6. Gao, W. P.; Liu, W. G.; Christensen, T.; Zalutsky, M. R.; Chilkoti, A. In Situ Growth of a Peg-Like Polymer from the C Terminus of an Intein Fusion Protein Improves Pharmacokinetics and Tumor Accumulation. *Proc. Natl. Acad. Sci. U. S. A.* **2010**, *107*, 16432-16437.
7. Gao, W. P.; Liu, W. G.; Mackay, J. A.; Zalutsky, M. R.; Toone, E. J.; Chilkoti, A. In Situ Growth of a Stoichiometric Peg-Like Conjugate at a Protein's N-Terminus with Significantly Improved Pharmacokinetics. *Proc. Natl. Acad. Sci. U. S. A.* **2009**, *106*, 15231-15236.
8. Heredia, K. L.; Bontempo, D.; Ly, T.; Byers, J. T.; Halstenberg, S.; Maynard, H. D. In Situ Preparation of Protein - "Smart" Polymer Conjugates with Retention of Bioactivity. *Journal of the American Chemical Society* **2005**, *127*, 16955-16960.

9. Magnusson, J. P.; Bersani, S.; Salmaso, S.; Alexander, C.; Caliceti, P. In Situ Growth of Side-Chain Peg Polymers from Functionalized Human Growth Hormone-a New Technique for Preparation of Enhanced Protein-Polymer Conjugates. *Bioconjugate Chem.* **2010**, *21*, 671-678.

10. Boyer, C.; Bulmus, V.; Liu, J. Q.; Davis, T. P.; Stenzel, M. H.; Barner-Kowollik, C. Well-Defined Protein-Polymer Conjugates Via in Situ Raft Polymerization. *J. Am. Chem. Soc.* **2007**, *129*, 7145-7154.

11. De, P.; Li, M.; Gondi, S. R.; Sumerlin, B. S. Temperature-Regulated Activity of Responsive Polymer-Protein Conjugates Prepared by Grafting-from Via Raft Polymerization. *J. Am. Chem. Soc.* **2008**, *130*, 11288-+.

12. Liu, J. Q.; Bulmus, V.; Herlambang, D. L.; Barner-Kowollik, C.; Stenzel, M. H.; Davis, T. P. In Situ Formation of Protein-Polymer Conjugates through Reversible Addition Fragmentation Chain Transfer Polymerization. *Angew. Chem.-Int. Edit.* **2007**, *46*, 3099-3103.

13. Trnka, T. M.; Grubbs, R. H. The Development of L2x2ru = Chr Olefin Metathesis Catalysts: An Organometallic Success Story. *Accounts Chem. Res.* **2001**, *34*, 18-29.

14. Bielawski, C. W.; Grubbs, R. H. Living Ring-Opening Metathesis Polymerization. *Prog. Polym. Sci.***2007**, *32*, 1-29.

15. Lynn, D. M.; Kanaoka, S.; Grubbs, R. H. Living Ring-Opening Metathesis Polymerization in Aqueous Media Catalyzed by Well-Defined Ruthenium Carbene Complexes. *J. Am. Chem. Soc.* **1996**, *118*, 784-790.

16. Fraser, C.; Grubbs, R. H. Synthesis of Glycopolymers of Controlled Molecular Weight by Ring-Opening Metathesis Polymerization Using Well-Defined Functional Group Tolerant Ruthenium Carbene Catalysts. *Macromolecules* **1995**, *28*, 7248-7255.

17. Manning, D. D.; Hu, X.; Beck, P.; Kiessling, L. L. Synthesis of Sulfated Neoglycopolymers: Selective P-Selectin Inhibitors. *J. Am. Chem. Soc.* **1997**, *119*, 3161-3162.

18. Kanai, M.; Mortell, K. H.; Kiessling, L. L. Varying the Size of Multivalent Ligands: The Dependence of Concanavalin a Binding on Neoglycopolymer Length. *J. Am. Chem. Soc.* **1997**, *119*, 9931-9932.

19. Claverie, J. P.; Viala, S.; Maurel, V.; Novat, C. Ring-Opening Metathesis Polymerization in Emulsion. *Macromolecules* **2001**, *34*, 382-388.

20. Lee, B. S.; Mahajan, S.; Clapham, B.; Janda, K. D. Suspension Ring-Opening Metathesis Polymerization: The Preparation of Norbornene-Based Resins for Application in Organic Synthesis. *J. Org. Chem.* **2004**, *69*, 3319-3329.

21. Monteil, V.; Wehrmann, P.; Mecking, S. A General Route to Very Small Polymer Particles with Controlled Microstructures. *J. Am. Chem. Soc.* **2005**, *127*, 14568-14569.

22. Quemener, D.; Heroguez, V.; Gnanou, Y. Latex Particles by Miniemulsion Ring-Opening Metathesis Polymerization. *Macromolecules* **2005**, *38*, 7977-7982.

23. Lipshutz, B. H.; Aguinaldo, G. T.; Ghorai, S.; Voigtritter, K. Olefin Cross-Metathesis Reactions at Room Temperature Using the Nonionic Amphiphile "Pts": Just Add Water. *Org. Lett.* **2008**, *10*, 1325-1328.

24. Lipshutz, B. H.; Ghorai, S. Transition-Metal-Catalyzed Cross-Couplings Going Green: In Water at Room Temperature. *Aldrichimica Acta* **2008**, *41*, 59-72.

25. Lipshutz, B. H.; Ghorai, S.; Aguinaldo, G. T. Ring-Closing Metathesis at Room Temperature within Nanometer Micelles Using Water as the Only Solvent. *Advanced Synthesis & Catalysis* **2008**, *350*, 953-956.

26. Lipshutz, B. H.; Ghorai, S. Pqs: A New Platform for Micellar Catalysis. Rcm Reactions in Water, with Catalyst Recycling. *Org. Lett.* **2009**, *11*, 705-708.

27. Lipshutz, B. H.; Ghorai, S.; Abela, A. R.; Moser, R.; Nishikata, T.; Duplais, C.; Krasovskiy, A.; Gaston, R. D.; Gadwood, R. C. Tpgs-750-M: A Second-Generation Amphiphile for Metal-Catalyzed Cross-Couplings in Water at Room Temperature. *J. Org. Chem.* **2011**, *76*, 4379-4391.

28. Lipshutz, B. H.; Ghorai, S.; Leong, W. W. Y.; Taft, B. R.; Krogstad, D. V. Manipulating Micellar Environments for Enhancing Transition Metal-Catalyzed Cross-Couplings in Water at Room Temperature. *J. Org. Chem.* **2011**, *76*, 5061-5073.

29. Gallivan, J. P.; Jordan, J. P.; Grubbs, R. H. A Neutral, Water-Soluble Olefin Metathesis Catalyst Based on an N-Heterocyclic Carbene Ligand. *Tetrahedron Lett.* **2005**, *46*, 2577-2580.

30. Hong, S. H.; Grubbs, R. H. Highly Active Water-Soluble Olefin Metathesis Catalyst. *J. Am. Chem. Soc.* **2006**, *128*, 3508-3509.

31. Lynn, D. M.; Mohr, B.; Grubbs, R. H. Living Ring-Opening Metathesis Polymerization in Water. *J. Am. Chem. Soc.* **1998**, *120*, 1627-1628.

32. Lynn, D. M.; Mohr, B.; Grubbs, R. H.; Henling, L. M.; Day, M. W. Water-Soluble Ruthenium Alkylidenes: Synthesis, Characterization, and Application to Olefin Metathesis in Protic Solvents. *J. Am. Chem. Soc.* **2000**, *122*, 6601-6609.

33. Mohr, B.; Lynn, D. M.; Grubbs, R. H. Synthesis of Water-Soluble, Aliphatic Phosphines and Their Application to Well-Defined Ruthenium Olefin Metathesis Catalysts. *Organometallics* **1996**, *15*, 4317-4325.

34. Quemener, D.; Heroguez, V.; Gnanou, Y. Design of Peo-Based Ruthenium Carbene for Aqueous Metathesis Polymerization. Synthesis by the "Macromonomer Method" and Application in the Miniemulsion Metathesis Polymerization of Norbornene. *J. Polym. Sci., Part A: Polym. Chem.* **2006**, *44*, 2784-2793.

35. Connon, S. J.; Blechert, S. A Solid-Supported Phosphine-Free Ruthenium Alkylidene for Olefin Metathesis in Methanol and Water. *Bioorg. Med. Chem. Lett.* **2002**, *12*, 1873-1876.

36. Lin, Y. A.; Chalker, J. M.; Floyd, N.; Bernardes, G. J. L.; Davis, B. G. Allyl Sulfides Are Privileged Substrates in Aqueous Cross-Metathesis: Application to Site-Selective Protein Modification. *J. Am. Chem. Soc.* **2008**, *130*, 9642-+.

37. Lin, Y. Y. A.; Chalker, J. M.; Davis, B. G. Olefin Metathesis for Site-Selective Protein Modification. *ChemBioChem* **2009**, *10*, 959-969.

38. Chalker, J. M.; Lin, Y. A.; Boutureira, O.; Davis, B. G. Enabling Olefin Metathesis on Proteins: Chemical Methods for Installation of S-Allyl Cysteine. *Chem. Commun.* **2009**, 3714-3716.

39. Lin, Y. A.; Chalker, J. M.; Davis, B. G. Olefin Cross-Metathesis on Proteins: Investigation of Allylic Chalcogen Effects and Guiding Principles in Metathesis Partner Selection. *J. Am. Chem. Soc*. **2010**, *132*, 16805-16811.

40. Kajetanowicz, A.; Chatterjee, A.; Reuter, R.; Ward, T. R. Biotinylated Metathesis Catalysts: Synthesis and Performance in Ring Closing Metathesis. *Catal. Lett.* **2014**, *144*, 373-379.

41. Lo, C.; Ringenberg, M. R.; Gnandt, D.; Wilson, Y.; Ward, T. R. Artificial Metalloenzymes for Olefin Metathesis Based on the Biotin-(Strept)Avidin Technology. *Chem. Commun.* **2011**, *47*, 12065-12067.

42. Carrillo, A.; Gujraty, K. V.; Rai, P. R.; Kane, R. S. Design of Water-Soluble, Thiol-Reactive Polymers of Controlled Molecular Weight: A Novel Multivalent Scaffold. *Nanotechnology* **2005**, *16*, S416-S421.

43. Chen, B. Z.; Metera, K.; Sleiman, H. F. Biotin-Terminated Ruthenium Bipyridine Ring-Opening Metathesis Polymerization Copolymers: Synthesis and Self-Assembly with Streptavidin. *Macromolecules* **2005**, *38*, 1084-1090.

44. Weber, P.; Ohlendorf, D.; Wendoloski, J.; Salemme, F. Structural Origins of High-Affinity Biotin Binding to Streptavidin. *Science* **1989**, *243*, 85-88.

45. Varray, S.; Lazaro, R.; Martinez, J.; Lamaty, F. New Soluble-Polymer Bound Ruthenium Carbene Catalysts: Synthesis, Characterization, and Application to Ring-Closing Metathesis. *Organometallics* **2003**, *22*, 2426-2435.

46. Manzini, S.; Poater, A.; Nelson, D. J.; Cavallo, L.; Slawin, A. M. Z.; Nolan, S. P. Insights into the Decomposition of Olefin Metathesis Precatalysts. *Angew. Chem.-Int. Edit.* **2014**, *ASAP*.

47. Alconcel, S. N. S., Functionalized and Protein-Reactive Polymers Synthesized Using Controlled Polymerization Techniques. PhD Disseratation, University of California, Los Angeles, Los Angeles, CA 2013.

Chapter 7

Progress Towards Protein-Heterodimers *via* Oxime Bond Formation

7.1. Introduction

In nature, many proteins exhibit biological activity only when multimerized, where there are two or more proteins interacting to form a complex.[1] As a result, covalently linking proteins could lead to higher activities,[2] since the entropic barrier to multimerization would be prepaid. Forming covalently linked protein dimers with synthetic polymer tethers should result in protein dimers that are stabilized by the synthetic polymer tether and are also biologically active.

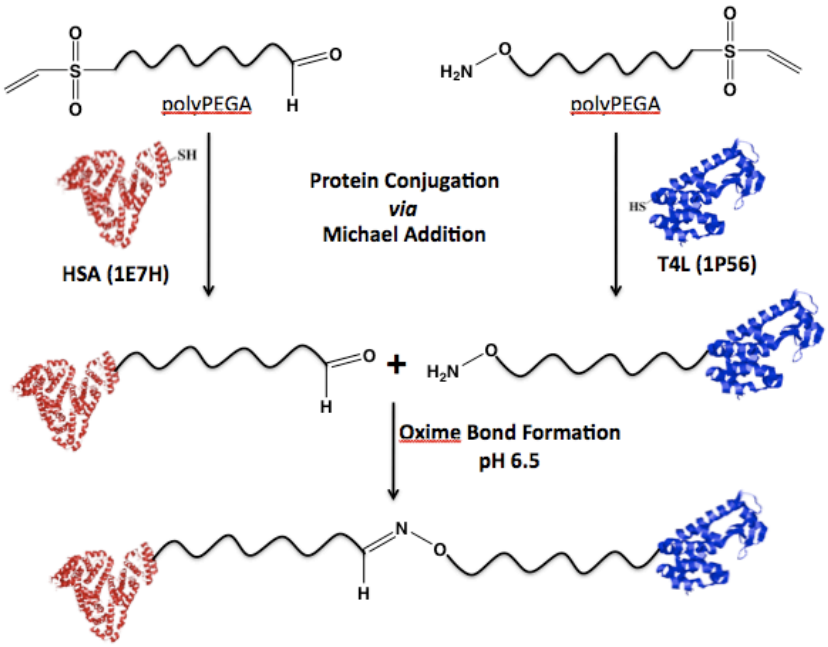

Figure 7.1. Proposed route to protein dimers through oxime bond formation.

Telechelic polymers have previously been applied towards the preparation of protein-dimers and higher ordered conjugates,[3-7] however these approaches are limited to the preparation of homo-dimers or by the sequential conjugation of proteins to polymer chain ends. We propose a new approach to prepare protein dimers (Figure 7.1) that should allow for a large diversity in

protein dimer synthesis. In particular, polymers with a vinyl sulfone at one end and either an aldehyde or an *o*-hydroxylamine at the other end were prepared by reversible addition-fragmentation chain transfer (RAFT) polymerization. RAFT is well suited to the preparation of protein-reactive polymers.[8,9] Functionality can be installed onto RAFT polymers through the use of functionalized RAFT CTAs,[10,11] as well as by post-polymerization modification of the RAFT thiocarbonyl endgroup.[3,4,12-17] We have previously developed methodology whereby RAFT thiocarbonyl polymer endgroups are rapidly and quantitatively transformed into cysteine reactive, Michael accepting, vinyl sulfone endgroups.[12,14] This allows for mild, site-specific conjugation of polymers to free cysteine residues. The vinyl sulfone will react with any biomolecule containing a free cysteine and the dimers will be assembled utilizing oxime chemistry. Oxime bond formation was chosen because it is chemoselective in the presence of proteins and because of the mild, aqueous conditions in which the oxime bond condensation occurs.[18,19] Herein, the preparation of a telechelic oxime and vinyl sulfone functionalized polymer for applications towards the development of protein dimers is discussed.

7.2. Results and Discussion

7.2.1. CTA Synthesis

Synthesis of a *Boc*-aminooxy dithiobenzoate RAFT CTA was accomplished through a four-step synthesis (Scheme 7.1). *N-Boc*-hydroxylamine (**1**) was prepared by reaction of hydroxyl amine hydrochloride with *di-tert*-butyl dicarbonate in 95% yield. *Tert*-butyl *2*-hydroxyethoxycarbamate (**2**) was prepared by the displacement of bromide of 2-bromoethanol with *N-Boc*-hydroxylamine in the presence of 1,8-diazabicycloundec-7-ene (DBU) in 77% yield. *N-Boc*-aminooxyethyl 2-bromopropanoate (**3**) was obtained by reaction of **2** with bromopropionyl bromide in poor yield, 42%. Compound **3** was then reacted with a dithiobenzoate, formed by the reaction of a phenyl magnesium bromide Grignard reagent with carbon disulfide, to produce CTA **4** in 87% yield.

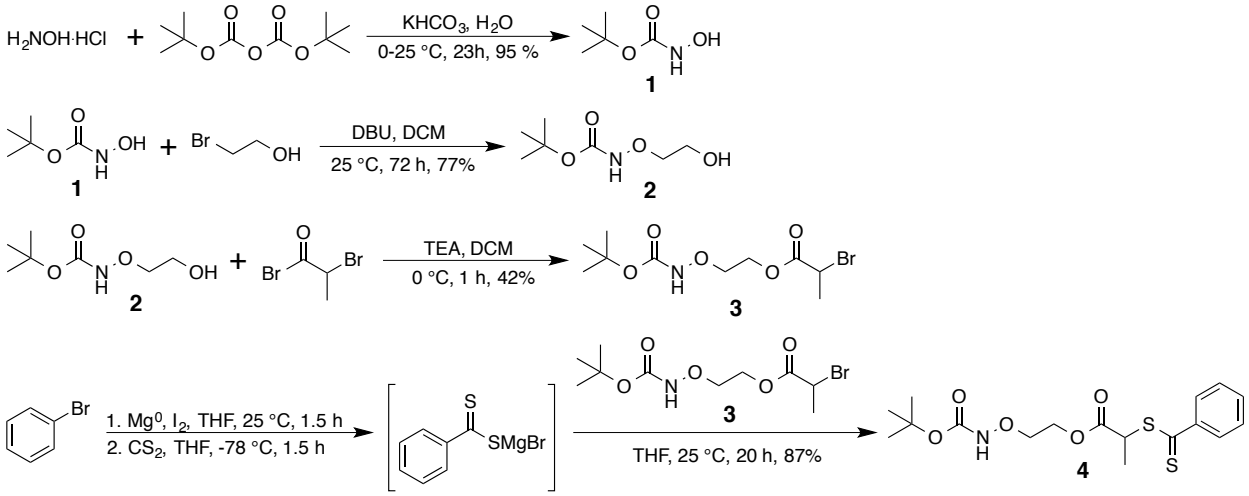

Scheme 7.1. Synthesis of a *Boc*-aminooxy functionalized dithiobenzoate CTA.

7.2.2. RAFT of PEGA

PEGA was polymerized in the presence of **4** in DMF at 70 ºC using a [0.1]:[1]][30] ratio of [AIBN]:[**4**]:[PEGA] (Scheme 7.2). The polymerization was stopped at 7.6 h at 70% conversion. Time point samples for kinetics analysis were collected at 0 h and approximately every hour after the polymerization was initiated. **Poly1** was obtained after extensive dialysis in 1:1 MeOH:EtOAc.

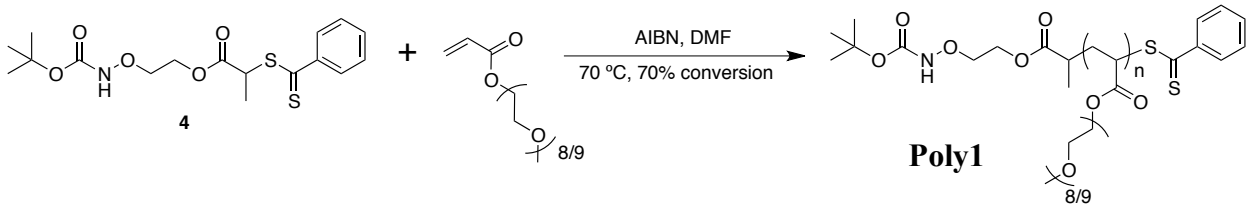

Scheme 7.2. RAFT polymerization of PEGA in the presence of CTA **4** to yield **Poly1**.

Analysis of **Poly1** by DMF gel permeation chromatography (GPC) calibrated with near monodisperse poly(methyl methacrylate) (PMMA) standards revealed a number average molecular weight (M_n) of 11.9 kDa and a polydispersity index (PDI) of 1.11. Because non-authentic standards were used, the M_n of **Poly1** obtained by GPC is likely inaccurate. ^{1}H NMR analysis of **Poly1** determined the M_n to be 24.3 kDa. As expected, a linear evolution of molecular weight versus monomer conversion was observed suggesting a controlled polymerization (Figure 7.2).

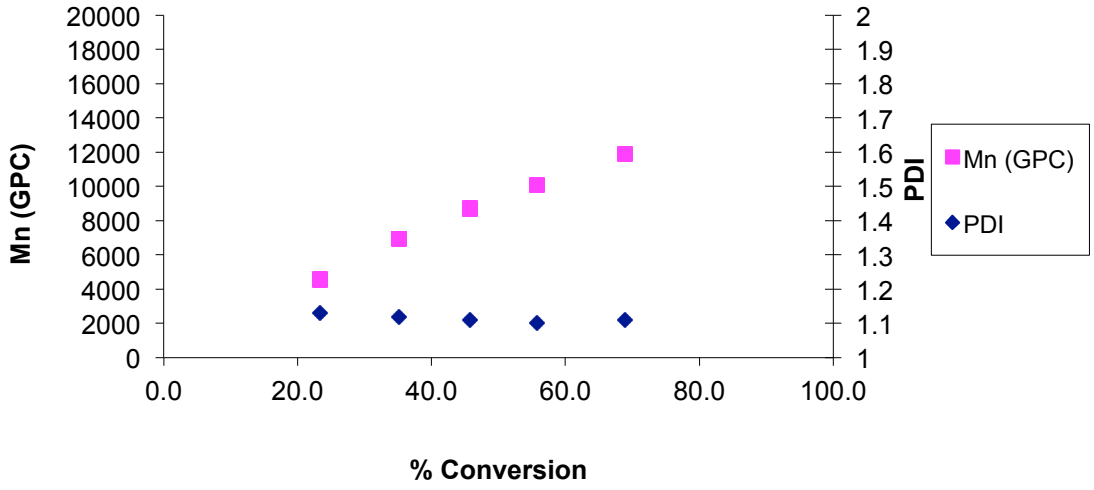

Figure 7.2. RAFT polymerization kinetics of the polymerization of pPEGA in the presence of CTA **4**.

7.2.3. RAFT Polymer Endgroup Modification

The ω-dithiobenzoate end-group of **Poly1** was readily converted into a cysteine-reactive vinyl sulfone endgroup *via* aminolysis with *N*-butylamine followed by *in situ* reaction with divinyl sulfone (Scheme 7.3).[14] α-*Boc*-protected aminooxy, ω-vinyl sulfone **Poly2** was obtained after extensive dialysis against 1:1 MeOH:EtOAc. ^{1}H NMR analysis of **Poly2** confirmed the presence of vinyl sulfone. Comparison of the ^{1}H NMR spectrum of **Poly1** (Figure 7.3.A) to that of **Poly2** (Figure 7.3.B), showed the loss of the aromatic peaks corresponding to the dithiobenzoate endgroup of **Poly1** at 9.0, 7.7, 7.5 ppm and the appearance of the vinyl sulfone endgroup at 6.8, 6.3, and 6.2 ppm.

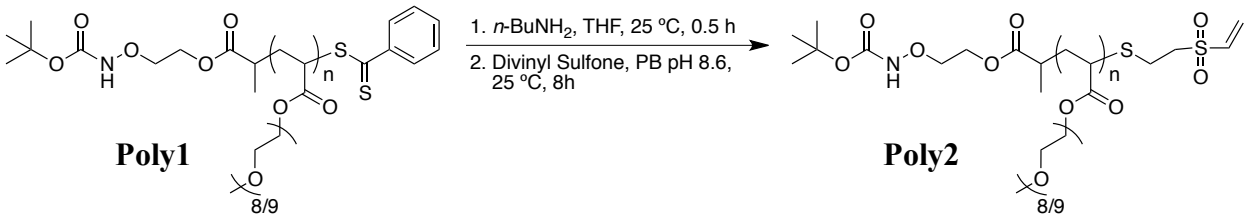

Scheme 7.3. End-group modification of **Poly1** by aminolysis followed by an *in situ* Michael addition to vinyl sulfone to yield **Poly2**.

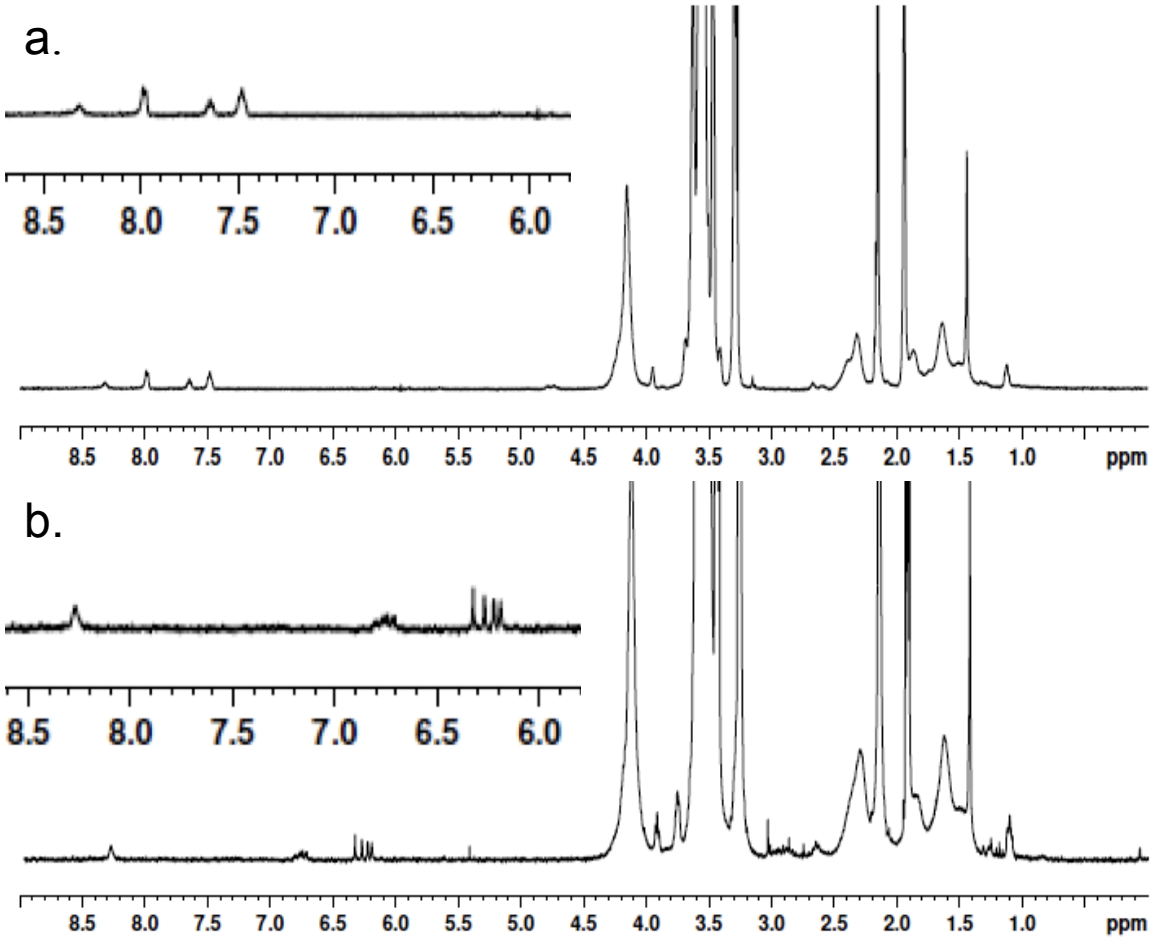

Figure 7.3. (a.) ^{1}H NMR of **Poly1** (benzoate end-group expanded at top left). **(b.)** ^{1}H NMR of **Poly2** (vinyl sulfone end-group expanded at top left).

7.3. Experimental

7.3.1. Materials

Chemicals were purchased from Sigma-Aldrich, Fisher Scientific, Acros, and EMD and used as received unless otherwise specified. AIBN was recrystallized twice from acetone. CH_2Cl_2 was distilled after stirring with CaH_2 and stored under argon. THF was distilled over sodium/benzophenone and stored under argon.

7.3.2. Analytical Techniques

NMR spectra were obtained on Bruker Avance 300 MHz AV, 500 MHz ARX, 500 MHz DRX, and 600 MHZ DRX spectrometers. Proton NMR spectra were acquired with a relaxation delay of 2 sec for small molecules and a relaxation delay of 30 sec for all polymers. UV-Vis spectra were obtained on a Biomate 5 Thermo Spectronic UV-Vis spectrometer and a Hewlett-Packard HP8453 diode-array UV-Vis spectrophotometer with Peltier temperature control spectrometer with quartz cells. Mass spectra were obtained by GC-MS on an Agilent 6890-5975 GC-MS with Autosampler and by MALDI-TOF spectrometry on an Applied Biosystems Voyager-DE STR and operated in linear mode with an external calibration. Infrared absorption spectra were recorded using a PerkinElmer FT-IR equipped with an ATR accessory. TLC plates were pre-coated with Grace Davisil 60Å 40-63 μm and were developed in the indicated solvent systems. Grace Davisil 60Å 40-63 μm silica gel was used for column chromatography. GPC was conducted on a Shimadzu HPLC system equipped with a refractive index detector RID-10A, one Polymer Laboratories PLgel guard column, and two Polymer Laboratories PLgel 5 μm mixed D

columns. LiBr (0.1 M) in DMF at 40 °C was used as an eluent (flow rate: 0.80 mL/min). Calibration was performed using near-monodisperse PMMA standards from Polymer Laboratories.

7.3.3. Methods

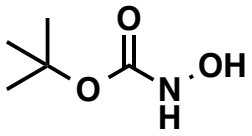

Synthesis of N-Boc-hydroxylamine (1): Synthesis of **1** was adapted from previous literature.[20] Hydroxylamine hydrochloride (6.00 g, 86.3 mmol) was dissolved in H_2O (60 mL). The temperature was then reduced to 0 ºC, and $KHCO_3$ (17.3 g, 172.79 mmol) was added slowly. A separate solution of di-*tert*-butyl dicarbonate (7.53 g, 34.5 mmol) in THF (60 mL) was prepared, and then added dropwise to the hydroxylamine solution and stirred for 23 h. Then solvent was removed *in vacuo*, and the remaining aqueous solution was washed with 3 x 30 mL DCM. The organic layers were combined and dried with $MgSO_4$, filtered, and solvent was removed *in vacuo*. **1** was obtained in 95 % yield (4.38 g). ^{1}H NMR (600 MHz, $CDCl_3$) δ: 7.00 (s, 1H), 6.48 (s, 1H), 1.49 (s, 9H).

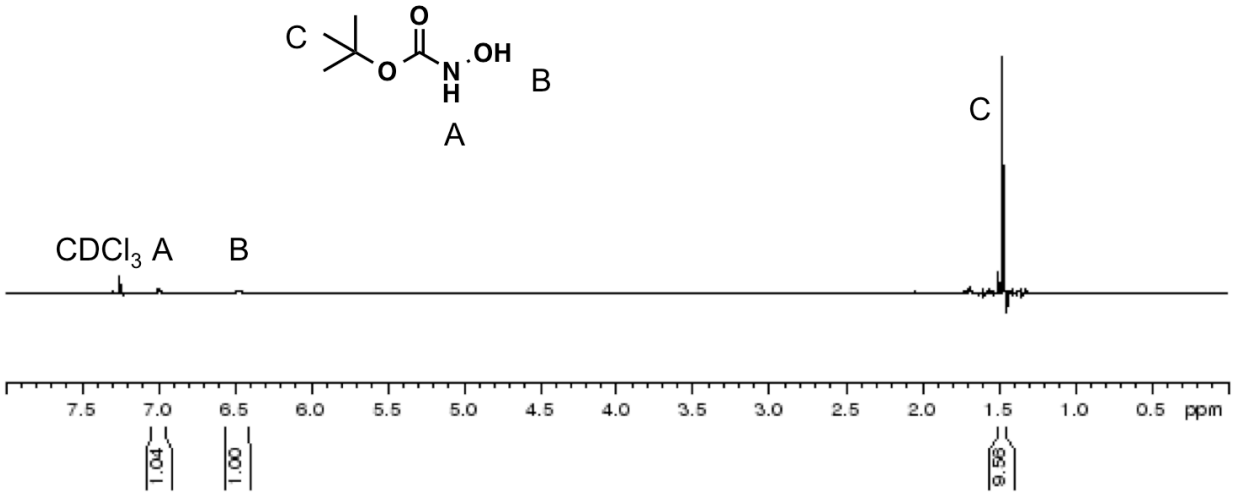

Figure 7.4. ^{1}H NMR (600 MHz, $CDCl_3$) *Boc*-hydroxyl amine (**1**).

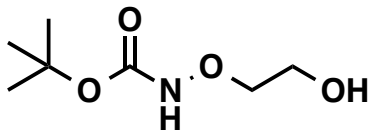

Synthesis of tert-butyl *2-hydroxyethoxycarbamate (**2**):* Synthesis of **2** was adapted from previous literature.[21] *N-Boc*-hydroxylamine (3.26 g, 24.4 mmol) and 2-bromoethanol were dissolved in dry DCM (30 mL). DBU (1.49 g, 9.79 mmol) was then added drop wise and stirred for 72 h. 20 mL DCM was then added, and the solution was washed with 3 x 40 mL H_2O. The organic layer was dried with $MgSO_4$, filtered, and solvent was removed *in vacuo*. The crude product was purified *via* silica gel chromatography using a 2/1 hexanes/EtOAc eluent. **2** was obtained in 77 % yield (1.08 g). ^{1}H NMR (500 MHz, $CDCl_3$) δ: 7.36 (s, 1H), 3.89 (m, 3H), 3.73 (m, 2H), 1.49 (s,

9H). ^{13}C NMR (500 MHz, $CDCl_3$) δ: 158.66, 82.59, 78.16, 59.61, 28.28. IR: 3299, 2977, 2933, 1704, 1482, 1454, 1392, 1367, 1277, 1251, 1162, 1116, 1071, 1049, 1016, 904, 871, 838, 771 cm^{-1}. HRMS calcd for [M + Na] $C_7H_{15}NNaO_4$ 200.0899, found 200.0907.

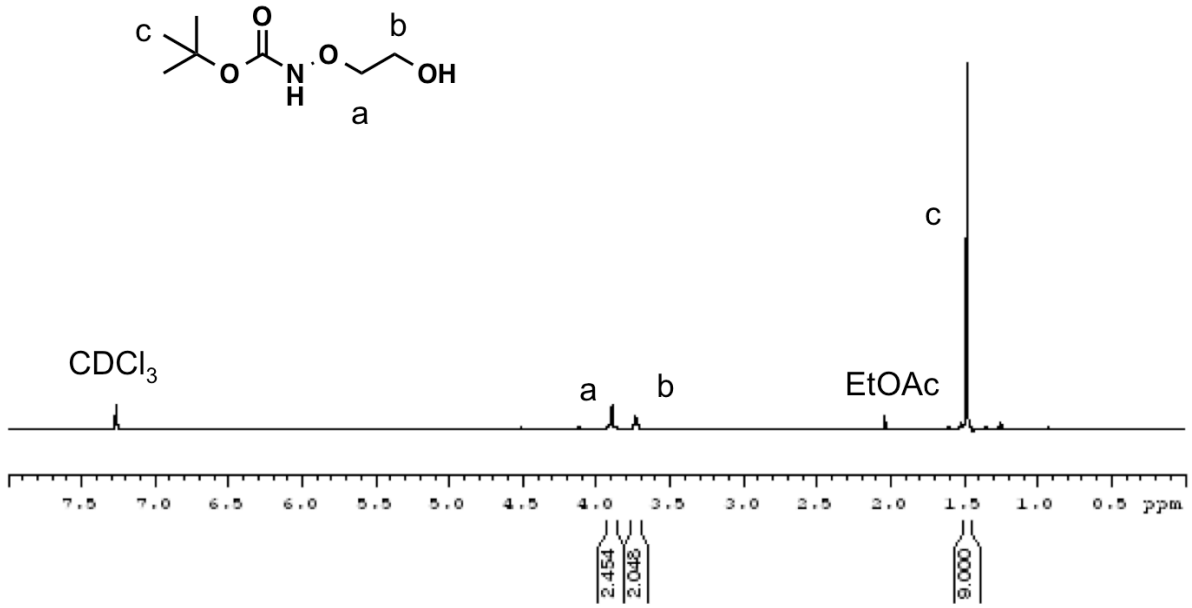

Figure 7.5. ^{1}H NMR (500 MHz, $CDCl_3$) of *tert*-butyl 2-hydroxyethoxycarbamate (**2**).

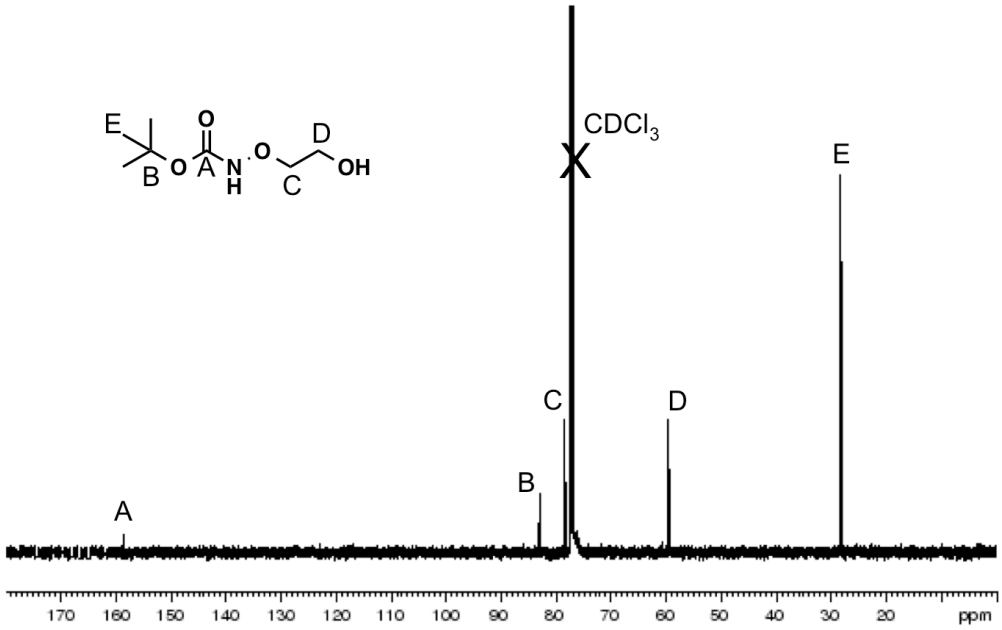

Figure 7.6. ^{13}C NMR (500 MHz, $CDCl_3$) of *tert*-butyl 2-hydroxyethoxycarbamate (**2**).

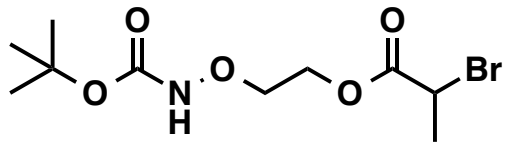

*Synthesis of N-Boc-aminooxyethyl 2-bromopropanoate (**3**)*: *tert*-Butyl 2-hydroxyethoxycarbamate (0.410 g, 2.31 mmol) and Et_3N (0.257 g, 2.54 mmol) were dissolved in dry DCM (20 mL). The temperature was then reduced to 0 ºC and 2-bromopropionyl bromide (0.749 g, 3.47 mmol) was added drop wise and stirred for 1 h. 20 mL DCM was then added and the solution was washed with 3 x 30 mL saturated sodium bicarbonate solution. The organic layer was dried with $MgSO_4$, filtered, and solvent was removed *in vacuo*. The crude product was purified *via* silica gel chromatography using a 3/1 hexanes/EtOAc eluent. **3** was obtained as a pale yellow oil in 42 % yield (0.290 g). ^{1}H NMR (500 MHz, $CDCl_3$) δ: 7.40 (s, 1H), 4.48-4.31 (m, 3h), 4.04 (t, *J* = 5.0 Hz, 2H), 1.81 (d, *J* = 7.0 Hz, 3H), 1.45 (s, 9H). ^{13}C NMR (500 MHz, $CDCl_3$) δ: 170.68, 156.84, 82.23, 74.01, 63.18, 40.11, 28.28, 21.86. IR: 3305, 2978, 2932, 1734, 1447, 1393, 1367, 1335, 1247, 1223, 1158, 1110, 1069, 1006, 913, 849, 770, 674 cm $^{-1}$. HRMS calcd for [M + Na] $C_{10}H_{18}BrNNaO_5$ 334.0266, found 334.0272.

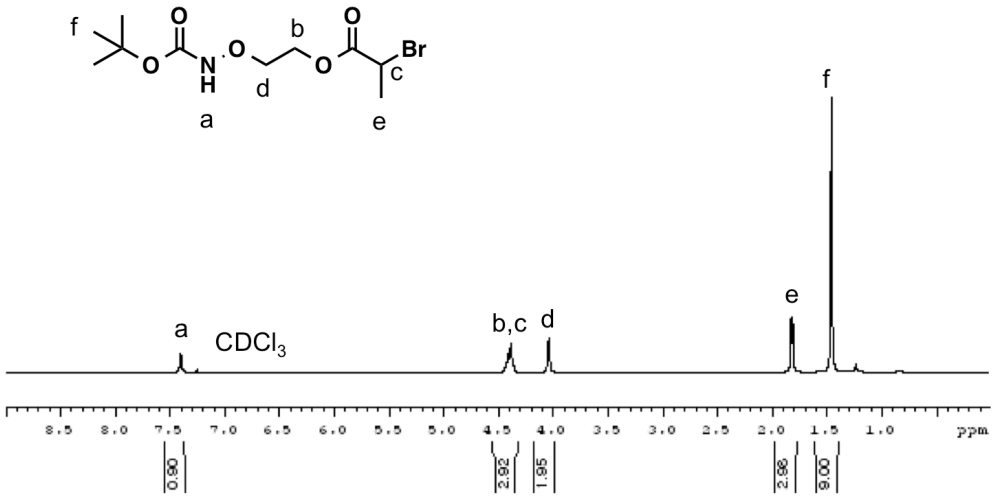

Figure 7.7. ^{1}H NMR (500 MHz, $CDCl_3$) of *N*-Boc-aminooxyethyl 2-bromopropanoate (**3**).

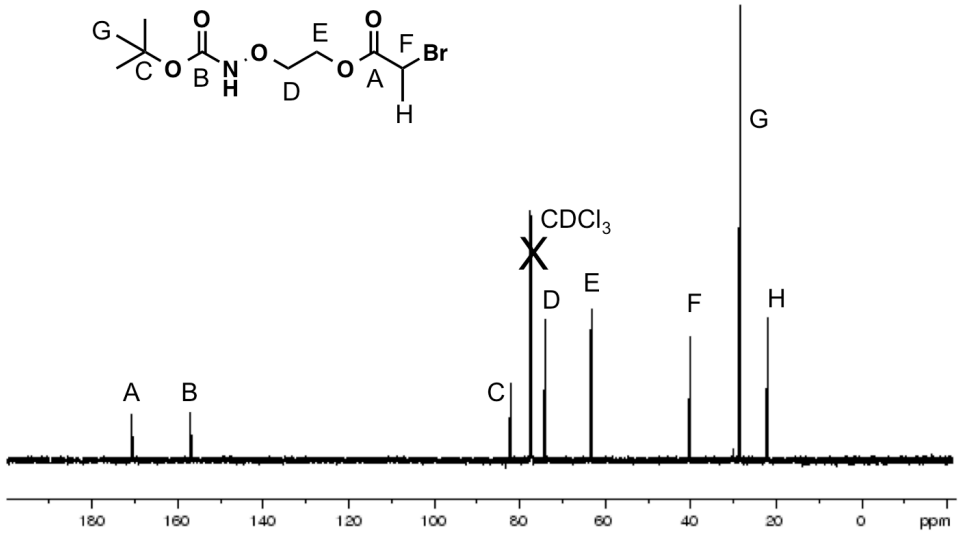

Figure 7.8. ^{13}C NMR (500 MHz, $CDCl_3$) of *N*-Boc-aminooxyethyl 2-bromopropanoate (**3**).

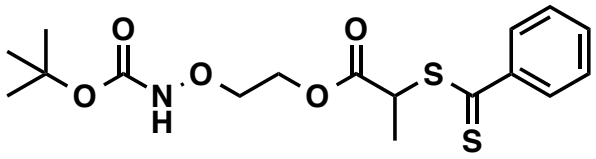

*Synthesis of N-Boc-aminooxyethyl 2-((phenylcarbonothioyl)thio)propanoate chain transfer agent (**4**):* Bromobenzene (0.615 g, 3.92 mmol) and magnesium (0.100 g, 4.11 mmol) were dissolved in dry THF (10.0 mL). I_2 (6.0 mg, 0.024 mmol) was added and the contents were stirred at 25 °C for 1.5 h. The temperature was then reduced to -78 °C and carbon disulfide (0.314 g, 4.12 mmol) was added drop wise and stirred for 1.5 h. The mixture was then brought to 23 °C, 4 mL of the solution was added drop wise to 2-(((*tert*-butoxycarbonyl)amino)oxy)ethyl 2-bromopropanoate (3) and stirred for 20 h. 30 mL DCM was then added, and washed with 3 x 30 mL of H_2O. The organic layer was dried with $MgSO_4$, filtered, and the solvent was removed *in vacuo*. The crude product was purified via silica gel chromatography using a 3/1 hexane/EtOAc eluent. **4** was obtained as red oil in 87.0 % yield (0.378 g). ^{1}H NMR (500 MHz, $CDCl_3$) δ: 7.99 (m, 2H), 7.54 (m, 1H), 7.39 (m, 2H), 7.34 (s, 1H), 4.78 (q, J = 7.35), 4.44 (m, 4H), 4.05 (m, 2H), 1.70 (d, J = 7.35, 3H), 1.47 (s, 9H).^{13}C NMR (500 MHz, $CDCl_3$) δ: 226.15, 171.71, 156.85, 144.60, 132.88, 128.71, 127.14, 82.07, 74.25, 63.05, 48.72, 28.40, 16.67. IR: 3303, 2977, 2934, 1732, 1590, 1475, 1445, 1392, 1367, 1243, 1158, 1107, 1078, 1043, 1026, 998, 919, 875, 761, 685 cm^{-1}. HRMS calcd for [M + Na] $C_{17}H_{23}NNaO_5S_2$ 408.4880, found 408.0908.

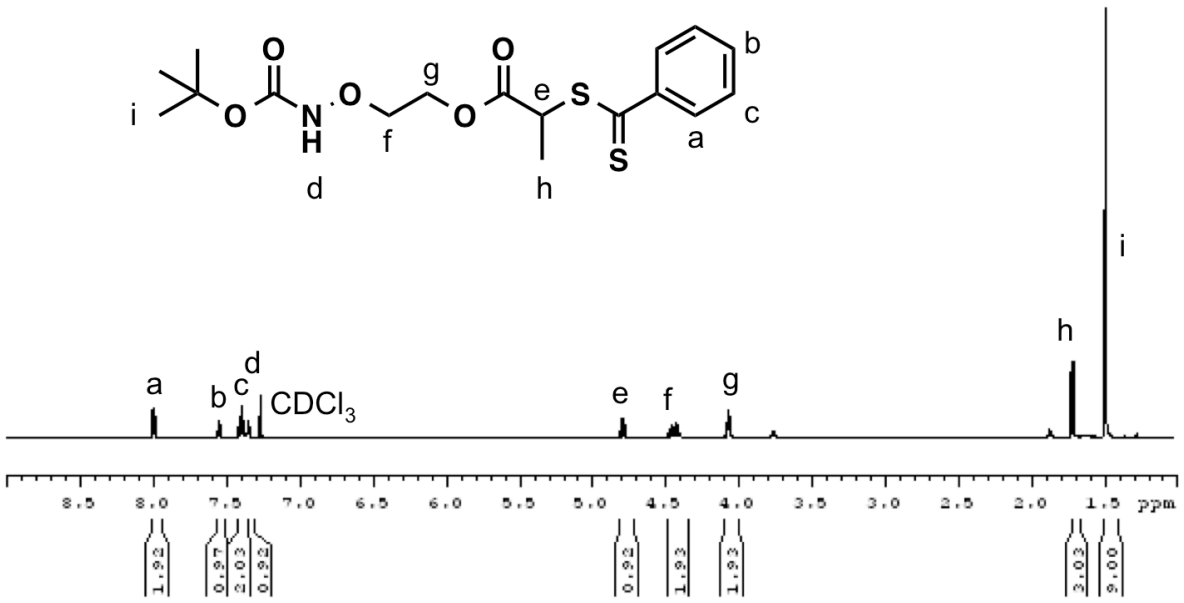

Figure 7.9. ^{1}H NMR (500 MHz, $CDCl_3$) of CTA **4**.

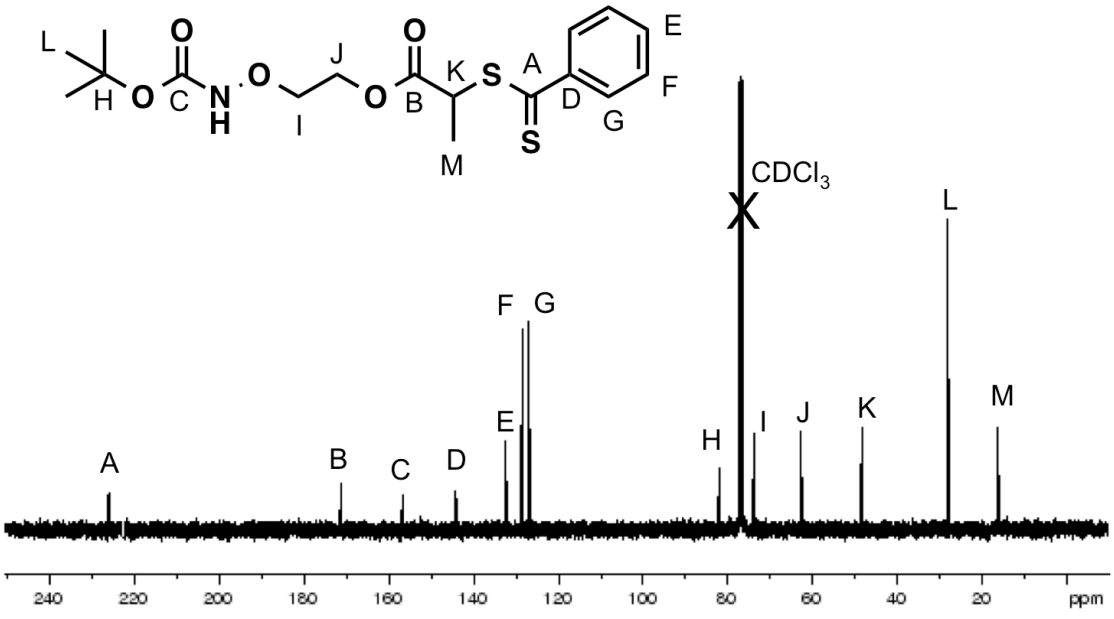

Figure 7.10. ^{13}C NMR (500 MHz, $CDCl_3$) of CTA **4**.

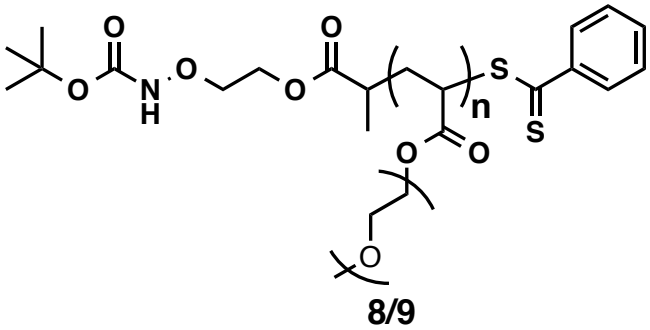

8/9

*Typical polymerization of PEGA in the presence of **4**:* **1** (50.6 mg, 0.131 mmol), AIBN (2.16 mg, 0.0132 mmol), and PEGA (1.79 g, 3.94 mmol) were loaded into a Schlenk tube. DMF (3.30 mL) was added to give a 25 mM solution of **1**, and then the flask was subjected to three freeze-pump-thaw cycles. Immersion of the Schlenk tube into a 70 °C oil bath initiated the polymerization. After 7.6 h (70.0 % conversion) the reaction flask was removed from the oil bath and opened to the atmosphere to give crude **poly1**. The polymer was purified by dialysis against 1/1 EtOAc/MeOH (MWCO 2,000 Da). Polymer conversions were calculated from the ^{1}H NMR spectra by averaging the integrations of the vinylic proton peaks of PEGA and the peak at 4.26 ppm (COOC**H$_2$**) of pPEGA and PEGA in CD_3CN. The molecular weight was calculated by averaging the integrations of three different peaks corresponding to the PEGA: 4.41-3.91 ppm (COOC**H$_2$**), 3.78-3.38 ppm (ethylene glycol units) and 3.36-3.19 ppm (OC**H$_3$**), and comparing them to the aromatic protons of the polymer. ^{1}H NMR (500 MHz, CD_3CN) δ: 8.32 (NH); 7.99 (*o*-CH); 7.65 (*p*-CH); 7.49 (*m*-CH); 4.41-3.91 (COOC**H$_2$**); 3.78-3.37; 3.36-3.19 (OC**H$_3$**); 2.72-2.54; 2.51-2.23; 2.21-2.06; 2.00-1.34; 1.12.M_n g/mol (^{1}H NMR): 24,300. M_n g/mol (0.1 M LiBr DMF GPC): 11,900. PDI: 1.11.

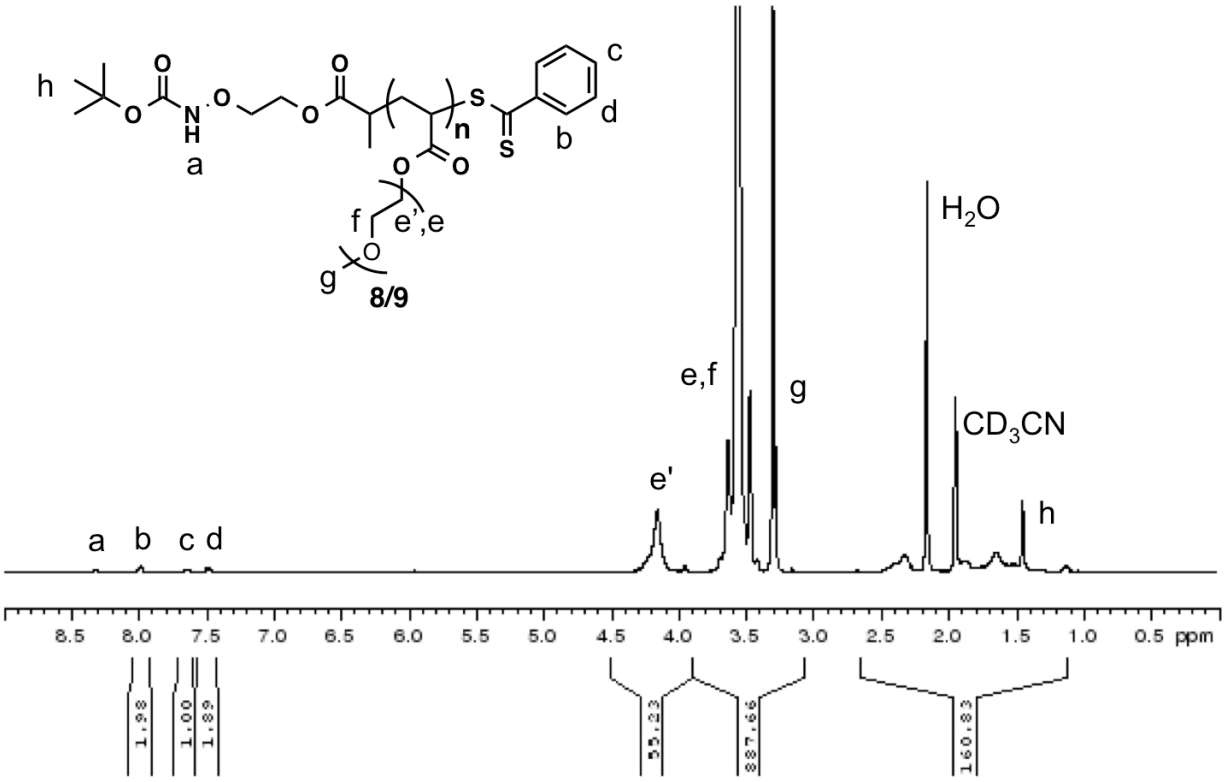

Figure 7.11. ^{1}H NMR (500 MHz, $CDCl_3$) of **Poly1**.

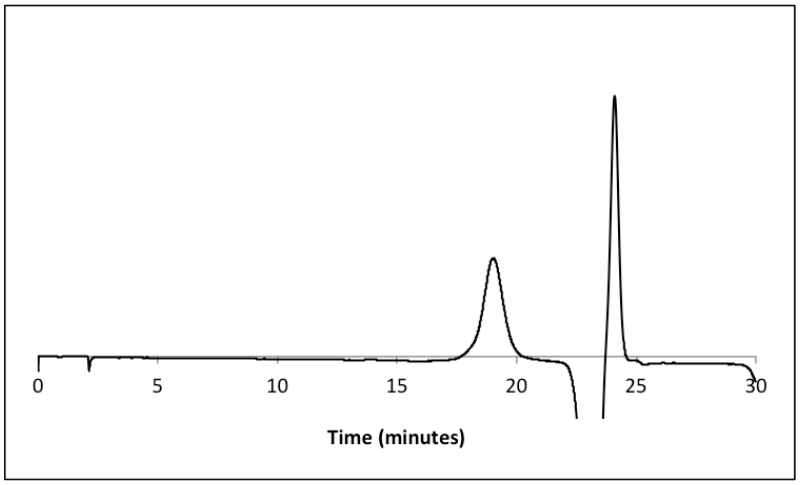

Figure 7.12. GPC chromatogram of **Poly1,** normalized and analyzed by comparison with monodisperse PMMA standards.

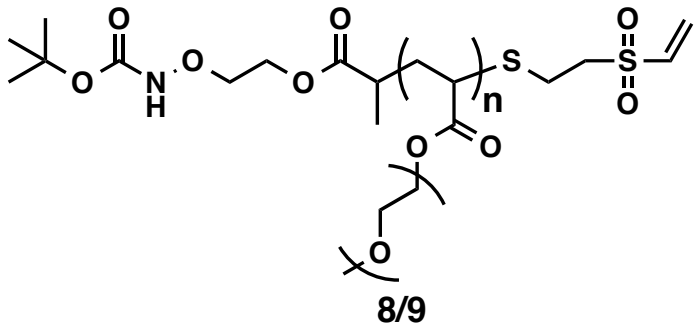

8/9

*Typical aminolysis and in situ conjugation of **poly1** with divinyl sulfone to afford PEGA-DVS (**poly2**):* **Poly1** (50.0 mg, 0.021 mmol) was dissolved in THF (0.210 mL) in Schlenk tube 1. *n*-Butylamine (0.008 mL, 0.840 mmol) was placed in Schlenk tube 2. Divinyl sulfone (0.021 mL, 0.227 mmol) was dissolved in a 0.1 M pH 8.6 phosphate buffer containing 10 mM TCEP, and 10mM EDTA (0.210 mL) in Schlenk tube 3. All three tubes were subjected to three freeze-pump-thaw cycles under argon. The contents of tube 1 were added to tube 2 and stirred for 30 minutes. With the disappearance of the red color of the polymer and the contents of tube 3 were added to tube 2. The solution was stirred for 8 h at 23 °C, followed by dialysis in 1/1 EtOAc/MeOH to afford **poly2** (MWCO 2000 Da). End group retention was determined by comparing the integrations of the peak at 4.14 ppm corresponding to the ester protons of the end group to the integrations of the vinyl sulfone at 6.80, 6.34, and 6.25 ppm. ^{1}H NMR (300 MHz, CD_3CN) δ: 6.36 (geminal-CH); 6.30 (cis-CH); 6.25 (trans-CH); 6.22 (NH); 4.40-3.80 (COOC**H$_2$**); 3.94 (CH); 3.77 (CH); 3.75-3.35 (OC**H$_2$**C**H$_2$**O), 3.35-3.2 (OC**H$_3$**), 2.5-2.25, 1.9-1.3. M_n g/mol (^{1}H NMR): 5,800. M_n g/mol (0.1 M LiBr DMF GPC): 7,600. PDI: 1.11.

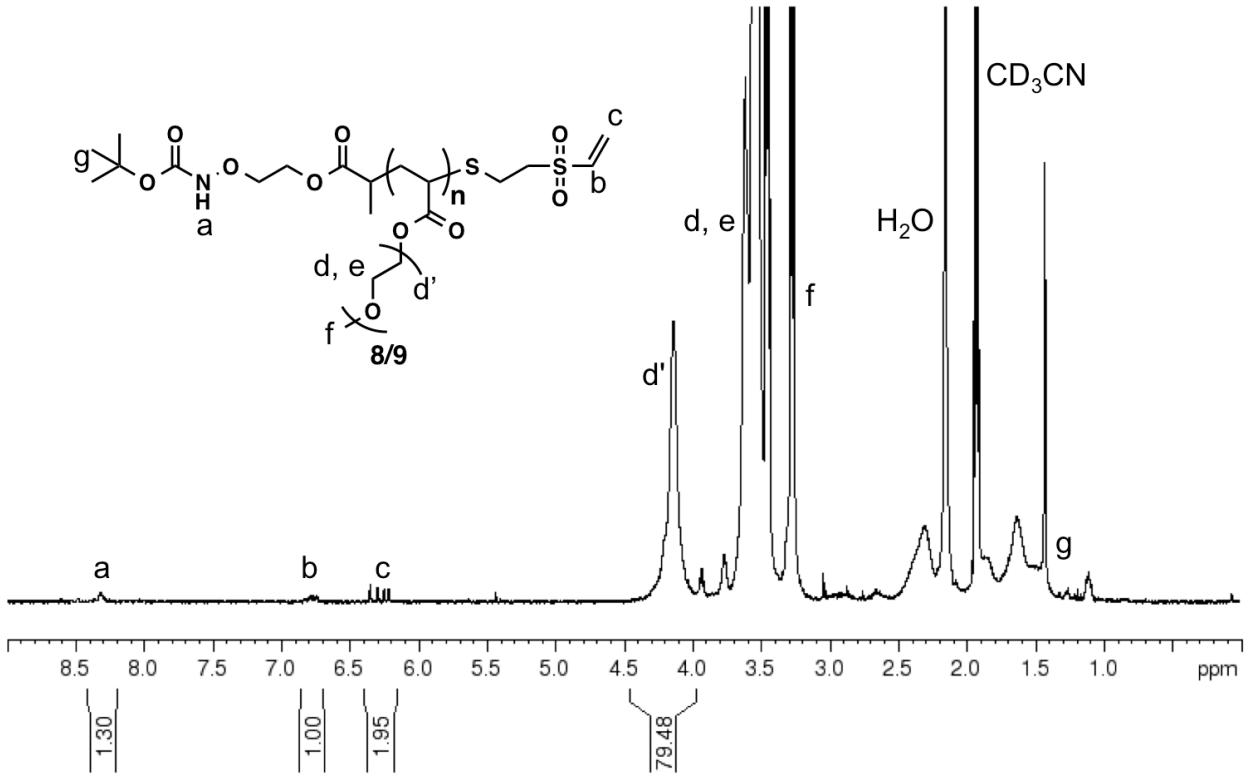

Figure 7.13. ^{1}H NMR (500 MHz, $CDCl_3$) of **Poly2**.

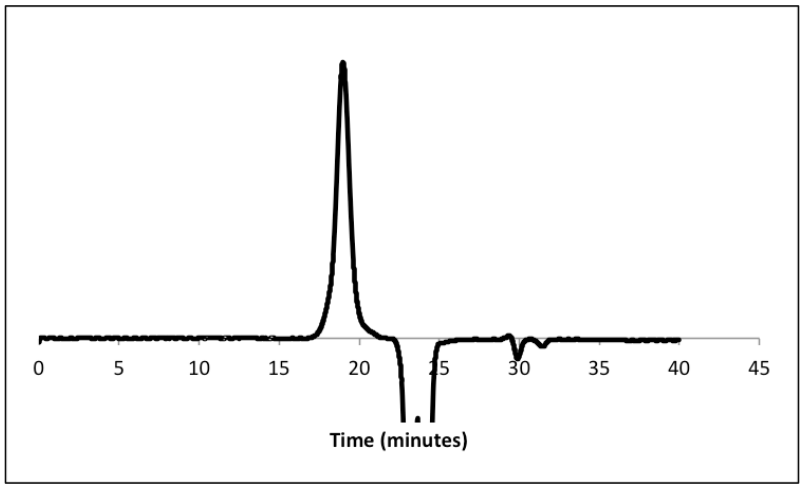

Figure 7.14. GPC chromatogram of **Poly2,** normalized and analyzed by comparison with monodisperse PMMA standards.

7.4. Conclusions

A novel *Boc*-protected aminooxy dithiobenzoate CTA was synthesized in moderate yield. Polymerization of PEGA in the presence of this CTA resulted in a well defined pPEGA. Post polymerization aminolysis followed by *in situ* conjugation to divinyl sulfone quantitatively yielded a α-*Boc*-aminooxy, ω-vinyl sulfone cysteine-reactive polymer. Conjugation of this polymer to proteins, as well as *Boc*-deprotection and subsequent oxime bond formation with aldehyde terminated polymers was explored (data not shown), however we were unable to efficiently gain access to protein dimers using this system.

7.5. References

1. Marianayagam, N. J.; Sunde, M.; Matthews, J. M. The Power of Two: Protein Dimerization in Biology. *Trends Biochem.Sci.* **2004**, *29*, 618-625.
2. Mammen, M.; Choi, S. K.; Whitesides, G. M. Polyvalent Interactions in Biological Systems: Implications for Design and Use of Multivalent Ligands and Inhibitors. *Angew. Chem.-Int. Edit.* **1998**, *37*, 2755-2794.
3. Heredia, K. L.; Grover, G. N.; Tao, L.; Maynard, H. D. Synthesis of Heterotelechelic Polymers for Conjugation of Two Different Proteins. *Macromolecules* **2009**, *42*, 2360-2367.
4. Tao, L.; Kaddis, C. S.; Loo, R. R. O.; Grover, G. N.; Loo, J. A.; Maynard, H. D. Synthetic Approach to Homodimeric Protein-Polymer Conjugates. *Chem. Commun.* **2009**, 2148-2150.
5. Boyer, C.; Liu, J.; Bulmus, V.; Davis, T. P.; Barner-Kowollik, C.; Stenzel, M. H. Direct Synthesis of Well-Defined Heterotelechelic Polymers for Bioconjugations. *Macromolecules* **2008**, *41*, 5641-5650.
6. Liu, J. Q.; Liu, H. Y.; Bulmus, V.; Tao, L.; Boyer, C.; Davis, T. P. A Simple Methodology for the Synthesis of Heterotelechelic Protein-Polymer-Biomolecule Conjugates. *J. Polym. Sci., Part A: Polym. Chem.* **2010**, *48*, 1399-1405.
7. Roth, P. J.; Jochum, F. D.; Zentel, R.; Theato, P. Synthesis of Hetero-Telechelic Alpha,Omega Bio-Functionalized Polymers. *Biomacromolecules* **2010**, *11*, 238-244.
8. Moad, G.; Rizzardo, E.; Thang, S. H. Living Radical Polymerization by the Raft Process - a Third Update. *Aust. J. Chem.* **2012**, *65*, 985-1076.

9. Boyer, C.; Bulmus, V.; Davis, T. P.; Ladmiral, V.; Liu, J.; Perrier, S. Bioapplications of Raft Polymerization. *Chem. Rev.* **2009**, *109*, 5402-5436.

10. Heredia, K. L.; Nguyen, T. H.; Chang, C. W.; Bulmus, V.; Davis, T. P.; Maynard, H. D. Reversible Sirna-Polymer Conjugates by Raft Polymerization. *Chem. Commun.* **2008**, 3245-3247.

11. Heredia, K. L.; Tolstyka, Z. P.; Maynard, H. D. Aminooxy End-Functionalized Polymers Synthesized by Atrp for Chemoselective Conjugation to Proteins. *Macromolecules* **2007**, *40*, 4772-4779.

12. Alconcel, S. N. S.; Grover, G. N.; Matsumoto, N. M.; Maynard, H. D. Synthesis of Michael Acceptor Ionomers of Poly(4-Sulfonated Styrene-Co-Poly(Ethylene Glycol) Methyl Ether Acrylate). *Aust. J. Chem.* **2009**, *62*, 1496-1500.

13. Boyer, C.; Liu, J. Q.; Bulmus, V.; Davis, T. P. Raft Polymer End-Group Modification and Chain Coupling/Conjugation Via Disulfide Bonds. *Aust. J. Chem.* **2009**, *62*, 830-847.

14. Grover, G. N.; Alconcel, S. N. S.; Matsumoto, N. M.; Maynard, H. D. Trapping of Thiol-Terminated Acrylate Polymers with Divinyl Sulfone to Generate Well-Defined Semitelechelic Michael Acceptor Polymers. *Macromolecules* **2009**, *42*, 7657-7663.

15. Heredia, K. L.; Tao, L.; Grover, G. N.; Maynard, H. D. Heterotelechelic Polymers for Capture and Release of Protein-Polymer Conjugates. *Polym. Chem.* **2010**, *1*, 168-170.

16. Spruell, J. M.; Levy, B. A.; Sutherland, A.; Dichtel, W. R.; Cheng, J. Y.; Stoddart, J. F.; Nelson, A. Facile Postpolymerization End-Modification of Raft Polymers. *J. Polym. Sci., Part A: Polym. Chem.* **2009**, *47*, 346-356.

17. Tao, L.; Kaddis, C. S.; Loo, R. R. O.; Grover, G. N.; Loo, J. A.; Maynard, H. D. Synthesis of Maleimide-End-Functionalized Star Polymers and Multimeric Protein-Polymer Conjugates. *Macromolecules* **2009**, *42*, 8028-8033.

18. Sletten, E. M.; Bertozzi, C. R. Bioorthogonal Chemistry: Fishing for Selectivity in a Sea of Functionality. *Angew. Chem., Int. Ed.* **2009**, *48*, 6974-6998.

19. Christman, K. L.; Broyer, R. M.; Tolstyka, Z. P.; Maynard, H. D. Site-Specific Protein Immobilization through N-Terminal Oxime Linkages. *J. Mater. Chem.* **2007**, *17*, 2021-2027.

20. Watson, K. D.; Carosso, S.; Miller, M. J. New and Concise Syntheses of the Bicyclic Oxamazin Core Using an Intramolecular Nitroso Diels–Alder Reaction and Ring-Closing Olefin Metathesis. *Org. Lett.* **2012**, *15*, 358-361.

21. Jones, D. S.; Hammaker, J. R.; Tedder, M. E. A Convenient Synthesis of N-(Tert-Butyloxycarbonyl)Aminooxy Ethers. *Tetrahedron Lett.* **2000**, *41*, 1531-1533.